From High-Dimensional Data to Disease Mechanisms

NOTCH Signaling in Hodgkin Lymphoma

D I S S E R T A T I O N

zur Erlangung des akademischen Grades

doctor rerum naturalium
(Dr. rer. nat.)
im Fach Biologie

eingereicht an der
Mathematisch-Naturwissenschaftlichen Fakultät I
Humboldt-Universität zu Berlin

von
Dipl.-Biochemiker Karl Köchert

Präsident der Humboldt-Universität zu Berlin:
Prof. Dr. Jan-Hendrik Olbertz

Dekan der Mathematisch-Naturwissenschaftlichen Fakultät I:
Prof. Dr. Andreas Herrmann

Gutachter:
1. Prof. Dr. Harald Saumweber
2. Prof. Dr. Georg Lenz
3. Prof. Dr. Joachim Selbig

eingereicht am: 27.10.2010
Tag der mündlichen Prüfung: 02.03.2011

Abstract

Inappropriate activation of the NOTCH signaling pathway, e.g. by activating mutations, contributes to the pathogenesis of various human malignancies. Using a bottom up approach based on the acquisition of high–dimensional microarray data of classical Hodgkin lymphoma (cHL) and non-Hodgkin B cell lymphomas as control, we identify a cHL specific NOTCH gene-expression signature dominated by the NOTCH co-activator Mastermind-like 2 (MAML2). This set the basis for demonstrating that aberrant expression of the essential NOTCH co-activator MAML2 provides an alternative mechanism to activate NOTCH signaling in human lymphoma cells. Using immunohistochemistry we detected high-level MAML2 expression in several B cell-derived lymphoma types, including cHL cells, whereas in normal B cells no staining for MAML2 was detectable. Inhibition of MAML protein activity by a dominant negative form of MAML or by shRNAs targeting MAML2 in cHL cells resulted in down-regulation of the NOTCH target genes *HES7* and *HEY1*, which we identified as overexpressed in cHL cells, and in reduced proliferation. In order to target the NOTCH transcriptional complex directly we developed short peptide constructs that competitively inhibit NOTCH dependent transcriptional activity as demonstrated by NOTCH reporter assays and EMSA analyses. We conclude that NOTCH signaling is aberrantly activated in a cell autonomous manner in cHL. This is mediated by high-level expression of the essential NOTCH co-activator MAML2, a protein that is only weakly expressed in B cells from healthy donors. Using short peptide constructs we moreover show, that this approach is promising in regard to the development of NOTCH pathway inhibitors that will also work in NOTCH associated malignancies that are resistant to γ-secretase inhibition.

Zusammenfassung

Die aberrante Aktivierung des NOTCH Signalweges, welche zum Beispiel durch aktivierende Mutationen der NOTCH-Rezeptoren hervorgerufen wird, trägt entscheidend zu verschiedensten malignen Erkrankungen im Menschen bei. Basierend auf der Analyse von hochdimensionalen Microarray-Datensätzen von klassischen Hodgkin Lymphoma Fällen und nicht-Hodgkin Fällen, haben wir eine Hodgkin Lymphoma-spezifische NOTCH Signatur identifiziert. Diese wird von dem essentiellen NOTCH-Koaktivator Mastermind-like 2 (MAML2) signifikant dominiert. Auf der Grundlage dieses Resultates haben wir die Rolle von MAML2 im Kontext des Hodgkin Lymphoma-spezifischen, aberrant re-gulierten NOTCH Signalweges weiter untersucht. Die signifikante Überexpression von MAML2 im Hodgkin Lymphom konnte in verschiedenen Hodgkin Lymphom Zelllinien und auch durch die immunhistochemische Analyse von primären Hodgkin Lymphom Fällen verifiziert werden. Mit Hilfe des Knockdowns von MAML2 bzw. der Inhibition des NOTCH Signalweges durch die Verwendung einer kompetitiv, dominant-negativ wirkenden, trunkierten Variante von MAML1 konnte daraufhin gezeigt werden, dass die Überexpression von MAML2 der limitierende Faktor für die Hodgkin Lymphoma-spezifische, pathologische Deregulation des NOTCH Signalweges ist. Die MAML2-vermittelte Überaktivierung des NOTCH Signalweges ist darüber hinaus essentiell für die Proliferation von Hodgkin Lymphom Zelllinien und die aberrante Expression der NOTCH Zielgene *HES7* und *HEY1*. Das konstitutive Vorhandensein von aktiviertem, intrazellulären NOTCH1 in Hodgkin Lymphom Zelllinien impliziert darüber hinaus, dass der Signalweg im Hodgkin Lymphom zellautonom aktiviert ist. Weiterhin wurde der NOTCH-Transkriptionelle-Komplex (NTK) somit als potentielles therapeutisches Ziel identifiziert. Zum Zwecke der Inhibition der NTK-Assemblierung wurden kurze, MAML1-basierte Peptid-Konstrukte entwickelt. Mit Hilfe von NOTCH-spezifischen Reporterassays und EMSA-Analysen konnte ge-

zeigt werden, dass *in vitro* effektiv die NTK-Assemblierung und NTK-abhängige transkriptionelle Aktivierung durch diese Peptid-Konstrukte inhibiert wird.

In dieser Arbeit wird damit ein neuer, pathologisch hochwirksamer Mechanismus der NOTCH Signalweg-Deregulation aufgedeckt. Gleichzeitig wird mit der Entwicklung NOTCH-inhibitorisch wirksamer Peptid-Konstrukte eine Möglichkeit aufgezeigt, diesen Mechanismus in dem essentiellsten Schritt, nämlich der NTK-Assemblierung, zu inhibieren. Dies ist eine Herangehensweise, die auch bei anderen malignen Erkrankungen mit pathologischer Deregulation des NOTCH-Signalweges als Ursache wirksam sein könnte, insbesondere bei solchen, bei denen sich die Behandlung mit γ-Sekretase Inhibitoren als nicht wirksam erweist.

Contents

1 Introduction

1.1 Hodgkin Lymphoma

1.1.1 Historical view on Hodgkin Lymphoma

As early as in 1832, the British physician Thomas Hodgkin published an article describing findings of the dissection of seven people showing 'Morbid Appearances of the Absorbent Glands and Spleen'. He reported, that these people suffered from massive enlargement of the spleen and the lymph nodes [1].
This was the first description of what was later to be called Hodgkin's Disease or according to the World Health Organization Hodgkin Lymphoma. Even though more than 150 years have passed since then, the aetiology of this malignancy has become explainable only in the last few decades.

1.1.2 Epidemiology of classical Hodgkin lymphoma (cHL)

Hodgkin lymphoma is a very common type of lymphoma with an incidence of around 3 per 100,000 in Europe and the USA [2]. Most people affected from Hodgkin lymphoma are aged around 30 or 50 years, thus following a bimodal distribution. Men are affected more often than women [3]. Interestingly, incidence of Hodgkin lymphoma in developing countries is predominant during childhood and decreases with age [3]. Hodgkin lymphoma is divided into various subtypes. The nodular-sclerosing-, the mixed-

(a) (b)

Figure 1.1: Defining a new disease, Thomas Hodgkin's work in the early 19^{th} century

A portrait (a) of Thomas Hodgkin and a picture (b) of what he found to be the Morbid Appearances of seven patients he dissected in 1832. (a), Reproduced courtesy of Gordon Museum, Guy's Hospital, GKT, King's College London. (b), Hodgkin's disease watercolor drawing by Robert Carswell in 1828.

cellularity- and lymphocyte-depleted subtypes are summarized as classical Hodgkin lymphoma (cHL). The lymphocyte-predominant subtype (LP) presents a distinct entity. As this work entirely focuses on cHL, no further description of the LP type will be provided. Readers interested in this particular entity of Hodgkin lymphoma are referred to [4].

Aspects of inheritance

Various studies indicate, that cHL is one of the malignancies, in which a significant association between cHL incidences and inheritance is to be assumed. One of these studies found cHL to be number four in a ranking list of cancers with high familial indices. Yet, the percentage of familial cHL of all cHL cases is very low and so far, no genetic markers could be identified, that would mediate such an inheritance mechanism [5].

1.1.3 Treatment of cHL, prognosis and caveats today

Clinicians divide the advancement of Hodgkin lymphoma in three stages, each of with different treatment regimens being used. Ongoing trials are trying to minimize the cycles of chemotherapy and the dose of radio therapy. Below, some common forms of treatment for each stage are listed as are percentages of survival rates from different studies.

- Early stage cHL, Engert *et al.* 2010 [6], treatment group 4: 2× chemotherapy doxorubicin, vinblastine, bleomycin, dacarbazine, radio therapy 20 Gy. 96.6% 5-year overall survival.
- intermediate early-stage cHL study EORTC H9U: 6× chemotherapy with doxorubicin, vinblastine, bleomycin and dacarbazine, radio therapy 30 Gy. 95% 4-year overall survival [7].
- advanced–stage cHL study GHSG HD12: 8× chemotherapy with bleomycin, etoposide, doxorubicin, cyclophosphamide, vincristine, procarbazine and prednisone. 88% 4-year overall survival [8].

The treatment regimens used presently have a number of severe side effects. Some acute side effects are for example myelosuppression with associated cytopenias and pulmonary toxicity [9, 10]. Long term toxicities include secondary cancers as for example Myelodysplastic syndrome (MDS) and acute myeloid leukaemia (AML) [11]. Studies show, that the 20-25 year cumulative actuarial risk of secondary cancers after traditional cHL treatment is 24-28%, with the most common secondary malignancy being breast-cancer [12, 13, 14, 15, 16]. There is a strong association of radio therapy with the onset of these secondary malignancies, yet some of them are also seen when only chemotherapy was applied [17].

Though, overall survival rates are high for patients treated with early–stage and intermediate early–stage cHL, the prognosis for elderly and advanced stage patients is poor. The overall survival rate with a follow up of seven years can be as low as 73% [18]. This emphazises the importance of advancing treatment strategies for cHL to higher overall survival rates at the same time reducing toxicity of treatment.

1.1.4 Aetiology of cHL

The character of HRS cells

The special character of Hodgkin lymphoma cells was already observed around the year 1900 by Carl Sternberg [19] and Dorothy Reed [20]. Both discovered, that the mono-nucleated Hodgkin cells and the multi-nucleated — and henceforth called — Reed–Sternberg cells are hallmarks of the disease described by Thomas Hodgkin. In this work, the two cell types will be summarized using the term Hodgkin–Reed–Sternberg (HRS) cells. A prominent pathohistological marker of cHL is the expression of CD30 [21], a TNF receptor family member (see figure 1.2). This marker is to some degree compromised

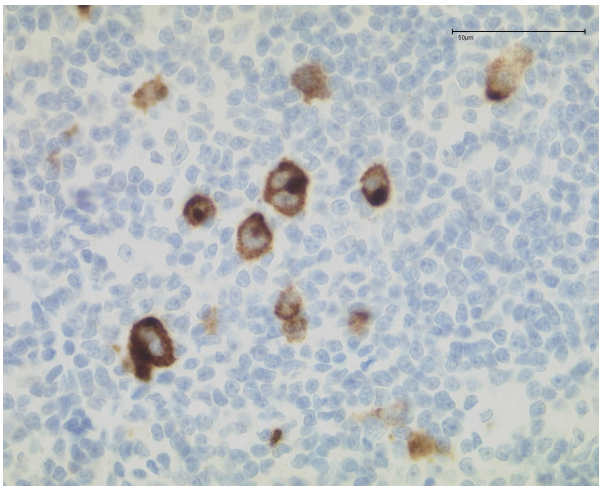

Figure 1.2: CD30 Staining of a lymph node from a cHL patient

CD30 staining is a typical histological cHL marker used by pathologists for cHL diagnosis. The blackly stained, enlarged cHL cells make up just around 1% of the tumor tissue.

by some T cell lymphomas that also express CD30 (e.g. $CD30^+$ anaplastic large T-cell lymphoma [22]). HRS cells are unusually large in comparison to normal cells of lymphatic origin and comprise usually about 1% of the tumor tissue [23]. The remaining 99% are composed of bystander cells that are attracted by signals given from the HRS cells. This attraction will result in the cHL-typical, inflammatory microenvironment

(for a thorough description, please see below). The rarity of HRS cells within the tumor tissue and the difficulty to separate them from bystander cells add substantially to the limitations of experimental characterisation, which is mainly done by the usage of HRS cell lines established from cHL patients. However, using e.g. laser-dissection techniques, it is nowadays also possible to isolate HRS cells from cHL patient biopsies which may be used for experimental characterisation (see e.g. [24]).

The cellular origin of HRS cells

HRS cells show an immunophenotype that is difficult to interpret, as lineage markers of several distinct lineages are found in these cells. However, in nearly all cases of cHL, these cells are characterized by the presence of rearranged and somatically hypermutated Ig variable genes [25]. As these rearrangements and hypermutations take place in germinal center B cells, the cellular origin and the differentiation stage (where development takes a turn to pathogenic events) of HRS cells was pinpointed to this particular B cell population.

However, HRS cells do not show a B cell phenotype and have lost a considerable part of the B cell specific gene expression pattern. In HRS cells a vast number of B cell lineage genes is down–regulated, whereas a large set of B cell lineage inappropriate genes is up–regulated [26, 27, 24].

Another aspect of the cellular origin of cHL is, that the tumor cells of a particular cHL patient display the very same Ig variable rearrangements, indicating that they are the clonal expansion of one original tumor cell [28, 29]. In 25% of cHL cases these mentioned processes lead to non-functional Ig variable genes, a fact that would normally result in apoptosis induction of the affected B cell. To evade apoptosis induction, HRS cells have developed a number of mechanisms. For example, mutations of the FAS gene found in cHL (yet only rarely) prevent apoptosis induction by FAS-ligands of effector cells. Moreover, several anti-apoptotic genes such as c-FLIP [30] and Bcl-2 family proteins are

expressed at aberrantly high levels in cHL [3].

There are also reports on cHL cases with a T-cell origin which, however, are very rare [31]. These cases show no rearrangement of Ig variable genes nor their hypermutation, yet carry T cell receptor gene rearrangements. Strikingly, those seemingly T cell derived cases of cHL are very similar to B cell derived cHL as they cluster with B cell origin cHL cases when their gene expression profiles are analyzed together with other B or T cell associated malignancies [32].

The cHL microenvironment

As mentioned above, cHL is characterized by the infiltration of various cell types of the immune system into lymphatic tissue. Cell types found in the microenvironment are mast cells, B cells, T cells and plasma cells to name just a few. Presumably, these cells are attracted through a number of cytokines (IL5, IL13, IL21) [33, 34, 35] and chemokines (CCL5, CCL17, CCL22) [36, 37] which are secreted by the HRS cells. In turn, the attracted cells seem to play an important role in the survival of HRS cells as there is evidence that they provide appropriate survival signals (see table 1.1 and [31]). This hypothesis is endorsed by the fact, that HRS cells are very difficult to grow in culture, are basically not found in peripheral blood and even if they metastasize into non-lymphoid tissue, they are embedded in their typical microenvironment [38, 31]. Hence, the cHL microenvironment is an important factor for the pathogenesis of this malignancy in that it maintains an appropriate environment for the tumor cells and plays a role in promoting tumor growth and immune escape [39]. A recent study additionally indicates the presence of $CD68^+$ macrophages in the tumor microenvironment in a subset of cHL cases. When these cells are found in the cHL microenvironment, prognosis is significantly poorer than when they are absent [40]. Table 1.1 shows, how a number of survival signals is given to HRS cells by diverse types of immune system cells.

HRS cells provide/secrete	**Attracted/interacting cell/antigen**	**Secondary Effects**
CD30	Eosinophil/CD30L	possibly growth stimulation of cHL [31]
IL5, CCL5, CCL28	Eosinophil	possibly growth stimulation of cHL
TNFα, TNFβ	Fibroblast	Attraction of Eosinophils
PD1L, IL10, TGFβ, galectin1	$CD8^+$ T_C cell / PD1	inhibition of $CD8^+$ T cells
TARC, CCL5, CCL20, CCL22, galectin1	$CD4^+$ T_{Reg} cell	expansion of $CD4^+$ T_{Reg} cell which will inhibit $CD8^+$ T_C cells through IL10 secretion
BCMA, TRKA	Granulocyte / APRIL	TRKA stimulation through secretion of NGF
TARC, CCL5, CCL22, CD54, CD40, MHCII, CD80	$CD4^+$ T_H cell / CD18, CD11A, CD40L, TCR, CD28	promotion of T_H to T_{Reg} differentiation [41]

Table 1.1: cHL cellular interactions with other immune system cell types - generation of the cHL microenvironment

T_C, cytotoxic T cell; T_H, T helper cell; T_{Reg}, regulatory T cell; TGFβ, transforming growth factor-β; TNFα, tumor necrosis factor-α. Adapted from [31].

Deregulated transcription factor networks in cHL

Normally, B cell lymphomas and leukemias maintain a substantial part of their B cell phenotype and expression pattern. In opposite, HRS cells show a nearly complete loss of the B cell–specific expression program (see above and [42]). Most of the remaining B cell specific factors they express are associated with antigen-presenting functions and T helper cell communication (MHCII, CD40 and CD80) [43, 44]. Generally, HRS cells have a very unspecific expression pattern. Markers of various hematopoetic lineages are expressed (CD3, CD4, CD40, granzyme B, CCL17, CSF1R) and many years had to pass before Hodgkin researchers began to understand how this is achieved [31, 45, 46]. A very significant factor towards understanding the pathogenesis of cHL is the broad deregulation of various transcription factor networks which contributes to the reprogramming of the former B cell specific gene expression program [27]. The list of these transcription factor networks is still growing and in context of this work, only a few will be mentioned (the interested reader may want to refer to Küppers *et al.* [31] for a thorough and broad description).

Besides the deregulation of the NF-κB transcription factor network (see table 1.2 be-

low), early B cell factor 1 (EBF1) is a B cell lineage transcription factor, that suppresses the expression of myeloid and T cell genes [47] and at the same time activates the transcription of B cell specific genes. As such, EBF1 is an important B-lineage commitment factor and its expression levels in cHL are vastly reduced in comparison to normal B cells [48]. It is thus commonly assumed, that EBF1 is one of the factors, that contributes to the cHL specific loss of the B cell phenotype [49].

Another very important B cell transcription factor is the gene E2A which codes for the two transcription factor proteins E12 and E47. Even though these proteins are detectable in cHL, they can not function properly, as in cHL various mechanisms have been elucidated, that impair E2A dependent transcriptional activation [48, 26, 50]. The high level expression of the inhibitor of DNA binding 2 (ID2) is one of these mechanisms. ID2 lacks a DNA binding domain, yet is able to dimerize with E2A proteins to a form a dimer, which is not capable of transcriptional activation. ID2 is normally expressed in dendritic cells and natural killer cells rather than in B cells and a number of studies have provided data, indicating that this factor effectively inhibits B cell generation [51, 52]. A second mechanism to inhibit E2A mediated transcription of B cell genes in cHL is the high level expression of activated B cell factor 1 (ABF1). ABF1 is a transcriptional repressor capable of forming heterodimers with E2A. These dimers are then transcriptionally inactive which will result in the down-regulation of E2A mediated transcriptional activation [48].

The effects of down-regulation of a number of other B cell transcription factors such as PU.1 [53] and OCT2 [54] and the up–regulation of T cell associated genes such as NOTCH1 and NOTCH2 [55, 56] stresses the great variety of transcription factor deregulation in cHL. Last but not least, recent publications indicate, that epigenetic silencing of B cell genes (e.g. CD19) and B cell atypical epigenetic modifications result in up–regulation of B cell inappropriate genes such as ID2 and CSF1R [46, 57] in cHL.

Gene	Type of alteration	Pathway	Frequency of cases with alterations(%)
REL	Gains, amplifications	NF-κB	50
NFKBIA	Point mutations, deletions	NF-κB	20
NFKBIE	Point mutations, deletions	NF-κB	15
TNFAIP3	Point mutations, deletions	NF-κB	40
BCL3	Gains, translocations	NF-κB	10
JAK2	Gains, amplifications	Jak-Stat	40
SOCS1	Point mutations, deletions	Jak-Stat	45
TP53	Point mutations, deletions	p53	10
MDM2	Gains	p53	60
CD95	Point mutations	FAS-mediated apoptosis	10

Table 1.2: Genetic lesions in cHL

In cHL, various major pathways involved in cellular decision-making processes have been identified to be deregulated. Often, genetic lesions play a pivotal role in their deregulation, however, as they never occur in 100% of cHL cases are just one of many important factors to consider. The table was adapted from [31].

Genetic lesions in cHL

In cHL, several major cellular pathways recurrently show genetic aberrations. Table 1.2 shows a short summary of those pathways and the pathway members, which have been shown to be prone to genetic lesions in cHL cases.

In case of NF-κB signaling, a whole set of different events has been identified over the past decades, all of which will lead to aberrantly activated NF-κB signaling . The same is the case for members of the Janus kinase–signal transducer and activator of transcription (Jak–Stat) signaling cascades. On the other hand, mutations of TP53 in cHL result in inhibition of TP53 induced apoptosis [58, 59, 60].

In summary, genetic lesions add to the pathologic deregulation of various transcription factor networks in cHL — taken together they are probably the major mechanisms contributing to cHL pathogenesis [31].

Role of Epstein Barr Virus (EBV) infection in cHL

Various cHL studies suggest that EBV infection may play a pivotal role in causing the onset of the disease: 40% of all cHL cases in Europe and the USA are EBV positive

and in developing countries even 90% of all cases show to be EBV positive [61, 62, 63]. Moreover, a number of population based studies propose a statistically significant relation of an EBV infection followed by infectious mononucleosis with the onset of cHL [64, 65, 66]. Although different mechanisms have been revealed, that show how EBV encoded proteins contribute to the pathogenetic mechanisms of cHL, the significance of their role is still not completely understood [31] — when comparing EBV positive cases to EBV negative cases, the EBV associated expression pattern is quite restricted and some essential pathogenic mechanisms — for example deregulated NF-κB activity — in terms of magnitude show no significant difference in between EBV positive and EBV negative cHL cases (though mechanistically there presumably is a difference in deregulation of NF-κB activity, as in EBV negative cases frequent mutations of the inhibitor of NF-κB activity, NFKBIA were detected, which are not found in EBV positive cases [67]). On the other hand EBV encoded proteins can replace pathogenetic mechanisms found in EBV negative cHL cases [68, 69, 70, 71]. Additionally, one EBV protein called latent membrane proteine 2A (LMP2A) migth play a pivotal role in EBV positive cHL pathogenesis — gene expression of B cells from LMP2A transgenic mice and ectopic LMP2A expression in human B cell lines resulted in alterations of gene expression similar to those found in HRS cells [72]. Recently, it was also shown, that LMP2A may constitutively activate the NOTCH1 pathway to autoregulate the LMP2A promoter and takes advantage of the NOTCH1 signaling system to alter levels of B cell specific transcription factors such as E2A and EBF [73].

1.1.5 Is NOTCH signaling deregulated in cHL?

Apart from playing a putative role in EBV associated cHL as mentioned above, data from other studies indicate that the NOTCH signaling pathway itself may be deregulated in cHL. NOTCH1 [56, 74] and NOTCH2 [56, 55] have been shown to be expressed in

HRS cells and it is assumed, that these receptors may be activated through cells in the microenvironment of the tumor, that express according NOTCH receptor ligands [31]. So far, no study provided *in vivo* evidence, that activation of the NOTCH signaling pathway indeed is mediated through the microenvironment. This hypothesis is thus still an assumption needing further clarification. However, a number of *in vitro* studies show that:

- ectopic stimulation of the HRS cell lines with JAG1 expressing HtTA-jag10 cells results in accelerated proliferation of HRS cells and up–regulation of the NOTCH target gene *HES1* [56]
- knockdown of NOTCH1 using siRNA results in the regulation of B lineage genes formerly lost / down-regulated in HRS cell lines (up-regulation of e.g. EBF1, E2A and CD79a, down-regulation of ABF1 [74] and GATA3 [75])
- *JAG1* mRNA is expressed in primary cHL cases [56]
- L428 HRS cells transduced with a tamoxifen-inducable NOTCH1 intracellular domain (NIC1) viral construct show growth inhibition [76]

Whereas these data give some indication that NOTCH signaling may be deregulated in a manner advantageous for cHL (though this is contradicted by the findings of Zweidler-McKay *et al.* [76] mentioned above), numerous points of this particular pathway and according questions had still to be answered:

- *Is the NOTCH signaling system deregulated in a global and systemic manner in cHL, i.e. is there a cHL specific NOTCH signature — if yes, why and how is it deregulated?*
- If a cHL NOTCH signature exists, is it dominated by a limited number of factors?

- What is the status of all genes associated with NOTCH signaling in cHL – is a significant number of them deregulated in any manner?
- Is the NOTCH signaling system possibly activated in a cell-autonomous manner in cHL?
- Are there cHL specific NOTCH target genes?

In the following part, an introduction on NOTCH signaling is provided as to give an overview on the complexity of this pathway. It shall also enable the reader to judge its possible impact on cHL pathogenesis.

1.2 Introduction to NOTCH signaling

The NOTCH signaling pathway is one of the most conserved and essential ones for a large number of cellular decision processes made in cellular differentiation and cell-cell communication [77]. This pathway was named after a X-linked, dominant Drosophila mutation, first found around 1916 by Mohr, Morgan and Bridges [78]. These mutants exhibited irregular notches of missing tissue at their wing blades. In 1940, Poulson found, that a complete loss of NOTCH gene activity caused lethal hyperplasia of the embryonic nervous system, indicating that this pathway plays a pivotal role in cellular differentiation [79].

In context of the hematopoetic compartment, NOTCH is involved in many processes as for example stem cell development [80, 81, 82, 83, 84], T cell differentiation [85, 86, 87, 88], marginal zone B cell development [89, 90, 91, 92] and various malignancies (see also section 1.2.2). The last decades have brought forward much data on NOTCH signaling in *Mammalia* and NOTCH signaling is much better understood nowadays. Yet, the growing number of players involved build up a very complex signaling network in which

it is quite difficult to link a specific input to a specific output as this is largely determined by a vast number of parameters and their concentration-, activity- and time-dynamics.

1.2.1 Core components of the NOTCH signaling cascade

In *Mammalia*, there are four types of proteins that compose the core components of the NOTCH signaling pathway:

- the NOTCH receptors NOTCH1, NOTCH2, NOTCH3, NOTCH4
- the co-activators of the Mastermind-like family (MAML1, MAML2, MAML3)
- the canonical NOTCH ligands, JAG1, JAG2, DLL1, DLL3 and DLL4
- the transcription factor CSL

The NOTCH receptors

In *Mammalia*, 4 NOTCH receptors have been identified so far. They are single-pass transmembrane proteins. The extracellular domain of either receptor protein is composed of 29-36 epidermal growth factor (EGF) repeats, of which especially EGF repeats number 11 and 12 are important for ligand binding [93]. The EGF repeats are followed by three cystein-rich LIN domains which prevent ligand independent activation, and the heterodimerization domain (HD). The NOTCH intracellular domain (NIC) possesses one to two nuclear localization signals and is composed of a RAM domain followed by six ankyrin repeats. These are important for binding to the transcription factor CSL. Finally, the cytoplasmatic domain contains — in case of NOTCH1 and NOTCH2 — a transactivation domain and all receptors possess a PEST domain important for proteasome-mediated degradation [77].

The Mastermind-like family of NOTCH co-activators

The first member of the human Mastermind-like family, MAML1, was identified by Wu *et al.* in 2000 [94], the other two known members, MAML2 and MAML3, were first described in 2002 independently by two groups [95, 96]. These proteins are human homologues of *Drosophila* Mastermind. The family members share high amino acid identity among each other, compared to MAML1, MAML2 has 45% and MAML3 has 34% identical amino acids [96]. All human MAML proteins share the same domain structure which is composed of a N-terminal binding domain (mediating binding to NIC and the transcription factor CSL) followed by two transactivation domains. MAML proteins are essential for the formation of a transcriptionally active NOTCH transcriptional complex (NTC) [97]. They activate NOTCH signaling with different potentials. As shown in [95], MAML2 has the highest potential to activate the NTC mediated transcription of the NOTCH target gene *HES1*. At the same time MAML proteins may also play a role in the degradation of the NTC, as MAML1 has been shown to recruit CDK8 which in turn phosphorylates NIC and thereby may coordinate NTC turnover [98]. In how far different MAML members may contribute to fine-tuning of NOTCH signaling is still at large, yet a recent study provides evidence, that the potential of MAML proteins to activate NOTCH signaling in general is in turn modified through SUMOilation [99].

In terms of their biological functions, recent studies have brought forward much data, indicating that MAML proteins are especially important and essential for lymphoid cell fate decisions [100, 101, 92]. Interestingly, MAML proteins are also involved in various other signaling pathways such as NF-κB and p53 (see for example [102, 103]) and — in case of MAML2 — have been shown to be a potent oncogenic inducer when aberrantly fused to TORC1 or MECTC1 by translocation [104, 105].

Canonical NOTCH ligands

The five conventional NOTCH ligands all contain EGF repeat domains and an amino-terminal domain called DSL (Delta, Serrate, and Lag-2). This domain is highly conserved among species and involved in NOTCH receptor binding. In case of JAG1 and JAG2 there is an additional cystein rich domain adjacent to the plasma membrane. In terms of functionality, one study indicates, that JAG1 expression is essential for the generation of hematopoietic cells in the aorta-gonad mesonephros [106]. This study also linked JAG1 expression to NOTCH1 mediated expression of the transcription factors GATA2 and RUNX1. JAG2, DLL1 and DLL4 have also been shown to be important in the process of differentiation of $CD34^+$ cord blood hematopoetic progenitor cells to Natural killer cells [107].

The transcription factor CSL

CSL (CBF1, Su(H) and LAG-1) is the key transducer of the NOTCH signaling pathway. It is a transcription factor sharing similarity with the Rel family of transcription factors, yet differs from Rel in that it contains a β-trefoil domain in between two Rel-homology domains. The β-trefoil domain contains a hydrophobic pocket that probably mediates interaction with NIC [93]. So far, four splice variants of CSL have been deposited in public databases (see e.g. http://www.ncbi.nlm.nih.gov/gene/).

NOTCH — from translation to activation

In canonical NOTCH signaling, each combination of one of each of the four protein-types described above comprises the essential components for the assembly of a transcriptionally active NTC – all other proteins necessary for transcriptional activation belong to the basic transcription machinery of a cell (e.g. CREBBP and EP300) and are not specific for the NOTCH transcriptional activation. After translation of the NOTCH receptors

the ≈300 kDa sized proteins are cleaved by furin-like convertases [108] (S1-cleavage) into two parts which are then re-assembled as a heterodimer. This heterodimer then translocates to the cellular membrane. Upon receptor-ligand interaction, the next — S2-cleavage called — step is mediated by ADAM metalloproteases and results in truncation of the extracellular domain of the NOTCH receptor (called NOTCH^{TM}). At that time, the receptor is still membrane-bound yet accessible for the final S3-cleavage step. This step is mediated by the γ-secretase complex and will result in the release of the NOTCH intracellular domain (NIC). NIC shuttles to the nucleus where it binds to CSL (an otherwise repressive transcription factor that is quasi-statically bound to DNA in complex with various co-repressors such as NCOR2). Thereby a dual binding interface is formed, to which Mastermind-like family members may bind. This complex consisting of DNA/CSL/NIC/MAML is the essential NTC-assembly necessary for transcriptional activation. Figure 1.3 shows, how the S2 and S3 cleavage steps of a NOTCH receptor will result in the cell-contact mediated activation of the pathway.

NOTCH transcriptional activation — adding to the complexity

A vast number of proteins and processes influence NTC dependent transcription. For example, the presence, number and spatial orientation of CSL binding sites has a major impact on the magnitude of the transcriptional read-out mediated by NOTCH signaling [111]. Additionally, it is not yet understood, in how far ligand-receptor interactions are integrated to an intracellular message. This is a complex, concentration dependent process, that recently has been mathematically modeled for DLL1-NOTCH1 mediated NTC activation [112].

Apart from that, many other mechanisms influence NOTCH activation at other parts of the signaling cascade. For example the ubiquitylation status of ligands which is determined by E3 ubiquitin ligases such as NEURL and MIB1 plays an important role [113, 114, 115, 116, 117] as does the glycosylation status of the NOTCH receptors (de-

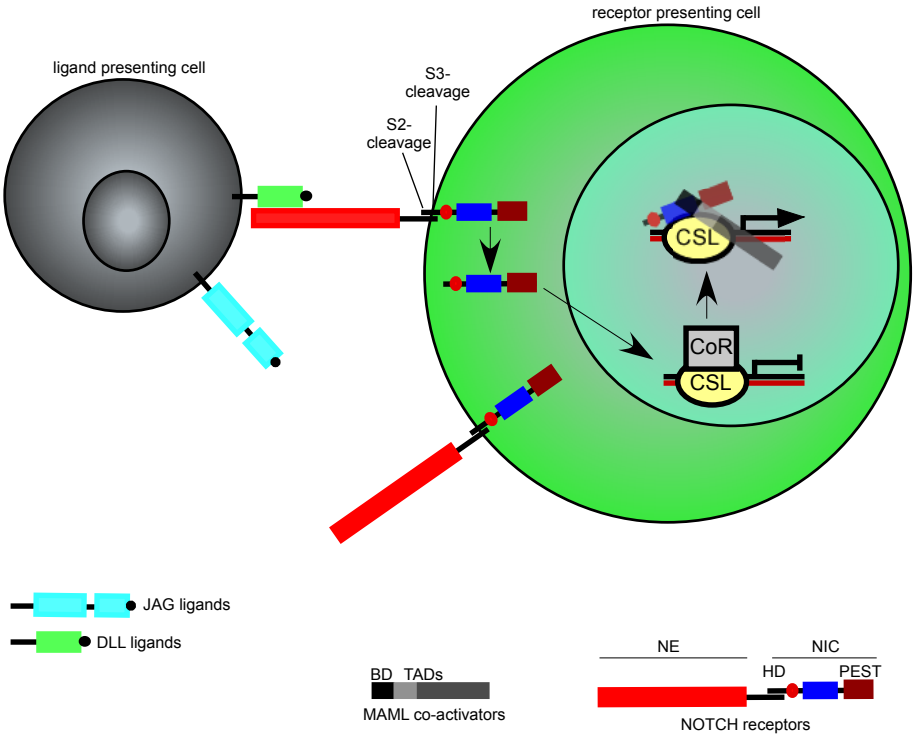

Figure 1.3: Activation of NOTCH signaling

Shown is a simplified scheme of NOTCH transcriptional activation. Note, that various other molecules such as glycosyl transferases and ring finger E3 ligases play important roles in tuning the NOTCH activation potential. For a thorough description of these proteins in regard to NOTCH signaling please refer to [93]. However, this scheme shows all proteins and steps that are absolutely essential for NOTCH transcriptional activation.
When NOTCH signaling is not activated, the repressive transcription factor CSL is bound to DNA and recruits various co-repressors (CoR). In this state, no transcription is possible from CSL-binding sites. As soon as the NOTCH receptors are translated, a first cleavage step (S1, not shown) will result in the production of two parts of the receptor. This step is done by furin-like convertases and takes place in the *trans*-Golgi compartment [108]. The NOTCH extracellular domain (NE) and the NOTCH intracellular domain (NIC) are assembled to form a singlepass, transmembrane recptor. Upon ligand binding, ADAM proteases will mediate S2 cleavage (resulting in the cleavage product NOTCH^{TM}), which is then followed by γ-secretase complex-mediated S3 cleavage. This results in the release of NIC which may then translocate to the nucleus (NIC possesses nuclear localization sequences [109, 110]). There it displaces the CoRs, binds to CSL, thereby forming a dual binding-interface for binding of the co-activators of the Mastermind-like family (MAML). Binding of MAML proteins occurs via their binding domain (BD), whereas their transcriptional activation is mediated through two trans-activation domains (TADs). The now formed complex can then recruit standard proteins involved in transcription (e.g. EP300) and will activate transcription from CSL binding sites. Note, that the magnitude of transcriptional activation also depends on the number and spatial positioning of CSL binding sites in immediate proximity to each other [111]. HD, heterodimerization domain; PEST, proline, glutamate, serine and threonine enriched domain.

termined by various glycosyl transferases of the fringe family, such as LFNG and MFNG [118, 119, 120, 121, 122]) and their ubiquitination (modified by the protein NUMB [123], which thereby inhibits NOTCH signaling). Moreover a recent study indicates that Nemo-like kinase physically modulates NOTCH signaling by interfering with the formation of the NOTCH transcriptional complex [124].
In turn all these NTC modifying molecules are regulated themselves, making it obvious that complete understanding of the complexity of the regulation of NOTCH signaling and the prediction of its dynamics are still far away.

1.2.2 Pathological deregulation of the NOTCH signaling pathway

Due to its involvement in decisive steps of cellular life, NOTCH signaling has to be controlled and fine-tuned in a very sophisticated and tightly controlled manner. Any deregulation of this pathway most probably results in severe effects leading to pathogenic events. Numerous diseases are associated with deregulated NOTCH signaling [77]. For example there are implications of pathologically deregulated NOTCH signaling in Alagille syndrome (a developmental disorder partly caused by mutations of NOTCH2 [125]), ovarian cancer (in a significant number of cases the NOTCH3 gene is amplified [126]), breast cancer (associated with the impaired NOTCH-inhibition mediated through NUMB [127]) and T cell acute lymphoblastic leukemia (T-ALL) [128].

In human cancers, T-ALL is best examined in regard to the mechanisms leading to pathologically deregulated NOTCH signaling. Two major mechanisms have been elucidated, that are responsible for aberrant NOTCH activation as found in T-ALL:

- Mutations within the NOTCH receptor, that may lead to ligand independent, facilitated cleavage of the receptor. These mutations are usually found in the NOTCH heterodimerization domain. Additionally, NOTCH mutations of the PEST domain are frequently found, these may impair turn-over of cleaved NOTCH and

thus increase its half-life [129]. Both types of mutations are found in around 50% of T-ALL cases [128].

- Mutations or deletions of ubiquitin ligases that mediate the turn over of the NOTCH transcriptional complex — e.g. FBXW7 — this results in increased half-life of the NTC [130].

Yet, exactly these two mechanisms diminish treatment possibilities of deregulated NOTCH signaling with γ-secretase inhibitors (GSIs) such as compound E or DAPT. GSIs target the NOTCH signaling cascade by inhibiting the S3 cleavage step through a variety of mechanisms and were originally developed for the treatment of Alzheimer's Disease (AD) in which deregulated γ-secretase activity presumably contributes to pathogenesis [131]. Though effective when NOTCH signaling is deregulated by for example NOTCH gene amplification these compounds are ineffective when NOTCH deregulation is mediated by mechanisms independent of γ-secretase mediated S3 cleavage. Nevertheless, for NOTCH-associated disease entities in which this is not the case, GSI usage may be an option. Recent clinical trials report, that there are no severe side effects or acute toxicities associated with treatment using GSIs [132, 133]. However, for malignancies with mechanisms rendering NOTCH activation independent of S3-cleavage, new therapeutic strategies will have to be developed.

1.3 Aim of this work

As mentioned above, at the beginning of this study a number of very relevant questions regarding the actual role of the NOTCH signaling system in Hodgkin lymphoma had not been satisfyingly answered. Hence, this study aimed to determine and describe the general and cell–biological characteristics of the NOTCH signaling system in cHL in a holistic fashion. The major working hypothesis was summarized as follows:

If the NOTCH signaling system is pathologically deregulated in classical Hodgkin lymphoma, this must result in and/or must be the result of the deregulation of a statistically and biologically significant number of NOTCH associated genes.

Accordingly, one would assume, that classical Hodgkin lymphoma should be characterized by a specific NOTCH signaling system signature, specifiable by quantifying mRNA or protein levels of all NOTCH associated genes. One would moreover assume, that experimental perturbation of the NOTCH signaling system in cHL should result in significant cell–biological effects.

Ergo, a holistic specification and definition of the NOTCH signaling system is the prerequisite for the systemic understanding of its role in cHL.

2 Materials and Methods

2.1 Materials

2.1.1 Antibiotics

The following antibiotics used for bacteria cultures were purchased from Sigma Aldrich and applied at the stated concentrations:

- Ampicillin (50 μg/ml)
- Kanamycin (30 μg/ml)
- Tetracyclin (12.5 μg/ml)

As additive in *mammalian* cell culture, Penicillin (10.000 Units/ml) and Streptomycin (10 mg/ml) were purchased from PAA Laboratories solved in 0.9% NaCl-H_2O.

2.1.2 Antibodies used for Western Blotting

Antibody	*Product number, Supplier*
β-actin	A5441, Sigma Aldrich
CD19	R0808, Dako
CD3	R0810, Dako
FLAG-tag	F3165, Sigma Aldrich
GFP	BA-0702, Vector Laboratories
MAML1	4608, Cell Signaling
MAML2	4618, Cell Signaling
MAML3	NB100-2129, Novus Biologicals
MYC-tag	46-0603, Invitrogen
cleaved NOTCH1	2421, Cell Signaling
NOTCH1	N6786, Sigma Aldrich
NOTCH2	clone C651.6DbHN, Developmental Studies Hybridoma Bank,

	University of Iowa
NOTCH3	34465, Cell Signaling
NOTCH4	2423, Cell Signaling
PARP1	sc-8007, Santa Cruz Biotechnology

2.1.3 Buffers

Where applicable, pH of a buffer was measured using a pH-meter.

1l of*Phosphate buffer pH 7.0* was prepared by mixing 39 ml of 0.1 M $K4_2HPO_4$ and 61 mL of 0.1 M KH_2PO_4 and addition of 900 ml H_2O.

10× *Phosphate buffered saline (PBS) stock solution* was prepared by dissolving 80 g/l NaCl, 2 g/l KCl, 26.8 g/l Na_2HPO_4-$7H_2O$ and 2.4 g/l KH_2PO_4 in double distilled H_2O. The pH was adjusted to 7.4 by adding HCl. Buffer was autoclaved before usage.

10× *Tris Borat EDTA (TBE) stock solution* were prepared by dissolving 108 g/l Tris, 55 g/l Boric acid in H_2O and addition of 40 ml/l Na_2EDTA pH 8.0.

1 M *Tris-HCL stock solution* was prepared by dissolving 121.14 g/l Tris in double distilled H_2O. The desired pH was adjusted by adding concentrated HCl. Buffer was autoclaved before usage.

High Salt Lysis (HSL) buffer: 20 mM HEPES pH 7.9, 350 mM NaCl,1 mM $MgCl_2$, 0.5 mM EDTA pH 8.0, 0.1 mM EGTA pH 7.6, 1% (v/v) Nonidet P-40. A protease inhibitor cocktail was added just before usage: 1 pill/10 ml HSL buffer Complete, Mini Protease Inhibitor Cocktail and NaF and Na_3VO_4 to final concentrations of 1 mM each.

Buffers for extraction of nuclear proteins:

- Buffer A: 10 mM HEPES pH 7.9, 10 mM KCl, 0.1 mM EDTA pH 8.0, 0.1 mM EGTA pH 7.6, 1 mM DTT. A protease inhibitor cocktail was added just before usage: 1 pill/10 ml buffer Complete, Mini Protease Inhibitor Cocktail and NaF and Na_3VO_4 to final concentrations of 1 mM each.
- Buffer C: 20 mM HEPES pH 7.9, 0.4 M NaCl, 1 mM EDTA pH 8.0, 1 mM EGTA pH 7.6, 1 mM DTT, 20% glycerol (v/v). A protease inhibitor cocktail was added just before usage: 1 pill/10 ml buffer Complete, Mini Protease Inhibitor Cocktail and NaF and Na_3VO_4 to final concentrations of 1 mM each.

Shift-buffer for CSL EMSA: 40 mM HEPES pH 7.9, 100 mM KCl, 5 mM EDTA pH 8.0, 16 mM $MgCl_2$, 10 mM Spermidine, 35 μg/ml Poly(dI-dC), 500 μg/ml BSA, 0.05% (v/v) Nonidet P-40, 30% glycerol (v/v), 8% Ficoll 400.000 (w/v).

SDS-PAGE sample buffer: 10% SDS (w/v), 10 mM DTT, 20% glycerol (v/v), 0.2 M Tris-HCl pH 6.8, 0.05% bromphenol blue (w/v).

SDS-PAGE running buffer: 25 mM Tris-HCl pH 8.3, 200 mM Glycine, 0.1% SDS (w/v).

Western blot transfer buffer: 25 mM Tris, 192 mM glycine, 10% MeOH.

1× TBS buffer: 150 mM NaCl, 7.7 mM Tris-HCl pH 7.5.

2.1.4 Chemicals

Chemical	*Supplier*
Agarose	ROTH
Acrylamide/Bis-solution 40%	ROTH
$CaCl_2$	Sigma Aldrich
bacto-tryptone	ROTH
bacto-yeast	ROTH
β-Mercapthoethanol	ROTH
bovine serum albumin (BSA) fraction V	ROTH
bromphenol blue	Sigma Aldrich
DMSO	ROTH
DTT	ROTH
EDTA	Sigma Aldrich
EtOH	MDC Distillery
Ficoll	PAA laboratories
Glycerol	Sigma Aldrich
HCl	ROTH
HEPES	ROTH
Imidazol	MERCK
IPTG	Roche
KCl	Sigma Aldrich
MeOH	ROTH
Milkpowder	Kaufland
Na_2HPO_4	Sigma Aldrich
Na_3VO_4	ROTH
NaCl	Sigma Aldrich
NaF	Sigma Aldrich
NaH_2PO_4	Sigma Aldrich
NaOH	Sigma Aldrich
Nonidet P-40	Roche
Poly(dI-dC) acid sodium salt	Roche
RbCl	Sigma Aldrich
Sodium-dodecyl-sulfate	ROTH
Spermidine	Sigma Aldrich
TEMED	ROTH
Tris	Sigma Aldrich
Triton X 100	Roche

2.1.5 Consumables

Consumable	*Supplier*
^{3}H-thymidine	New England Biolabs
^{32}P-dCTP	New England Biolabs
4 mm electroporation cuevettes	Invitrogen
BCA Protein Assay	Pierce
Complete, Mini; Protease Inhibitor Cocktail	Roche
dNTPs	Fermentas
DreamTaq™ and additives	Fermentas
Falcons	FalCon GmbH
HG-U133 Plus 2.0	Affymetrix
MicroBeads (CD19 and CD3)	Miltenyi Biotec
MACS cell seperation columns	Miltenyi Biotec
Optical 96-well plates	Thermo Scientific
Power SYBR® Green	Applied Biosystems
Prescission-protease	GE Healthcare
Reaction tubes / tips	Eppendorf
Smart Pool siRNA (MAML2 /control)	Thermo Scientific
Nitrocellulose membrane	Whatman
Quick Spin Columns Sephadex G50 fine	Roche

2.1.6 Kits

Product	*Supplier*
Dual-luciferase Kit	Promega
First strand cDNA synthesis kit	Roche
Invisorb Spin Plasmid Mini	Invitek
Invisorb Plasmid Maxi Kit	Invitek
Invisorb Spin Dna Extraction	Invitek
RNeasy Mini Kit	Qiagen

2.1.7 Machines

Machine	*Supplier*
ABI StepOnePlus	Applied Biosystems
ÄTKA-FPLC system	Amersham Biosciences
ÄTKA*prime* fraction collector	Amersham Biosciences
Beckman counter	Beckman Coulter
FACSAria™III	BD Biosciences

FACSCanto™II	BD Biosciences
Eppendorf Mastercycler gradient	Eppendorf
Gene-Pulser II	BioRad
HP xw4600 workstation	HP
MicroCal VP-ITC	GE Healthcare
Mithras LB940 Luminometer	Berthold Detection Systems
Nanodrop ND-100	Peqlab

2.1.8 Media for bacteria culture

Lysogeny broth (LB): 10 g/l bacto-tryptone, 5 g/l bacto-yeast extract, 10 g/l NaCl.
Terrific broth (TB): 12 g/l Bacto-tryptone, 24 g/l bacto-yeast extract, 2,13 g/l KH_2PO_4, 12,54 g/l K_2HPO_4.
Media were autoclaved before usage. Appropriate antibiotics were added after autoclaving.

2.1.9 Media for eukaryotic cell culture

Product	*Supplier*
RPMI1640	Invitrogen
Opti-MEM® I	Invitrogen
GlutaMAX®	Invitrogen

2.1.10 Software

Software	*Supplier*
Bioconductor 2.5	http://www.bioconductor.org
Canvas X	AOD Systems
EndNote X2	Thomson Cooperation
JAVA GSEA implementation	http://www.broadinstitute.org/gsea/
MiKTeX 2.8	http://miktex.org/
R 2.10	www.r-project.org
SigmaPlot 9.0	SysStat Software Inc
UCSF Chimera 1.4.1	http://www.cgl.ucsf.edu/chimera/

2.1.11 Used vector-backbones

Product	*Supplier*
pEGFP-N3	Clontech
pcDNA3.1(+)	Invitrogen
pcDNA3.1/V5-His	Invitrogen

pGL2	Promega
pGEM-TEasy	Promega
pCMV-Myc	Clontech
pSuper	Brummelkamp *et al.*
pSKB2LNB	Daumke *et al.*

2.2 Methods

2.2.1 Cell lines and culture conditions

cHL (L428, L1236, KM-H2, L591, HDLM-2, L540, L540Cy), pro-B lymphoblastic leukemia (Reh), Burkitt's lymphoma (Namalwa, BL-60, BJAB), diffuse large B-cell lymphoma (DLBCL, SU-DHL-4), T lymphoblastic lymphoma (SUP-T1), T cell acute lymphoblastic leukemia (ALL-SIL) and HEK293 cells were cultured at 37°C, 5% CO_2 in RPMI1640 supplemented with Penicillin (100 Units/ml), Streptomycin (0.1 mg/ml), sodium pyruvate (0.11 g/l) and L-Glutamine (2 mM).

2.2.2 Electrophoretic Mobility Shift Assay (EMSA) for NTC assembly monitoring

CSL EMSA was performed using the high-affinity CSL binding site (described previously [134]) from the HES1 promoter using the following oligonucleotides (overhang for labeling in small letters, binding sequence in capitals):

sense	5'-gatcCTAGGTTACTGTGGGAAAGAAAGTCC-3'
antisense	5'-gatcGGACTTTCTTTCCCACAGTAACCTAG-3'

As for the shift buffer, see section 2.1.3 for the complete buffer composition. 0.33μg/μl of each oligonucleotide were dissolved in annealing buffer (10×-annealing buffer: 500 mM TRIS-HCL pH 8.0, 700 mM NaCl in H_2O) and then annealed by incubating the mixture

at 95°C for 20 min and slow cooling down to room temperature. Labeling of the annealed oligonucleotides was done with ^{32}P-dCTP, a final oligonucleotide concentration of 10 ng/μl, Klenow enzyme (6U), a final concentration of 360 nM of each dATP, dGTP and dTTP and the appropriate Klenow-buffer. The labeling mixture was incubated at 37°C for 30 min and then purified using Quick Spin Columns Sephadex G50 fine for radiolabeled DNA Purification. EMSAs were performed with 5 μg of nuclear extracts on non-denaturing, 5% polyacrylamide gels using 1×TBE pH 8.3 as buffer.

For preparation of nuclear extracts for CSL EMSAs, HEK293 were transfected with different combinations of 10 μg Myc-tagged CSL, 10 μg Flag-tagged ICN1, 20 μg MAML1, 40 μg DnMAML1-pEGFP AA 13-74, 40 μg DnMAML1-pEGFP AA 13-50, 70 μg of DnMAML1-pEGFP AA 19-35, and total DNA amount was adjusted with empty plasmid. Cells were harvested after 48 hours.

2.2.3 Generation of plasmids and DNA constructs

MAML1 and MYC-CSL constructs were described before [95]. MAML2 was mobilized from the previously described MAML2-pEFBOS construct [96] by digestion with *Not*I and *Xho*I and cloned into pcDNA3.1(+). The DnMAML1-pEGFP amino acids (AA) 13-74 and the ICN1-pcDNA3.1 expression constructs as well as the Hes1-pGL2 reporter construct were described previously [135]. The truncated versions DnMAML1 AA 13-50 and AA 19-35 were cloned into pEGFP via *Hind*III and *Kpn*I restriction sites using HPLC grade oligonucleotides. Sequences for the shMAML2 constructs were selected based on siRNA sequences from the Dharmacon MAML2 ON-TARGETplus SMARTpool (L-013568-00, Dharmacon, Lafayette, CO). To generate shRNA expression constructs, the sequences (targeting sequence in bold, backbone sequence in normal)

- 5'-GATCCCC**GGACAAAGTCAGATTATGT**TTCAAGAGA**ACATAATCTGACTTTGTCC**TTTTTGGAAA-3'
- 5'-GATCCCC**CGAAAGTAATGGCTAACTA**TTCAAGAGA**TAGTTAGCCATTACTTTCG**TTTTTGGAAA-3'
- 5'-GATCCCC**AGACCAAATTTAACCCATA**TTCAAGAGA**TATGGGTTAAATTTGGTCT**TTTTTGGAAA-3'

were cloned via *Bgl*II and *Hind*III restriction sites into pSUPER using HPLC grade oligonucleotides. The scrambled shRNA construct has been previously described [136]. All constructs were verified by sequencing.

2.2.4 Immunohistochemistry (IHC)

IHC was kindly done by Prof. Dr. Anagnostopoulos and Dr. Jöhrens from the Institute of Pathology, Charité, Berlin. All cases were drawn from the files of the Consultation and Reference Center for Hematopathology at the Institute of Pathology, Campus Benjamin Franklin, Medical University Berlin. Diagnoses were established according to the WHO criteria. The primary antibody used was anti-MAML2 (see section 2.1.2). Bound antibodies were made visible using the streptavidin-biotin-alkaline phosphatase method and FastRed as chromogen (all from DakoCytomation, Glostrup, Denmark).

2.2.5 Isothermal Titration Calorimetry (ITC)

ITC measurements of concentration-dependent compound-protein binding were performed on a VP–ITC instrument from MicroCal. The injection syringe (500 μl volume) was loaded with a 100 μM solution of either compound. The calorimetry cell was loaded with purified human CSL at a concentration of 2 mg/ml in 20 mM phosphate buffer supplemented with a final concentration of 1 mM of BME. The protein solution was degassed before usage. After equilibration at the desired temperature, a series of 21 injections of 10 μl of the compound solution were done and the heat response was measured by the instrument using a power-compensation mechanism.

2.2.6 Isolation of primary lymphocytes

Primary $CD19^+$ B cells and $CD3^+$ T cells were isolated from human tonsils with CD19 or CD3 MicroBeads according to the manufacturer's recommendations. Purity of $CD19^+$

B and $CD3^+$ T cells was greater than 95%, as determined by staining of purified cells with CD19- and CD3-specific antibodies and subsequent FACS analysis.

The use of human material was approved by the local ethics committee of the Charité, and performed in accordance with the Declaration of Helsinki.

2.2.7 MAML2 knockdown and DnMAML1 based NOTCH inhibition experiments

Cells were transfected with 60 μg DnMAML1-pEGFP AA 13-74 fusion construct or 60 μg of pEGFP control plasmid, or with each 20 μg of three different shMAML2-pSuper based expression constructs or 60 μg of scrambled shRNA construct as control, both along with 10 μg of pEGFP. 48 hours after transfection, GFP^+ cells were enriched by FACS sorting and enriched cells were used for proliferation assays as well as RNA and protein extraction.

2.2.8 Preparation of whole-cell and nuclear extracts, SDS-PAGE and Western Blotting (WB)

Whole-cell extracts were prepared as follows:

1. cells were taken from culture flasks, centrifuged 5 min at 1200 ×g, RT, supernatant was decanted
2. cells were resuspended in PBS, centrifuged 5 min at 1200 ×g, RT, supernatant was decanted
3. cells were resuspended in an appropriate volume of HSL buffer and put on ice for 15 min
4. cell-suspension was centrifuged 5 min at 1200 ×g, 4°C, supernatant was transferred to a new reaction tube, protein concentration was determined using a standard BCA protein assay by measuring light absorption of the BCA-protein solution at 595 nm
5. proteins were put on liquid nitrogen and then stored at -80°C until usage

Nuclear extracts were prepared as follows:

1. cells were taken from culture flasks, centrifuged 5 min at 1200 ×g, RT, supernatant was decanted
2. cells were resuspended in PBS, centrifuged 5 min at 1200 ×g, RT, supernatant was decanted
3. cells were resuspended in an appropriate volume of nuclear buffer A and put on ice for 15 min
4. Nonidet P-40 was added to a final concentration of 1% (v/v) and cell suspesion was vortexted vigorously for 15 sec
5. cells centrifuged 5 min at 1200 ×g, 4°C, supernatant was decanted
6. nuclear pellets were resuspended in nuclear buffer C and put on ice for 15 min
7. nuclear pellet-suspension was centrifuged 5 min at 1200 ×g, 4°C, supernatant was transferred to a new reaction tube, protein concentration was determined using a standard BCA protein assay by measuring light absorption of the BCA-protein solution at 595 nm
8. proteins were put on liquid nitrogen and then stored at -80°C until usage

SDS-PAGE: For SDS-PAGE separation of proteins, polyacrylamide concentrations were used according to the size of the protein of interest, in case of MAML and NOTCH proteins the concentration was 7.5%. SDS-PAGE gels were put into the appropriate chamber and filled with SDS-PAGE running buffer. Protein samples were incubated at 95°C for 5 min prior to application on the SDS-PAGE gel. SDS-PAGE were run at 80-120 V.

Western blot analyses: SDS-PAGE gels were transferred to a nitrocellulose membrane and then put into the appropriate blotting chamber which was filled with WB transfer buffer. For large proteins like MAML and NOTCH members, wet-blotting was used (100 V at 4°C for 2 hours), for smaller proteins semi-dry blotting was used instead (20 V at RT for 45 min). Western blots were developed using 1× TBS buffer supplemented with 10 g/l skim milk powder and 0.1% Triton X-100 (v/v).

2.2.9 Proliferation assays

24 hours before proliferation assay set up, cells were diluted to ≈ 100000-400000 cells/ml. At the day of assay set up, cells were diluted to 50000 cells/ml and 200 μl of cell suspension were put into the wells of a 96 well plate (each sample was pipetted and measured in quadruplicates). 24 hours before the desired time of measurement each cell-containing well was pulsed with [^{3}-H]-thymidine to a final concentration of 1 μCi/ml. Cells were harvested and [^{3}-H]-thymidine incorporation measured 24 hours after pulsing.

2.2.10 Reporter assays

For measurement of luciferase activity, HEK293 and SUP-T1 cells were transfected with 10 μg of the Hes1-pGL2 promotor construct and 100 ng pRL-TKLuc as an internal control. Where indicated, cells were cotransfected with 5 μg Flag-tagged ICN1, 30 μg (HEK293) or 60 μg (SUP-T1) MAML2 expression constructs or both. Equal DNA loads were achieved by adding according amounts of empty plasmid. For assaying the functional activity of MAML1-based peptide-pEGFP constructs, SUP-T1 cells were co–transfected with 80 μg of either pEGFP, or the various DnMAML1-pEGFP constructs, as indicated, along with 10 μg of the Hes1-pGL2 promotor construct and 100 ng pRL-TKLuc as an internal control. 48 hours after transfection, cells were lysed and the ratio of the two luciferases was determined.

2.2.11 RNA preparation, semi-quantitative (sqPCR)and quantitative PCR (qPCR) analyses

Total RNA was extracted from cells using the Qiagen RNeasy Mini Kit according to the manufacturer's recommendations. Upon completion of the process, RNA was shock-frozen in liquid Nitrogen. cDNA first strand synthesis was performed using the Roche

1^{st} Strand cDNA Synthesis Kit according to the manufacturer's recommendations using oligo-dT primers and 1 μg of total RNA, whenever there was no amount-limitation. If there was an amount-limitation, total RNA amounts used were adjusted to the sample with the lowest RNA concentration.

Primer sequences used in sqPCR and qPCR are listed in table 2.1. sqPCR were performed as standard two-step program (annealing and elongation in two different temperature steps). qPCR analyses were performed using Power SYBR® Green Mastermix and the ABI StepOnePlus real-time PCR system in a one-step procedure (annealing and elongation at one temperature). Relative quantities were calculated using the $2^{-\Delta\Delta Ct}$ method taking into account the according primer efficiencies. For primer efficiency determination, CT values for five different cDNA concentrations were measured and then fitted according to the simple linear model:

$$\mathrm{CT}_i = \mathrm{a}_i + \mathrm{x}_i \times \log_{10} \mathrm{c} + \epsilon_i$$

where a_i is the y-intercept of the model for primer pair i, x_i the slope-estimator, c the concentration and ϵ_i the error of the model for each primer pair i. The efficiency E was then calculated from the slope-estimator:

$$\mathrm{E} = -1 + 10^{-1/x_i}$$

All PCR products were verified by sequencing.

Table 2.1: Primers used for sq- and qPCR

Name	PCR type	Forward primer (5'-3')	Reverse primer (5'-3')	Product size (bp)
CSL	sq	GTTGAATGGCGGTGGGGACGT	CAGCACTTGCAGGGAGACAACGG	575
GAPDH	sq	ATGCTGGCGCTGAGTAC	TGAGTCCTTCCACGATAC	257
MAML1	sq	CGAGCAGAACTCCCTGTTTC	CCCTGTGAACTGTCCAACCT	414
MAML2	sq	TGCAGGAATGGGATACCAAG	TGCCAAAGCCTGGTTAGAGT	399
MAML3	sq	CCTGAGCGAAGACCAGAAAC	TGGCTTCTTACGGCTGCTAT	461
HEY1	sq	TCATTTGGAGTGTTGGTGGA	CCAGTTCAGTGGAGGTCGTT	399
HES7	sq	GCGGGTGAGATGTGGTCTAT	GTTCGAATCCCACCAGAGTC	451
GAPDH	q	CTCTGCTCCTCCTGTTCGAC	TTAAAAGCAGCCCTGGTGAC	144
HES7	q	TACTCTCTCTGCCCCTCAGC	GACGTCGAGATAAAGGCAGG	119
HEY1	q	CGAGGTGGAGAAGGAGAGTG	TCGGCGCTTCTCAATTATTC	127
MAML1	q	CACTCCCATGTCAGATGACTTGCAC	GGGTCTCACCCTGTGCTTACCA	198
MAML2	q	ACATTTGTCAAGGCCACCTC	GTTTGCCAAAGCCTGGTTAG	125
MAML3	q	AAGCCCAGGGACCGAGGCAA	GCAGCCTTGGAGGGGCTTGG	160
NOTCH1	q	CCAGCTCGTCCCCGCATTCC	GCGCGCCGTTTACTTGAAGGC	115
NOTCH2	q	GGGGACCCTGTCATACCCTCTTGTG	TCCCACTGGCTCACGACGCT	225
NOTCH3	q	ABI Taqman # Hs01128541_m1	ABI Taqman # Hs01128541_m1	81
NOTCH4	q	TCCGTAGCAGACAAACTGCAGTGG	CTTTATCGGCTCCGGCCTGGAG	221
JAG1	q	CAATAGGATGGGCTTCTGTGCCCAG	TGCAGCAGATCACCTGCCTGTCT	209
JAG2	q	TGAGTGTGAAGGGAAGCCATGCC	TGCCCGCGACAGTCGTTGAC	128
DLL1	q	TCGTCAACAAGAAGGGGCTGCTG	TCGGGCAGACTGAAGGAGTCGAC	192
DLL3	q	CCGACTCCGCCAGAGCTTTTCC	GCAGAGACTGGGCACCACCGA	176
DLL4	q	GTCTCCACGCCGGTATTGGGC	CCGGTAAGAGTAGCGCAGCCTTG	281

sq, semi-quantative; q, quantitative

2.2.12 Size exclusion chromatography (SEC)

SEC was performed using 20 mM phosphate buffer pH 7.0 with a Sephadex G-200 column and the ÄKTA-FPLC system with an ÄKTA*prime* fraction collector. Buffers were filtered and degassed before usage.

2.2.13 Statistical analyses of experimental and microarray data

All statistical analyses were done in R v2.9.1 (http://www.r-project.org/)[137]). Independent Student's t-test was used to analyze data from proliferation- or real-time PCR-experiments. For analyses of luciferase assays, one way analysis of variance (ANOVA) was done before applying Tukey's Honestly Significant Differences test with 95% family-wise confidence level.

For microarray analysis of the various cell lines, RNA processing and hybridization to Affymetrix Human Genome U133 Plus 2.0 arrays were performed according to the manufacturer's recommendation. Raw microarray data was processed using the Bioconductor v2.4 framework [138]. RMA background correction and quantile normalization were applied. The LIMMA package was used for fitting gene-wise linear models and to calculate moderate t- and F-statistics for determination of significantly differentially expressed genes [139]. Fisher's Exact test was used for testing significance of deregulation of the NOTCH gene set. Unrotated principal component (PC) analysis was applied for analysis of intensity values of NOTCH associated genes. Gene set enrichment analysis (GSEA) was done as described in [140], ranking array-features according to their signal to noise ratio defined by:

$$\text{ratio}_i = \frac{\mu_A - \mu_B}{\sigma_A^2 + \sigma_B^2}$$

where μ_i is the average intensity of anyone feature in the biological groups and σ_i^2 the standard deviation of the intensity of anyone feature in the according biological group.

Microarray data are available through Gene Expression Omnibus accession number GSE20011.

2.2.14 Transfection of mammalian cells

24 hours before transfection, cells were diluted to ≈ 100000-400000 cells/ml. Cells were electroporated in OPTI-MEM I using a Gene-Pulser II with 950 μF and 0.18 kV (L428, HEK293), 500 μF and 0.3 kV (L591), 500 μF and 0.28 kV (SUP-T1), 50 μF and 0.5 kV (BJAB). Transfection efficiency was determined by pEGFP cotransfection and FACS analysis or by FACS analysis of pEGFP-fusion constructs, where used.

3 Results

3.1 Part I: High-dimensional data as basis for identification of a cHL-NOTCH disease mechanism

3.1.1 Defining a NOTCH gene set

Publicly available NOTCH gene sets (http://www.broadinstitute.org/gsea/msigdb) were screened and found to represent only core components of the signaling pathway in addition to some classical NOTCH target genes. Hence, these sets are incomplete in terms of comprising every gene that has been found to be associated with NOTCH. They for example lack various proteins that may fine tune NOTCH activation, proteins that are known to interact physically with NOTCH receptors of whom a direct function is yet to be shown but presumably exists (see e.g. the BioGrid database, http://thebiogrid.org/). They moreover do not include a vast number of described NOTCH target genes such as for example GATA3 [75], ABF1 [74] and HOXA5 [141]. To obtain a set of all genes where there is evidence of either

- protein interaction with NOTCH receptors
- tuning of the NOTCH signaling pathway
- target gene regulation through NOTCH transcriptional activity

the following databases where screened: BioGrid, KEGGpathway, Pubmed and NetAffx. Appendix A lists all genes that were found to be associated with the NOTCH signaling pathway.

To check NOTCH specificity of this set, it was analyzed against three pathway databases (BBID, KEGG_Pathway, biocarta), three GO-term sources (BP/CC/MF_FAT), three functional categories (cog_ontology, SP_PIR_Keywords, UP_seq_Feature), one disease source (OMIM) and 3 protein-domain database sources (Interpro, Pir-Superfamily, Smart) using the Database for Annotation, Visualization and Integrated Discovery (DAVID) version 6.7 (http://david.abcc.ncifcrf.gov/). This resulted in 82 annotation clusters. The annotation cluster with the highest enrichment score of 73.4 was found for the terms NOTCH signaling pathway (GOTERM_BP_FAT term 'NOTCH signaling pathway'; adjusted p-value=1.4^{-100}; SP_PIR_KEYWORDS term 'NOTCH signaling pathway'; adjusted p-value=8.7^{-92}) and the GOTERM_BP_FAT term 'cell surface receptor linked signal transduction' (adjusted p-value=9.7^{-22}).
Accordingly, the compiled NOTCH gene set is highly representative for the NOTCH signaling pathway.

3.1.2 Acquisition of data, quality control and processing

In order to detect a putative NOTCH signature, mRNA gene expression profiling was performed with HRS cell lines L428, L1236, KM-H2, HDLM-2, L540 and L540Cy and with the non-Hodgkin cell lines Reh (pre-B cell line), Namalwa (Burkitt's lymphoma, BL) and SU-DHL-4 (diffuse large B cell lymphoma, DLBCL). The Affymetrix array platform HG U133 Plus 2.0 was used. Biological replicates of cell lines (except for L540 and L540Cy) were acquired at different times, as to account for biological variance introduced through culturing cell lines over periods of time. From that point on, all samples were processed at the same times and by the same person as to exclude the

Array name/cell line and replicate number	coding number
HDLM-2_1	1
HDLM-2_2	2
KM-H2_1	3
KM-H2_2	4
L1236_1	5
L1236_2	6
L428_1	7
L428_2	8
L540	9
L540Cy	10
Namalwa_1	11
Namalwa_2	12
Reh_1	13
Reh_2	14
SU-DHL-4	15

Table 3.1: Array codings

All arrays were assigned a coding-number from 1-15. These numbers were used for naming the arrays in the quality assessment process.

possibility of introducing a batch effect. The second array for cell line SU-DHL-4 failed and could not be used for any analysis. In table 3.1, the numerical coding for all arrays is shown and will be used in the various quality assessment plots below.

Affymetrix default quality controls and RNA degradation plots

Looking at the Affymetrix quality plot of the data (figure 3.1(a)), the ratios of 3'-positioned probes to 5'-positioned probes of both *ACTIN* and *GAPDH* show to be according to quality standards. In case of *GAPDH* the ratio is centered around 0 and in case of *ACTIN* the ratios are between 0 and 1. This finding is confirmed when looking at the RNA degradation plots (figure 3.1(b)), no array shows 5'-positioned to 3'-positioned probe-slopes being significantly different from the other slopes. The calculated inter-array scaling factors and percentages of presence calls are uniformly distributed around -1 and between ≈37-47%, respectively. However, the average background is not evenly distributed, with a value of 133.26, array #12 shows significantly higher background than any other array (the other arrays have values of around 50).

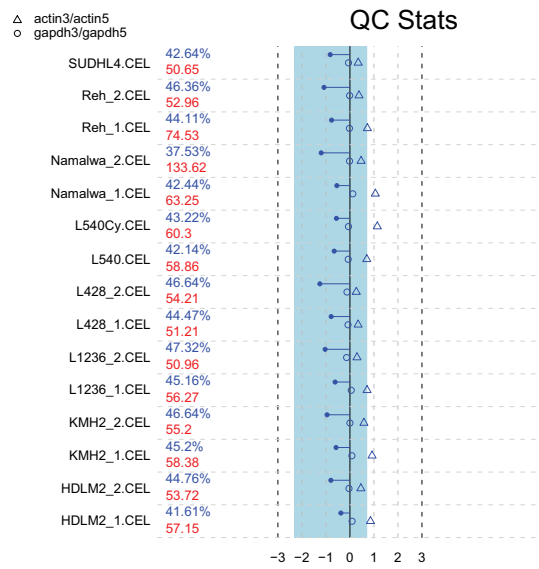

(a)

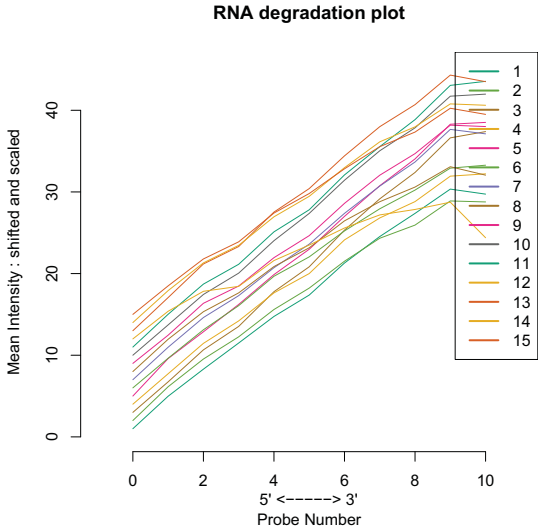

(b)

Figure 3.1: Affymetrix array quality controls

Quality plots recommended by Affymetrix and RNA degradation plots of the arrays show, that quality standards are met. *GAPDH* and *ACTIN* rations are of good quality for all arrays, as are the scale-factors and presence calls (a). RNA degradation is present, yet for all arrays the degradation slopes (b) are very similar.

MA-, intensity-density- and intensity box-plots

In figure 3.2, MA-, intensity-density- and intensity box-plots are shown for all 15 arrays. Except for array #12, MA-plots of all arrays show similar distributions of the data. Array #12 shows M-values shifted up to values of around 2.0 (M values should be centered around 0), indicating, that array #12 has over all higher intensities than all the other arrays. This is confirmed when looking at intensity-density- and intensity box-plots, where there is a clear shift of the distribution to higher intensities.

NUSE, RLE and PM/MM intensity distribution diagnostics

On the relative log expression (RLE) plot (see figure 3.3(a)), arrays' median RLE is centered around 0 and RLE values are evenly distributed across all arrays (both of which are expected) except array #12, where the distribution is a little broader. Looking at the normalized unscaled standard error (NUSE) plots (where the median standard error over all arrays was set to 1, see figure 3.3(b)) all arrays center around 1 (which is expected) except for arrays #1, #12 and #13.

Looking at the intensity distribution of perfect matches (PM) and mismatches (MM), one notes that PM intensities are shifted to higher intensities when compared with the mismatch intensity distribution (see figure 3.3(c)). This is expected as MM probes have poorer hybridization than PM probes.

In summary, especially array #12 shows to be an outlier array in many aspects tested. Array #13 also shows to slightly differ from the other arrays. A subsequent cluster analyses should help to determine, whether background correction and normalization of all arrays would result in the expected biological clustering of a main cHL cluster and a main non-Hodgkin cluster.

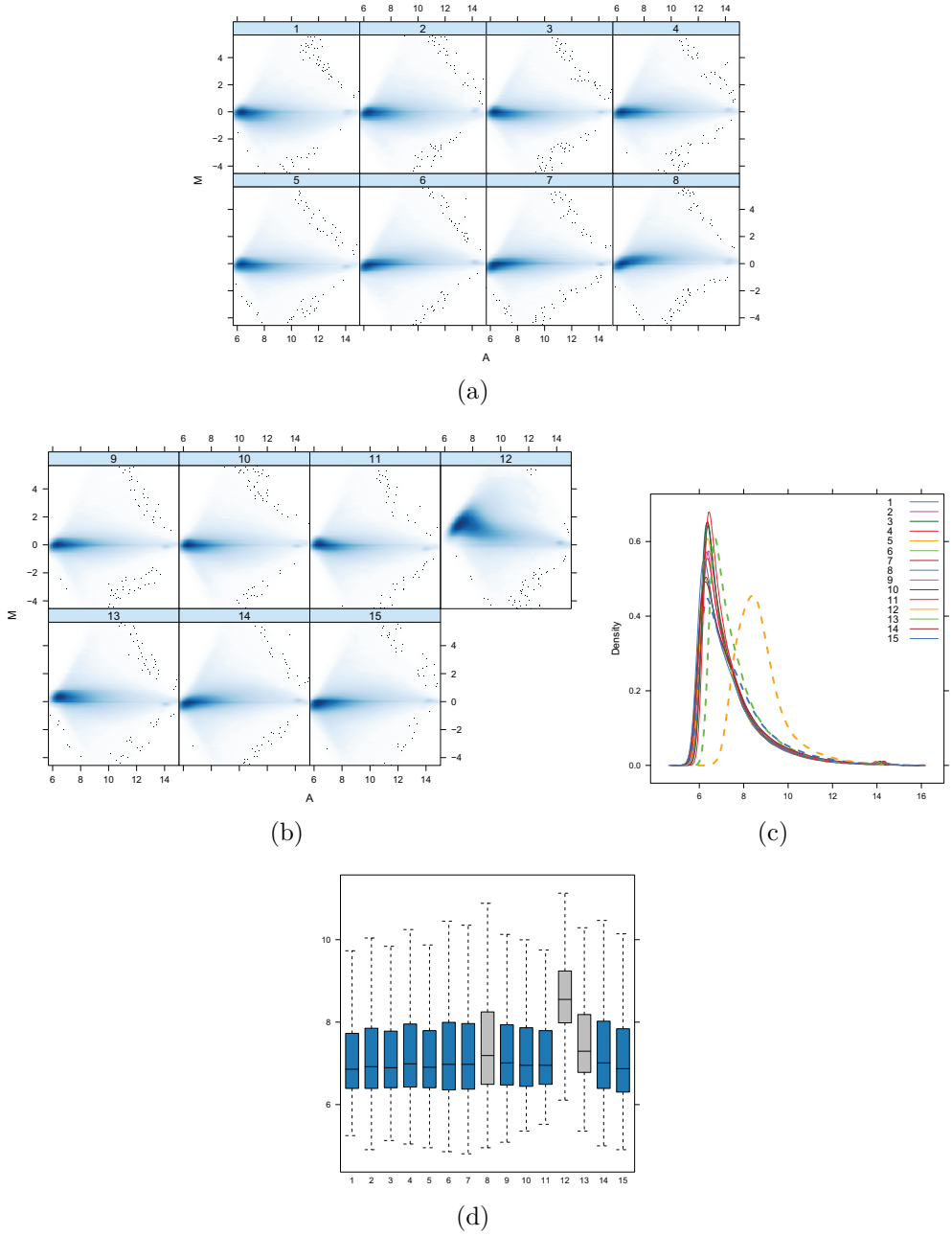

Figure 3.2: Quality assessment plots I

In (a) and (b), MA-plots show the similarity of each individual array to a pseudo-array calculated from the mean-intensity of every probe on the Affymetrix HGU 133 Plus 2.0 platform. For arrays with good quality, the expected distribution of values should center around the x-axis. The intensity-density- (c) and intensity box-plots (d) reveal information about array-individual intensity distributions, the spread of the distributions is expected to be more or less the same for all arrays, as is their median. All quality plots shown here indicate, that array #12 shows intensities shifted to higher values than seen for all other arrays.

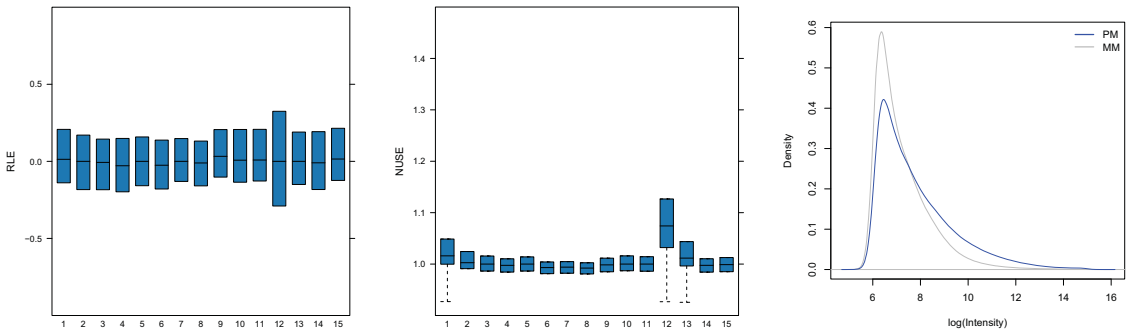

(a) (b) (c)

Figure 3.3: Quality assessment plots II

Shown are RLE (a), NUSE (b) and PM/MM (c) plots for arrays 1-15. The NUSE and RLE quality plots shown here indicate, that array #12 shows quality problems.

Biological clustering

The cluster analysis in figure 3.4 was done after robust multi-array average (RMA) background correction and quantile normalization of unprocessed data. It shows, that our samples cluster according to their biological groups, even arrays #12 (Namalwa_2) and #13 (Reh_1) cluster as expected with their biological replicates with a Pearson correlation coefficient of ≈0.99. In respect of this result, it is assumed, that the technical quality issues of array #12 and #13 are accounted for by the used processing approach. This and the aim not to reduce statistical power by reducing sample numbers led to the decision, to use all arrays for all further analyses.

3.1.3 Gene wise fitting of linear models

To determine genes significantly deregulated in cHL, gene-wise fitting of linear models was performed using the LIMMA [139] framework. All 54675 features present on the Affymetrix HGU 133 2.0 Plus array were used without applying any filters. The following

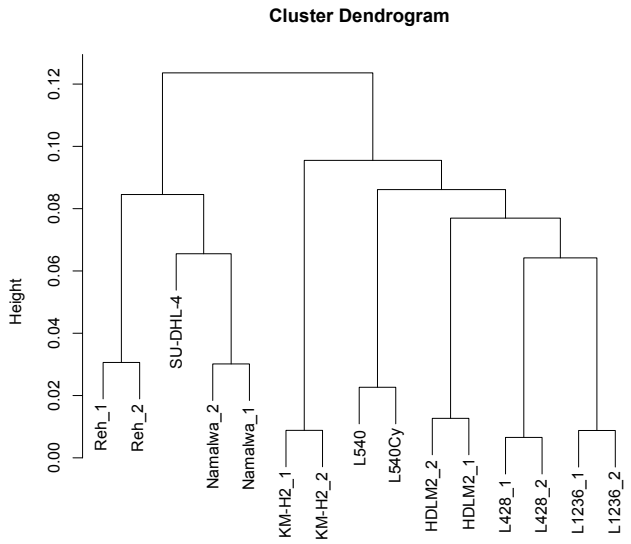

Figure 3.4: Pearson cluster analysis of cell lines

Biological clustering (Pearson distance and complete linkage were used as clustering parameters) of all 15 arrays using data of all features present on the Affymetrix HG U133 Plus 2.0 platform. Note that, where available, biological replicates cluster together. Moreover, there are two distinct biological clusters: one non-Hodgkin sample cluster and one cHL sample cluster. This suggests, that there is a substantial number of differentially regulated genes in between the two groups. It also confirms, that processing accounts and adjusts for technical problems with array #12 (Namalwa_2).

linear model was used for fitting:

$$y_i = 0 + x_1 HL + x_2 nHL + \epsilon_i \tag{1}$$

where y_i is the feature present in row i of the expression value matrix, x_1 and x_2 are the estimators with $x_n \in R$ for each of the dummy regressors of the factor group (which has two levels: HL and nHL). Models were forced through the origin, as no common reference or population mean was assumed. In R pseudo-code this will reduce to:

$$y_i = 0 + \text{group} \tag{2}$$

where group is the factor mentioned above.

Fold change in between groups was then calculated by multiplying an according contrast matrix with the calculated estimators of both group levels to get contrast estimators. Contrast estimators were then used for calculation of p-values using moderate t-tests [139]. Resulting p-values were adjusted to account for multiple testing using the method of Benjamini and Hochberg [142].

All features showing at least a $\log_2$-fold change of $\geq$0.5 or $\leq$-0.5 and an adjusted p-value of $p \leq 0.05$ were deemed significantly deregulated and thus were used for further analyses. These limitations resulted in the identification of $\approx$4400 significantly deregulated features in cHL.

3.1.4 Identification of a NOTCH signature

Principal Components Analysis

Data of the intensity values of all Affymetrix features representing genes of our NOTCH gene set were extracted resulting in a high-dimensional 270×15 matrix. To reduce dimensionality of this matrix to a visualizable level, unrotated Principal Components Analysis (PCA) was applied. Principal component (PC) 1 accounts for 82%, PC2 for 7% and PC3 for 3% of data set variance. The factor loadings are plotted in figure 3.5. As seen by this graphical representation, cHL samples are clearly separated from non-Hodgkin B cell control samples, indicating the presence of a cHL specific NOTCH signature. This result also suggests, that the NOTCH signaling system is globally regulated in a different manner in HRS cell lines than in non-Hodgkin cell lines. To address the question whether the separation seen in the PCA analysis is due to chance or whether it represents a true effect, Fisher's Exact Test was applied with the counts of genes that do or do not show statistically significant deregulation as defined in section 3.1.3. 63 of 270 features of our NOTCH gene set were deregulated according to the defined

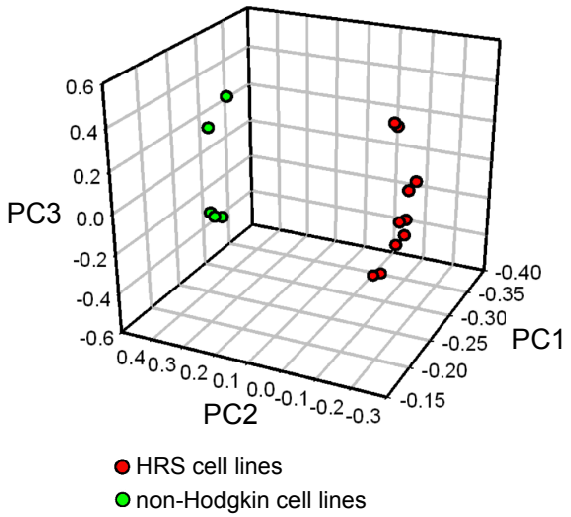

Figure 3.5: Principal Components Analysis of cell lines

Unrotated Principal Components Analysis was done with the intensities of 270 NOTCH associated features measured in 10 HRS cell line samples and 5 non-Hodgkin cell line samples. cHL samples separate from non-Hodgkin samples, suggesting, that cHL samples are characterized by a distinct NOTCH signature.

limitations. The result of the Fisher test, $p<10^{-10}$, shows that our NOTCH gene set is highly significantly deregulated in cHL.

Extending the analyses to arrays from primary cases

As to gain more biological and statistical power and in order to substantiate our cell line results, array data from the Gene Expression Omnibus (www.ncbi.nlm.nih.gov/geo/) data set GSE12453 were analyzed [24]. From this data set, 12 primary cHL cases, 5 primary BL cases and 11 primary DLBCL cases were taken and merged with our dataset. Assessing these data and our data in comparison there clearly is a batch effect present (see figure 3.6), resulting in the necessity to account for this effect in all subsequent analyses.

Quality assessment of the GSE12453 data was done separately, all arrays passed quality standards (a quality summary is given in Appendix B). Our dataset and the specified

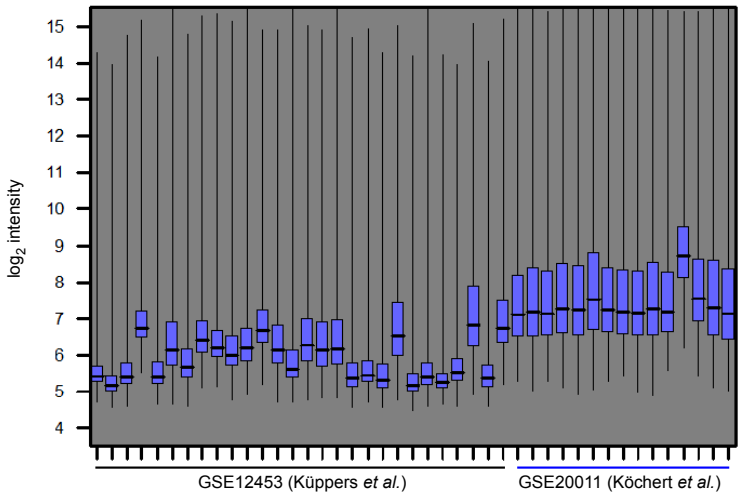

(a)

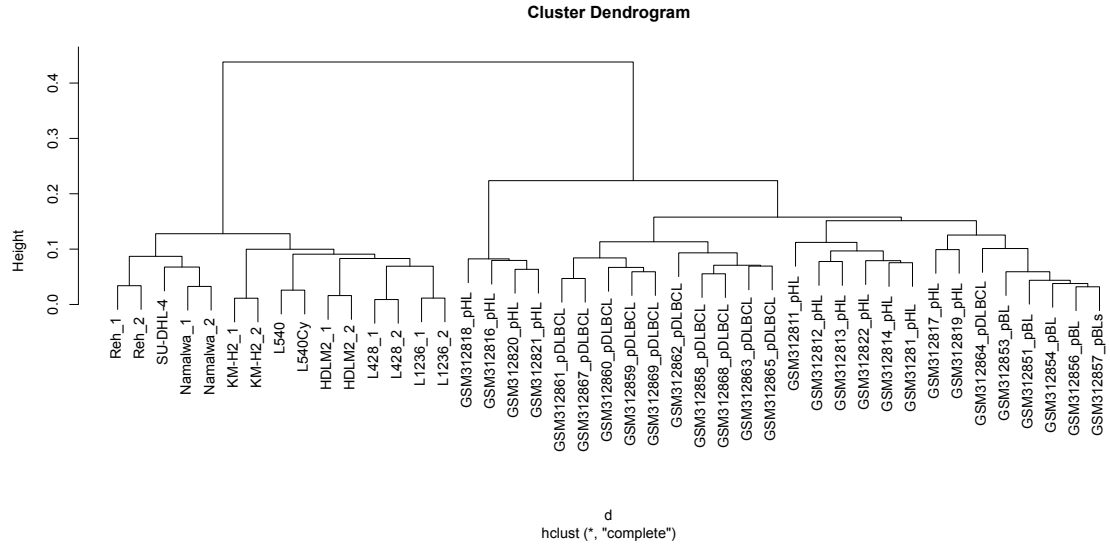

(b)

Figure 3.6: Batch effect detection in between datasets

Visualization of the intensity data of all features present on the used HGU 133 Plus 2.0 platform using a boxplot representation (a) and a Pearson distance cluster analyses (b) using complete linkage were performed. Note, that our data shifts to significantly higher intensity-distributions and that samples do not cluster according to their biological groups, yet according to their technical batches. This indicates the presence of a batch effect. All sample names starting with 'GSE' were taken from data set GSE12435. pHL, primary Hodgkin Lymphoma sample; pDLBCL, primary Diffuse Large B Cell Lymphoma sample; pBL, primary Burkitt Lymphoma sample.

data from GSE12453 were then processed together (RMA background-correction and quantile normalization were applied). To account for the batch effect in the statistical analyses, the linear model used for determination of differentially expressed genes was subsequently extended to following R pseudo-code representation:

$$y_i = 0 + \text{group} + \text{batch} \tag{3}$$

where batch is a factor with two levels representing the batch of our data set or the data from GSE12453, respectively. Adjustment of the data using linear models for batch effect estimator determination and the subsequent batch-correction resulted in clustering of the samples according to their biological groups (see figure 3.7).

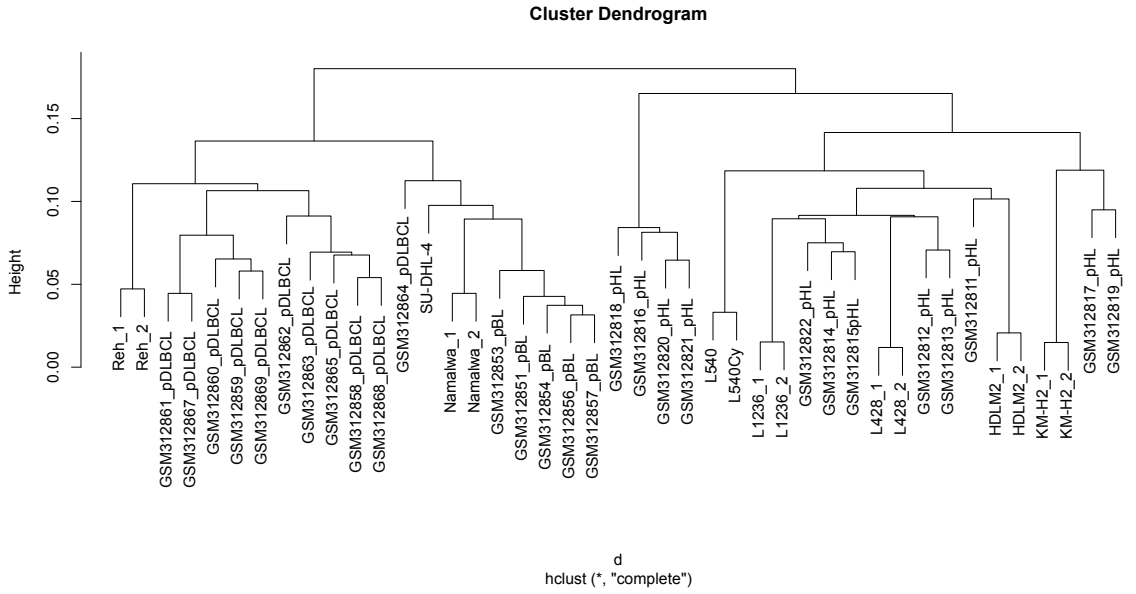

Figure 3.7: Cluster analysis after correction for the batch effect

The batch effect for each feature present on the used HGU 133 Plus 2.0 platform was estimated using linear models and than corrected for. Note, that after correction for the batch effect, samples cluster according to their biological groups. All sample names starting with 'GSE' were taken from data set GSE12435. pHL, primary Hodgkin Lymphoma sample; pDLBCL, primary Diffuse Large B Cell Lymphoma sample; pBL, primary Burkitt Lymphoma sample.

Statistically significant differential expression of genes was then determined as de-

scribed above. Altogether, ≈4300 of 54675 features were significantly deregulated in the pooled cHL samples when compared with the non-Hodgkin samples. Again, Fisher's Exact test was performed with the data of all features of our NOTCH gene set. All together, 48 of 270 features of the NOTCH gene set were significantly deregulated. Fisher's exact test rendered this result to be significant with $p<10^{-4}$.

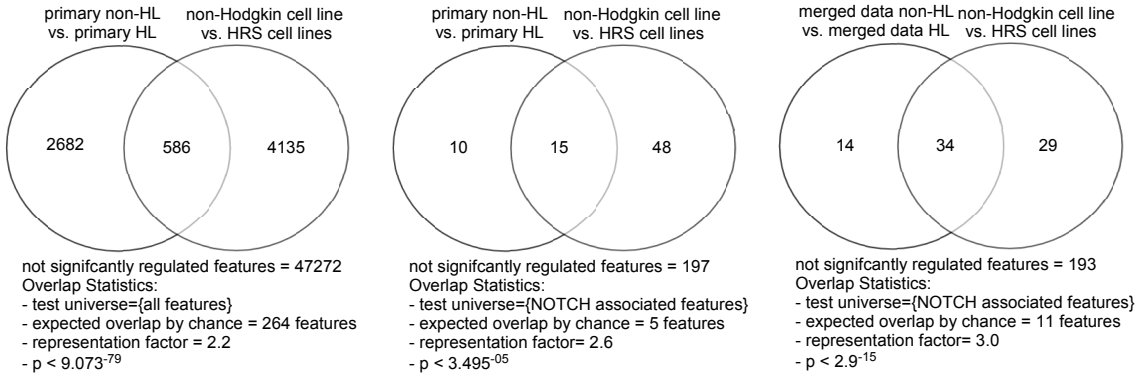

(a) (b) (c)

Figure 3.8: Overlap of significantly deregulated features in between different data sets

Venn diagrams are shown for (a) the comparison of all significantly deregulated features in primary and cell line samples, respectively. (b) shows the same comparison as in (a) for all NOTCH associated features and (c) shows the overlap of significantly deregulated NOTCH associated features when comparing cell line data and the merged data sets. The significance of any overlap was determined by calculating the exact hypergeometric probability. The number of features n expected to overlap by chance was calculated using the numbers a and b representing the count of features in either set used for the comparison and the total number of features N: $n=(a\times b)/N$.

Comparing the overlap of NOTCH gene set deregulation in the different data sets used

As to assess in how far deregulation of all genes and of the NOTCH gene set is similar in between the disjunct cell line, primary sample and merged data sets, the overlapping sets of their significantly deregulated genes was determined. As seen in figure 3.8, there is a significant intersection of significantly deregulated genes when all features of the used HGU 133 Plus 2.0 platform are analyzed, when comparing primary samples to cell lines.

The overlapping set of significantly deregulated NOTCH associated genes is significant for the comparison of primary to cell line data sets as well as for comparison of cell line data to the merged data set. This implies, that quality and magnitude of NOTCH deregulation is very similar in HRS cell lines and cHL primary cases. Appendix C lists the NOTCH gene set and the regulation of each feature in the different comparisons.

3.1.5 Gene Set Enrichment Analysis (GSEA)

For GSEA analysis we used – in addition to our NOTCH gene set – two publicly available NOTCH gene sets from the Molecular Signatures Database of the Broad Institute (http://www.broadinstitute.org/gsea/). Analyzing the data set with GSEA using our NOTCH gene set and the publicly available NOTCH gene sets shows that all sets are highly enriched as seen in figure 3.9 and table 3.2.

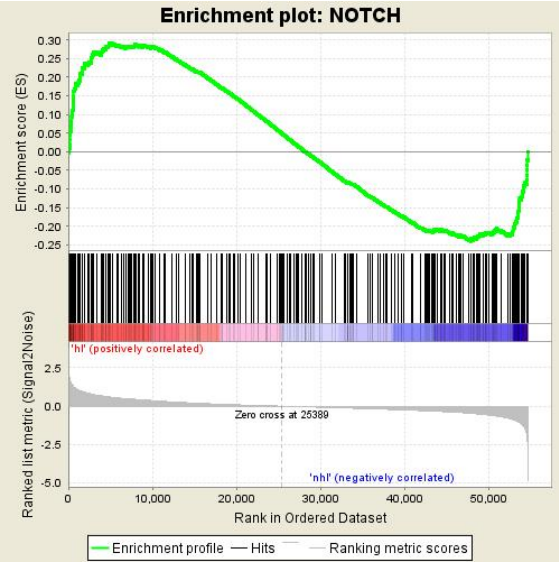

Figure 3.9: NOTCH Gene Set Enrichment Analysis

GSEA analysis plot for the NOTCH gene set developed in this study. Array features were ranked according to their signal to noise ratio and enrichment was calculated according to the algorithm developed by [140]. Cell line data was used as input. Note, that there is a significant enrichment of NOTCH associated genes that are up–regulated (e.g. MAML2 and NOTCH2, i.e. positive regulators of NOTCH signaling) or down–regulated in cHL (e.g., DTX1, i.e. a negative regulator of NOTCH signaling).

Gene Set Name	Feature Count	Normalized Enrichment Score	FDR q-value
NOTCH (Köchert *et al.*)	270	1.34	0.016
NOTCH_SIGNALING_PATHWAY	39	2.10	0.000
NOTCHPATHWAY	16	1.76	0.002

Table 3.2: GSEA results with different NOTCH gene sets

3.1.6 Conclusions from statistical analyses of array data

Taken together, the statistical analyses of array data gained from HRS and non-Hodgkin cell lines in combination with array data from primary cHL and non-Hodgkin cases showed, that there is a statistically significant deregulation of the NOTCH signaling pathway in cHL. The quality of this deregulation is not directly concludable from the analyses, as the NOTCH gene set members that show to be deregulated in cHL may have different impacts with the outcome possibilities:

a) positive regulation of NOTCH signaling

b) negative regulation of NOTCH signaling

c) direct/indirect result of activation/inactivation of NOTCH signaling

Thus, the next step was to combine the available context knowledge about NOTCH signaling with the results of the statistical analyses, as to draw conclusions about the actual characteristics of the deregulation of the NOTCH signaling system in HL.

3.1.7 Identifying top hits within the NOTCH gene set — hypothesis generation

To identify genes of high interest for further analyses, different parameters were taken into account:

- $\log_2$-fold change ($\log_2$intensity(cHL)-$\log_2$intensity(non-Hodgkin))

- adjusted p-values calculated from moderate t-tests
- GSEA rank metric scores
- relevance of gene for the NOTCH signaling pathway

Table 3.3 shows the top 10 NOTCH associated genes and the values of the mentioned parameters. The analysis is in good agreement with studies published by Jundt *et al.* and Kapp *et al.*: our analyses shows a significant up–regulation of NOTCH2 [55, 56] and a significant down–regulation of an inhibitor of NOTCH signaling, DTX1 [74]. The analyses moreover have shown, that the NOTCH associated genes are deregulated in cHL in a manner, that — according to todays knowledge about NOTCH signaling — will result in aberrant up–regulation of this pathway. Looking at table 3.3, one finds that MAML2, one of the three essential co-activators of NOTCH signaling, is highly (23.6-fold) up–regulated in cHL. This significant up–regulation of MAML2 is also found when analyzing the primary sample and merged data sets (see appendix C, Affymetrix Probe ID 235457_at). With respect to their subjective importance for NOTCH signaling and the degree of their deregulation, none of the other NOTCH associated genes found to be deregulated has such a high impact on the activation of NOTCH signaling.

Thus, MAML2 was determined to be the most important gene of interest for further mechanistic and functional analyses of NOTCH signaling in cHL.

There are various other genes involved in the processing of the NOTCH receptors, such as ADAM10 (responsible for S2-cleavage of NOTCH receptors) and members of the γ-secretase complex (PSEN1, PSEN2) which — according to these analyses — show to be up–regulated in cHL. Their up–regulation may also be interpreted as facilitating mechanism for NOTCH cleavage processes. In turn, the found up–regulation of NOTCH2 as described in [55, 56], also points into the direction of aberrant activation of the NOTCH signaling pathway in cHL. However, interplay of different NOTCH-ligands

Gene symbol	log_2-fold change	adjusted p-value	GSEA rank metric score	NOTCH association
GATA3	6.38	2.5×10^{-5}	1.86	c
MAML2	4.56	1.0×10^{-5}	1.70	a
PSEN2	3.12	6.0×10^{-5}	1.33	a
NOTCH2	2.97	0.01	1.54	a
PSEN1	1.09	0.03	1.34	a
SEL1L	1.60	0.03	1.26	unknown
ADAM10	0.77	0.05	1.00	a
DTX4	-1.93	0	-1.44	b
TCF3	-1.40	0	-1.73	c
DTX1	-4.00	0	-3.33	b

Table 3.3: 10 top hits - deregulated NOTCH genes in cHL

with different NOTCH receptors is poorly understood to date. The mere up–regulation of a NOTCH receptor is therefore not as important as the deregulation of an essential co-activator, such as MAML2, that by itself will activate NOTCH signaling with any cleaved NOTCH receptor [96, 95] and without whom NOTCH transcriptional activation may be impossible.

3.1.8 Assessing the expression status of Mastermind-like family members MAML1, MAML2 and MAML3

To verify the findings of the array analyses, the mRNA expression status of the various NTC components of HRS compared to non-Hodgkin cell lines was assessed using qPCR. Special emphasis was put forward on the analyses of the members of the Mastermind-like family. As seen in figure 3.10, relative quantification of the MAML family members is in accordance with the array analyses.

MAML1 shows no significant regulation in between HRS and non-Hodgkin cell lines, it is expressed at robust levels in all cell lines tested.

MAML2 in opposite shows a significant up–regulation in HRS cell lines which in relative comparison to the non-Hodgkin cell line Reh is up to 8-fold. The highest, relative levels of *MAML2* are found in the cell lines L1236 (5.5-fold up regulation), L591 (6-fold up regulation) and HDLM-2 (8-fold up regulation). All tested HRS cell lines show at least

2-fold up regulation of *MAML2* compared to Reh cells. Within the non-Hodgkin cell lines, Reh shows the highest levels of *MAML2*. Namalwa has around 0.1-fold *MAML2* levels when compared to Reh, BL-60 around 0.3 fold-levels and BJAB and SU-DHL-4 show *MAML2* CT values that are at the level of undetectability (CT=34-35).
In turn *MAML3* qPCR shows a slight, yet significant up–regulation of *MAML3* mRNA levels in non-Hodgkin cell lines. Reh and BJAB cells show the highest *MAML3* levels in all cell lines tested, in cHL only cell lines L1236 and KM-H2 show non-Hodgkin cell line comparable *MAML3* mRNA levels. All other HRS cell lines tested show *MAML3* CT values close to the level of undetectability (CT=33-35).
To get an impression of the relative abundance of the different MAML members in HRS cell lines, ΔCT values were analyzed and plotted in figure 3.10(b). Relative abundance of *MAML2* mRNA (median ΔCT of ≈5) is thus significantly higher than the mRNA levels of *MAML1* (median ΔCT of ≈9.3) and *MAML3* (median ΔCT of ≈15.5). This is suggestive of the quantitative importance of MAML2 in the suspected deregulation of NOTCH signaling in cHL.

Validating MAML members qPCR data on protein level

Next, MAML1, MAML2 and MAML3 protein levels were assessed in our cell line panel in order to validate qPCR analyses. As seen in figure 3.11, western blot analyses confirms the qPCR data.

All cell lines tested show expression of MAML1. In case of the HRS cell lines, L428, L1236 and L591 MAML1 expression is only weak, in opposite HRS cell lines KM-H2, L540 and L540Cy show robust expression. As for the non-Hodgkin cell lines, Reh and Namalwa show robust expression, whereas BL-60, BJAB and SU-DHL-4 show weak expression.

MAML2 protein is highly expressed in all HRS cell lines tested. In Reh, BL-60 and BJAB there is only weak expression and in cell lines Namalwa and SU-DHL-4 expression

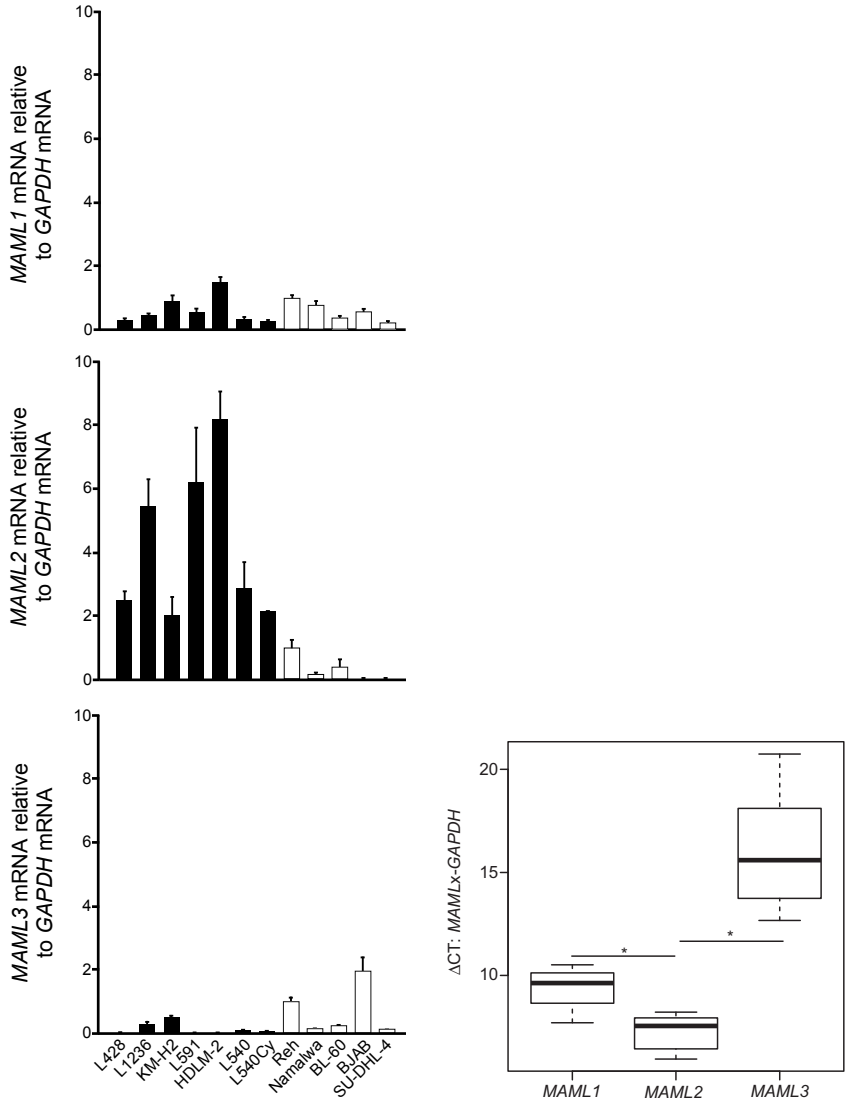

Figure 3.10: qPCR quantification of all three Mastermind-like family members in cHL and non-Hodgkin cell lines.

mRNA levels of all human Mastermind-like family members were quantified relative to *GAPDH* using qPCR (a). There is robust expression of *MAML1* in all cell lines tested, with little differences within them. In opposite, *MAML2* is highly up–regulated in all HRS cell lines tested, when compared with non-Hodgkin cell lines. *MAML3* mRNA levels are slightly higher in non-Hodgkin cell lines than in cHL. (b) is a box-and-whisker plot presentation of HRS cell line ΔCT values for all MAML members and shows, that there is significantly more *MAML2* mRNA present in cHL than *MAML1* or *MAML3*. Efficiencies of all primer pairs used was 91%±1.3%, allowing for this estimation of comparative MAML abundance. Error bars denote 95% confidence intervals (a), Black bars: HRS cell lines, empty bars: non-Hodgkin cell lines. *:$p < 0.001$,

is not detectable.

MAML3 protein levels, as seen in the according qPCR analysis, vary substantially across different cell lines. In regard to the HRS cell lines, MAML3 protein is detectable in L1236, KM-H2, L540 and L540Cy. The non-Hodgkin cell lines Reh and BJAB show high levels of MAML3, whereas Namalwa, BL-60 and SU-DHL-4 show weak expression.

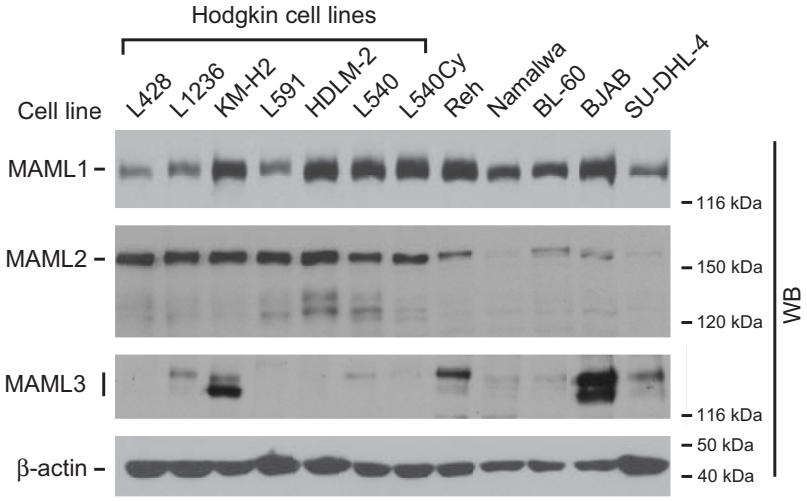

Figure 3.11: Western Blot analyses of MAML members

Western blot analyses of MAML1, MAML2 and MAML3 protein using whole cell extracts is in good agreement with qPCR analyses. MAML1 is expressed in all cell lines tested without there being a significant difference of expression levels in the biological groups, cHL and non-Hodgkin. Contrarily, MAML2 is highly expressed in HRS cell lines, whereas in non-Hodgkin cell lines there is only weak or barely detectable expression. MAML3 protein levels are somewhat up–regulated in non-Hodgkin cell lines, in cHL, only cell line KM-H2 shows high MAML3 protein levels. β-actin was analyzed as control.

Since only few data regarding MAML2 expression in human lymphoid cells were available, *MAML1*, *MAML2* and *MAML3* mRNA expression and MAML2 protein expression was determined in $CD19^+$ B cells and $CD3^+$ T cells. *MAML1* and *MAML3* mRNA is expressed at robust levels in all cell types tested. Contrarily, *MAML2* mRNA is most prominently expressed in the HRS cell line L428 and primary $CD3^+$ T cells whereas there is no expression in the non-Hodgkin cell line Namalwa and very weak expression in $CD19^+$ B cells (see figure 3.12(a)). MAML2 protein was strongly expressed only in

$CD3^+$ T cells, whereas it was hardly detectable in $CD19^+$ B cells, (see figure 3.12(b)).

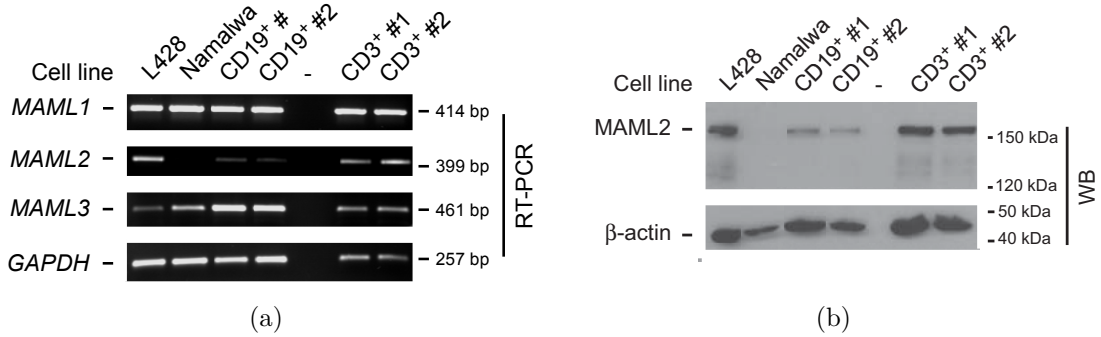

(a) (b)

Figure 3.12: MAML member expression in primary B and T cells

The mRNA expression status of all human MAML members in primary $CD3^+$ T and $CD19^+$ B cells was assessed using sqPCR (a). *GAPDH* was analyzed as control. (b) Western blot analysis using whole cell lysates. MAML2 protein levels were assessed in primary $CD19^+$ B cells and $CD3^+$ T cells isolated from two independent tonsils of healthy donors. As comparison, HRS cell line L428 and non-Hodgkin cell line Namalwa are shown. In $CD3^+$ T cells there is robust MAML2 expression comparable to levels found in L428. In comparison, there is only very weak expression of MAML2 in $CD19^+$ B cells, which also might be the result of remaining technical T cell contamination of the samples. These results imply that MAML2 expression is normal for T cells and is not normal for B cells. β-actin was analyzed as control.

3.1.9 MAML2 immunohistochemistry of primary material

To confirm the cell line data in primary material, immunohistochemistry was performed in non-neoplastic lymphoid tissue and 180 B cell-derived primary human lymphoma cases. This was done for MAML2 only, and not the other MAML members, as the data shown and analyses done so far show MAML2 to be the significantly deregulated MAML co-activator in cHL. In contrast, MAML1 and MAML3 are not significantly deregulated and thus — in regard to the scope of this study — it was decided not to perform immunohistochemistry of these MAML members.

In several B cell-derived primary human lymphoma cases we detected high levels of MAML2 expression. In cHL, 30 of 61 cases stain highly positive for MAML2 (see figure

3.13), in B-ALL 8 of 8 cases stained positive and in MCL 4 of 10 cases stained positive for MAML2. In the described cases, staining was found to be cytoplasmatic and nuclear. In contrast, B cells of non-neoplastic lymphoid tissue did not stain positive for MAML2. Some exemplary stainings are presented in figure 3.13, table 3.4 shows a summary of the findings for all B-cell associated malignancies stained. In summary, these data show, that MAML2 expression in various B cell-derived primary human lymphomas is unusually high when compared to normal B cells of tonsillar origin. The results moreover suggest, that aberrant, high-level MAML2 expression may play an important pathogenic role in various B cell derived malignancies.

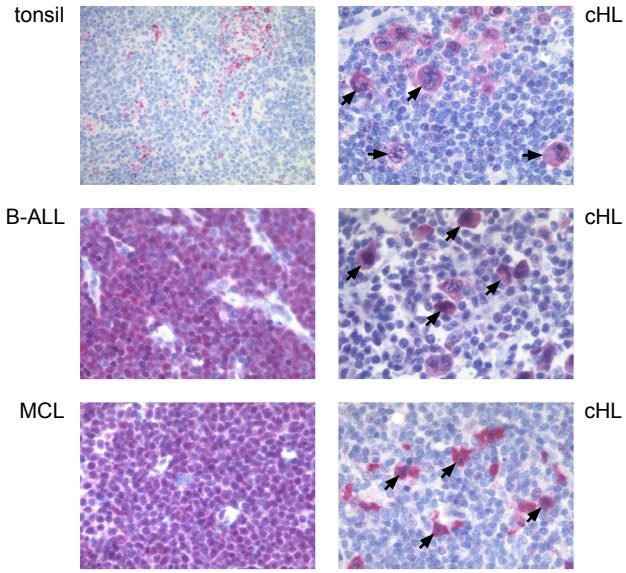

Figure 3.13: MAML2 Immunohistochemistry

The analysis of non-neoplastic lymphoid tissue and 180 B cell-derived primary human lymphoma cases by MAML2 immunohistochemistry revealed, that MAML2 is not expressed in normal B cells. All tonsils from healthy donors (here, 1 representative case is shown) did not show MAML2 staining of their B cells, only Macrophages and Dendritic cells stained positive. In opposite ≈50% of all cHL cases stained highly positive for MAML2. Here, three representative cHL cases are shown, arrows point to cHL cells. Massive MAML2 staining is also found in B cell lymphoblastic leukemia and Mantle cell lymphoma (one representative case of each malignancy is shown).

Disease type	≥90% cells pos.	50-90% cells pos.	0-49% cells pos.	all cells neg.	pos. cases/ cases examined
B lymphoblastic leukemia	7	1	0	0	8/8
B cell chronic lymphocytic leukemia	2	0	3	2	5/7
Lymphoplasmacytic lymphoma	2	0	2	3	4/7
Plasma cell myeloma	0	0	2	6	2/8
Nodal marginal zone lymphoma	3	0	1	6	4/10
Extranodal marginal zone lymphoma	0	4	1	5	5/10
Follicular lymphoma (FL), grade 1	0	2	1	5	3/8
FL, grade 2	1	0	0	7	1/8
FL, grade 3a	0	0	0	8	0/8
FL, grade 3b	0	0	2	6	2/8
Mantle cell lymphoma	3	0	1	6	4/10
DLBCL, GCB type	0	1	1	6	2/8
DLBCL, non-GCB type	0	1	5	4	6/10
Burkitt's lymphoma	0	0	1	8	1/9
cHL	25	2	3	31	30/61

Table 3.4: MAML2 Immunohistochemistry of 180 B cell-derived primary human lymphoma cases

pos.: positive; neg.: negative

3.1.10 Quantification of NOTCH receptors, NOTCH ligands and CSL in HRS- and non-Hodgkin cell lines

As the high-level expression of MAML2 alone would not suffice for activation of the NOTCH signaling pathway, assessment of NOTCH receptor mRNA and protein expression was of vital importance for a thorough characterization of the cHL-specific NOTCH signaling system. Also, as to get a complete picture of the expression status of the essential components composing the NTC (see above), the mRNA expression of all canonical NOTCH ligands was quantified using qPCR and the mRNA expression of *CSL* was assessed by sqPCR.

These data were of great importance in order to systemically specify the NOTCH pathway in the cHL context.

qPCR analyses of NOTCH receptors in cHL

In figure 3.14, the results of qPCR quantification of all human NOTCH receptors is shown. *NOTCH1* is expressed in all HRS cell lines (except L1236) at levels that are found in the tested non-Hodgkin cell lines. Levels are slightly higher than in the non-Hodgkin cell lines in KM-H2, L591 and HDLM-2.

Confirming earlier studies [55, 56], *NOTCH2* levels are up to 4-fold higher (L1236) in HRS cell lines than in non-Hodgkin cell lines. Within the HRS cell panel, L540 and L540Cy show the lowest levels of *NOTCH2*, however, these are still higher than in Namalwa, BL-60, BJAB and SU-DHL-4.

NOTCH3 mRNA is detected in almost all cell lines tested at very low levels (except HRS cell line L1236) and hardly detectable in KM-H2 and L591. In case of *NOTCH4* mRNA, only HDLM-2 and BJAB show levels that are well detectable, whereas all other cell lines tested, have *NOTCH4* CT values close to undetectability.

Analyses of NOTCH receptor protein expression in HRS cell lines

To verify qPCR data of NOTCH receptor mRNA expression on protein level, we performed western blot analyses of all human NOTCH receptors in HRS and non-Hodgkin cell lines. The according analysis for NOTCH1 was extended to assessment of the activation status of this particular receptor and is shown below in section 3.1.11. The analyses done for NOTCH2-4 are shown in figure 3.15. They confirm the qPCR data shown above. NOTCH2 is expressed at high levels in all HRS cell lines and is weakly expressed in non-Hodgkin cell line Reh and merely detectable in all other non-Hodgkin cell lines (figure 3.15(a)). No NOTCH3 (figure 3.15(b)) or NOTCH4 (figure 3.15(c)) protein expression is detectable in any cell line tested.

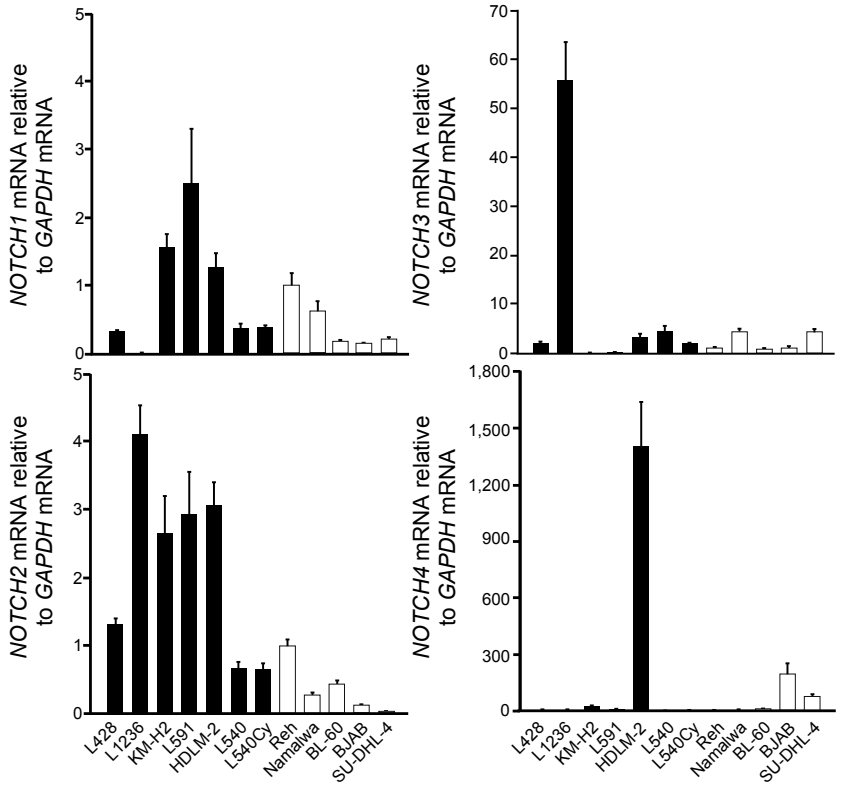

Figure 3.14: Expression status of NOTCH receptors in cHL

Quantification of all human NOTCH receptors was measured relative to *GAPDH* using qPCR. In the HRS cell lines analyzed, *NOTCH1* is expressed at levels comparable to those found in non-Hodgkin cell lines. Only L591 cells show *NOTCH1* levels that are substantially higher (≈2.5-fold of Reh levels) than in non-Hodgkin cell lines. Confirming earlier studies [55], *NOTCH2* is significantly up–regulated in HRS cell lines, e.g. L1236 have ≈4-fold more *NOTCH2* than Reh cells. For the receptors *NOTCH3* and *NOTCH4* no systematic regulation or differential expression in between the two biological groups is detectable. Error bars denote 95% confidence intervals, black bars: HRS cell lines, empty bars: non-Hodgkin cell lines.

qPCR analyses of NOTCH ligands

Next, the mRNA levels of all canonical NOTCH ligands were assessed. As shown in figure 3.16(a), *JAG1* is expressed at low levels in HRS cell lines with the exception of L591, where expression is at least 25-fold higher then in according non-Hodgkin cell lines. The non-Hodgkin cell line Namalwa also shows up to 5-fold higher levels of *NOTCH1* mRNA than, e.g. cell line Reh.

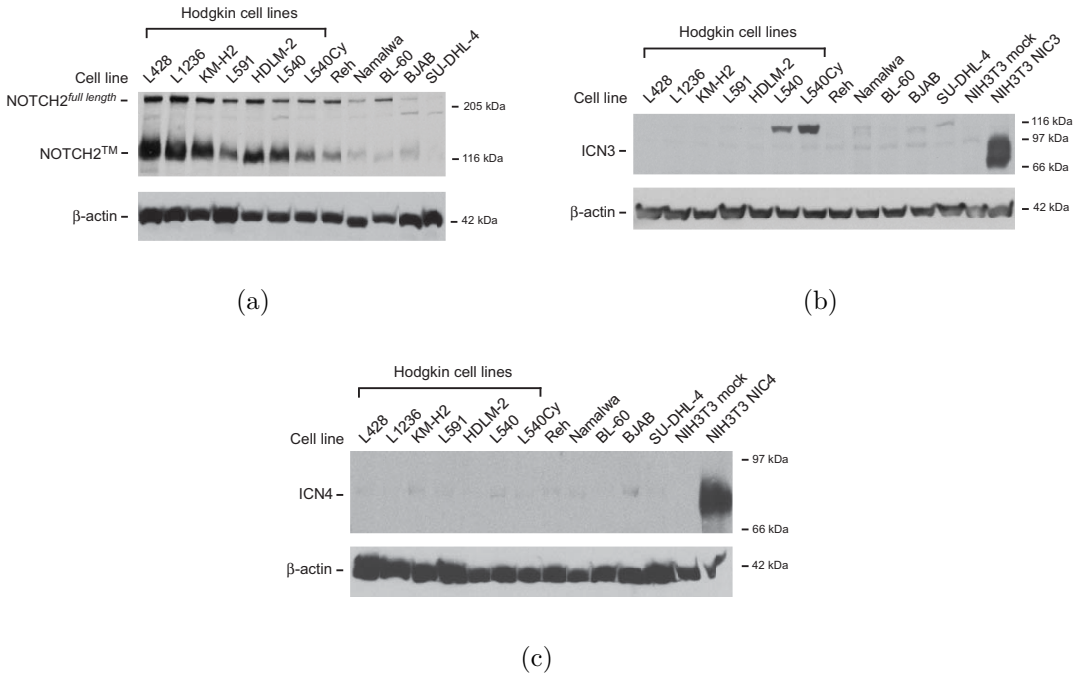

Figure 3.15: NOTCH receptor protein expression

Whole cell lysates were used for western blot assessment of NOTCH receptor protein expression in HRS- and non-Hodgkin cell lines. (a) shows protein expression of NOTCH2. Note, that it is highly expressed in HRS cell lines in comparison to non-Hodgkin cell lines and is in agreement with previously published data [56]. Neither NOTCH3 (b), nor NOTCH4 (c), show protein expression in any cell line analyzed. In case of these two receptors, whole cell lysates of NIH3T3 cells transduced with a control construct (mock) or an viral expression construct coding for NIC3 and NIC4, respectively, were used as protein control. β-actin was analyzed as control.

JAG2 in turn is highly up–regulated (up to 100-fold) in cHL, especially in the cell lines L1236, KM-H2 and HDLM-2. For the ligands *DLL1*, *DLL3* and *DLL4*, expression levels are low across all cell lines tested (see figure 3.16(b)). No systematic differential regulation is observed when HRS and non-Hodgkin cell lines are compared.

mRNA expression status of *CSL*

As CSL is the canonical transcription factor necessary for transcriptional activation mediated by NIC and MAML proteins, its mRNA expression status was determined in HRS- and non-Hodgkin cell lines. As seen in figure 3.17, *CSL* mRNA expression was

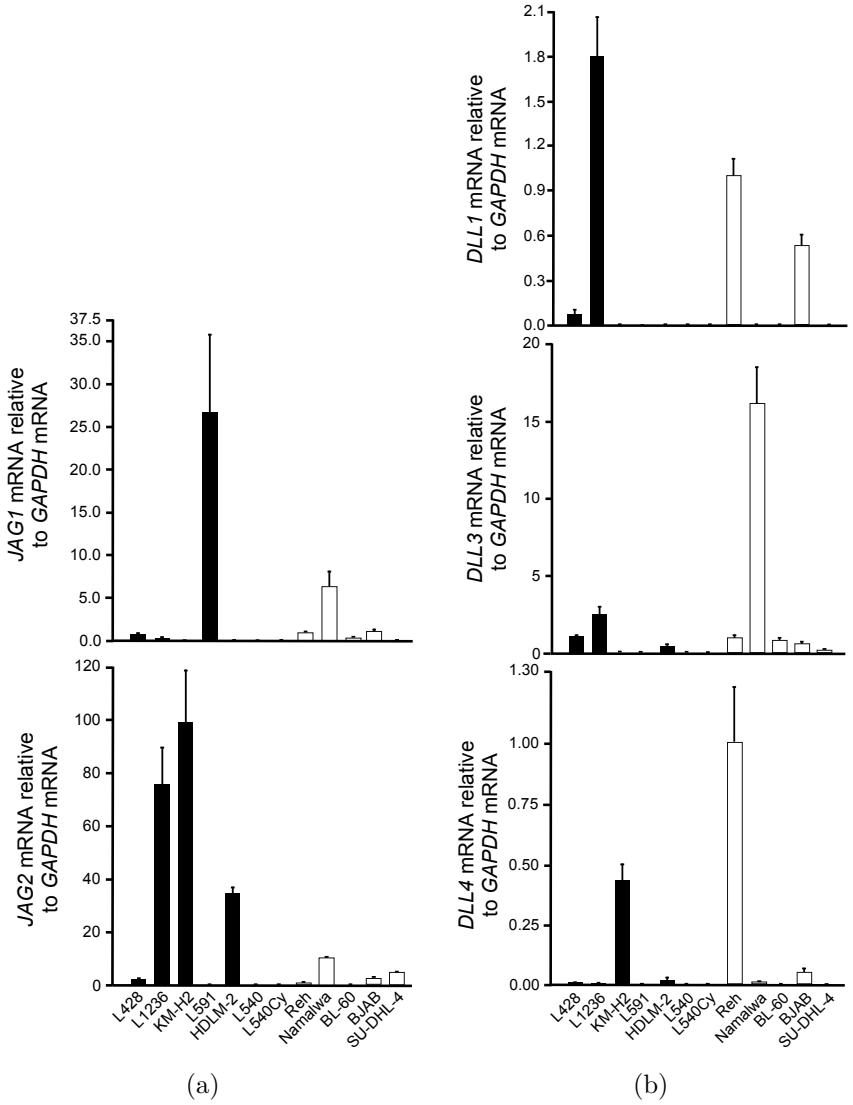

Figure 3.16: Expression status of NOTCH ligands in cHL

qPCR quantification of the canonical NOTCH ligands *JAG1* and *JAG2* (a), *DLL1*, *DLL3* and *DLL4* (b) in HRS and non-Hodgkin cell lines relative to *GAPDH*. Note, that especially *JAG2* is significantly up–regulated in HRS cell lines. For all other ligands, there is no systematic, group-dependent regulation observable. Error bars denote 95% confidence intervals, black bars: HRS cell lines, empty bars: non-Hodgkin cell lines.

detectable at robust levels in all cell lines analyzed.

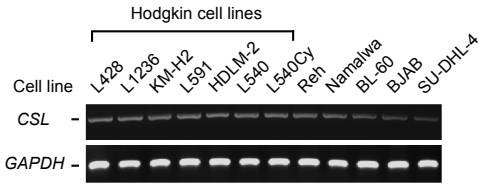

Figure 3.17: mRNA expresseion of *CSL*

CSL mRNA expression was assessed using sqPCR. Primers were designed to amplify all four known human splice variants. *GAPDH* was analyzed as control.

3.1.11 Cleavage status of NOTCH1

In order to determine whether the NOTCH1 signaling pathway is activated in HRS cell lines in terms of NOTCH receptor cleavage, western blot analyses were performed with whole cell and nuclear extracts of various HRS and non-Hodgkin cell lines. Confirming previous studies [56], the NOTCH1 receptor is expressed at robust levels in all HRS cell lines tested except for L1236 (this being in accordance with results from section 3.1.10). However, it is also expressed in non-Hodgkin cell lines (figure 3.18, upper panel). This was assessed by usage of an antibody detecting NOTCH1 and NOTCH1^{TM}.

A different antibody specific to the N-terminal S3 cleavage site of NIC1 was then used to assess the actual cleavage status of NOTCH1, as a positive control the T-ALL cell line SUP-T1 was used. This cell line shows constitutive NOTCH1 signaling due to a t(7;9)(q34;q34.3) translocation [143] which results in the constitutive expression of NIC1. As seen in figure 3.18 (lower panel), except BL-60, every cell line tested shows some level of NIC1 which is enriched in the nucleus when compared to whole cell extracts. In case of cHL, cell lines KM-H2, L591 and HDLM-2 show high levels of activated NOTCH1, all other HRS cell lines show low to medium levels. In the non-Hodgkin cell lines, BJAB and SU-DHL-4 cells show the highest levels of NIC1.

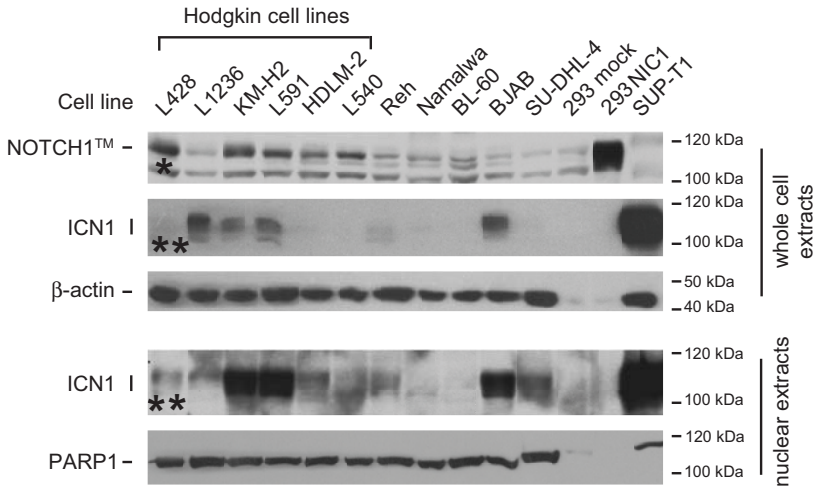

Figure 3.18: Expression and cleavage status of the NOTCH1 receptor

Western blot analyses of NOTCH1 receptor expression and NOTCH1 cleavage in HRS and non-Hodgkin cell lines. NOTCH1 is expressed in all cell lines analyzed except L1236 (upper panel). In nuclear extracts, there is cleaved NOTCH1 (NIC1) in all cell lines analyzed, except BL-60. The T-ALL cell line SUP-T1 (which constitutively expressed NIC1) was used as control for positioning of the NIC1 protein band. HRS cell lines KM-H2, L591 and HDLM-2 show high levels of NIC1. In opposite, L1236 NIC1 levels are barely detectable. HEK293 cells transfected with a control-vector (mock) or a NIC1-flag (this NIC1 construct does not possess the native NOTCH1 S3-cleavage epitope) expression vector were used for testing the specificity of the NIC1 specific antibody. β-actin or PARP1 were analyzed as control. $*$, antibody recognizing NOTCH1^{TM};$**$, antibody specifically recognizing the N-terminus of NIC1, which becomes accessible only after S3 cleavage.

3.1.12 Assessing the potential of MAML2 to activate NOTCH signaling

We next wanted to assess the potential of MAML2 to super-induce NOTCH1 dependent transcription in a system where NIC1 is present to some degree. To this end we used a NOTCH reporter assay that has been described in previous studies as detection system for NOTCH transcriptional activation [144]. The HES1 promotor region (-194 bp to +160 bp) was cloned in front of a firefly luciferase using the pGL2 vector as backbone (HES1 being a well characterized NOTCH target gene [144]). A thymidine-kinase driven luciferase construct was used for signal normalization. HEK293 cells were transfected with these reporter-constructs and different combinations of constructs coding for NIC1

and MAML2. HEK293 cells show low levels of endogenous MAML2 and NIC1. As seen in figure 3.19, there is a 3-fold activation of the NOTCH-reporter construct in HEK293 cells when transfected with NIC1, ectopic expression of MAML2 in turn leads to a 1.9-fold induction of the reporter construct. Ectopic expression of MAML2 and NIC1 leads to a 5.5-fold super-induction.

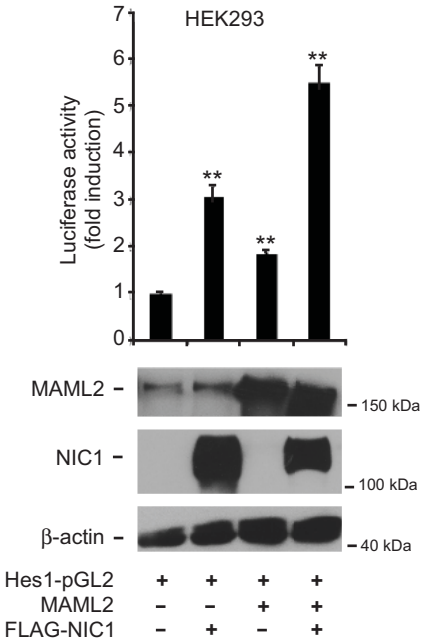

Figure 3.19: NOTCH1 reporter assay in HEK293 cells

HEK293 cells were used for a dual luciferase-based NOTCH reporter assay. Cells were transfected with different constructs and lysed 48 hours after transfection. In this cellular context, NIC1 as well as MAML2 activate this reporter system significantly, the combination of both expression constructs results in a super-induction of the reporter. Expression of all constructs was monitored using western blotting with whole cell lysates, β-actin was used as control. Error bars denote standard deviation. **:$p<0.001$

To extend this model system, we used the lymphatic cell line SUP-T1. This cell line shows only very weak MAML2 protein expression and high levels of NIC1 (see section 3.1.11). Thus we aimed to determine the effect of ectopic MAML2 expression on this system with inherent, aberrant NOTCH1 activity. Again, ectopic expression of NIC1

drives the reporter even more then just the already present levels of endogenous NIC1 (2-fold). This effect is observed to the approximately same extend (2.3-fold) when MAML2 is ectopically expressed. A 5.2-fold induction of the reporter is the result of ectopical expression of both members of the NOTCH transcription machinery (see figure 3.20).

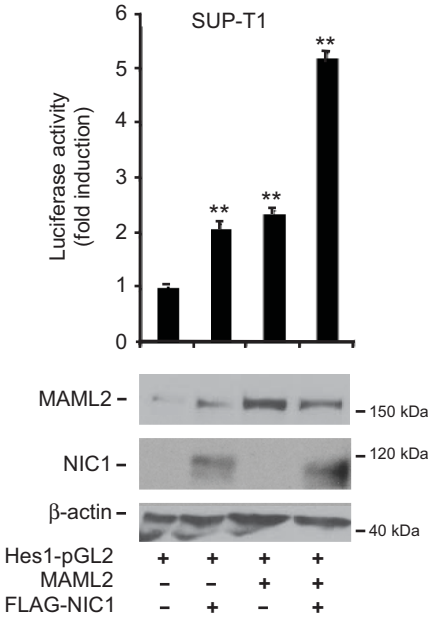

Figure 3.20: NOTCH1 reporter assay in SUP-T1 cells

SUP-T1 cells were used for a dual luciferase-based NOTCH reporter assay. Cells were transfected with different constructs and lysed 48 hours after transfection. In this cellular context, NIC1- as well as the MAML2-construct activate this reporter system significantly, the combination of both expression constructs results in a super-induction of the reporter. Expression of all constructs was monitored using western blotting with whole cell lysates, β-actin was used as control. Error bars denote standard deviation. **:$p<0.001$

From these data we concluded, that in a system, where NIC1 is present, high-level expression of MAML2 suffices to super-induce the NOTCH signaling pathway. Taken together, the data accumulated by then stated, that every core component of the NOTCH signaling pathway is present in cHL. As NOTCH1 is also present in its activated form, this argues for B cell inappropriate activation of the NOTCH signaling pathway in cHL, which might be essentially mediated by high-level expression of MAML2.

3.1.13 Establishing knockdown of MAML2 in HRS cell lines

To evaluate the contribution of MAML2 to cHL specific NOTCH signaling, we wanted to test the effect of MAML2 knockdown on different biological readouts. Initial attempts to do so by transfection of Dharmacon ON-TARGETplus SMARTpool MAML2 siRNA were confounded by weak MAML2 knockdown, especially when looking at MAML2 protein levels over time course. To overcome this limitation three of the sequences from the MAML2 siRNA SMARTpool were cloned into the pSUPER expression vector, which results in the efficient production of shRNA transcripts (hereafter these constructs are referred to as shMAML2). Almost complete knockdown of MAML2 was achieved using this approach (figure 3.21) over up to 72 hours of time. A respective control shRNA (hereafter referred to as shControl) construct was kindly provided by Dr. Martin Janz as described in [136].

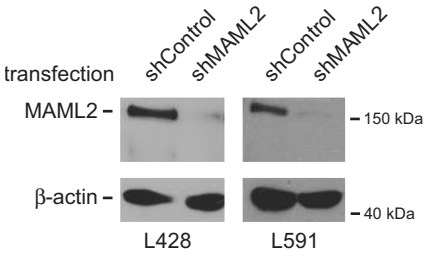

Figure 3.21: shRNA based knock down of MAML2

L428 and L519 cells were transfected with GFP and pSuper based constructs coding for shControl (targeting the firefly luciferase gene) or shMAML2 (targeting human MAML2). After 48 hours, GFP^+ cells were FACS-enriched, lysed and total protein extracts were analyzed using western blotting. MAML2 protein levels were knocked down almost completely in both L428 and L591. β-actin was analyzed as control.

3.1.14 cHL specific target gene regulation through MAML2 mediated NOTCH signaling

To identify NOTCH target genes that may be cHL-specifically deregulated through MAML2 mediated NOTCH signaling, we screened our NOTCH gene set for deregulated NOTCH target genes.

Re-screening the NOTCH GSEA analysis from section 3.1.5 (because of its less conservative statistical approach, GSEA also detects deregulated genes not detected by robust single-gene statistics), we found the NOTCH target genes HES7 and HEY1 to be part of the GSEA leading edge with a rank metric score of 0.75 and 0.66, respectively. Deregulation of these genes were subsequently tested with the known cell panel shown in figure 3.22 (a) using sqPCR. In comparison to non-Hodgkin cell lines, *HES7* mRNA is found at high levels in all HRS cell lines. In opposite, it is completely lacking in the non-Hodgkin cell lines. In case of *HEY1*, mRNA levels are robust in all HRS cell lines (except HDLM-2) and in non-Hodgkin cell lines comparatively low (Namalwa and BJAB) or lacking (Reh, BL-60, SU-DHL-4).

To assess the potential regulation of these two genes by MAML2 dependent NOTCH signaling, their mRNA levels were determined 48 hours after transfecting L428 and L591 with shControl or shMAML2 constructs (see figure 3.22 (b)). In L428, knockdown of MAML2 resulted in *HES7* levels significantly reduced to 58% of the respective control sample and in case of *HEY1* to 37%. In L591 this significant reduction was 51% for *HES7* and 63% in case of *HEY1* in comparison to according control samples. These results indicate, that high-level MAML2 expression in HRS cell lines is essential for *HES7* and *HEY1* mRNA expression. This argues in favour for aberrant NOTCH activation through MAML2 in cHL.

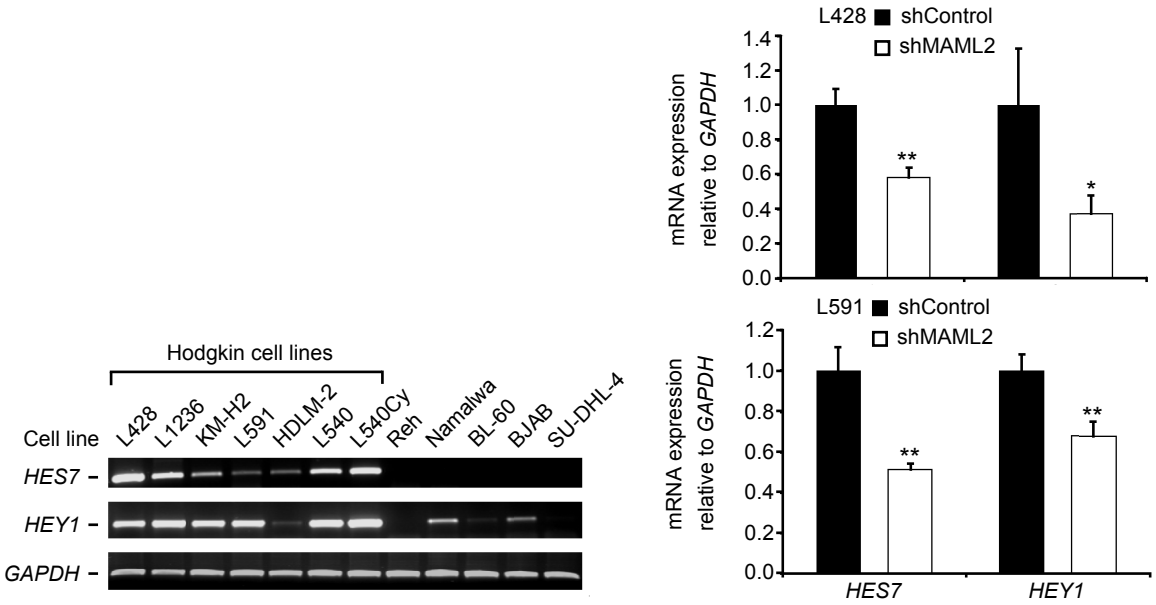

Figure 3.22: Expression status of *HES7* and *HEY1*

Analyses of *HES7* (a, upper panel) and *HEY1* (a, lower panel) mRNA expression were done using sqPCR. Compared to non-Hodgkin cell lines, *HES7* is highly expressed in HRS cell lines except in L591 and HDLM-2, which show comparatively low levels. In non-Hodgkin cell lines, no *HES7* mRNA was detectable. *HEY1* also is expressed at high levels in HRS cell lines except HDLM-2 when compared to its weak expression in non-Hodgkin cell lines (Namalwa and BJAB). *HEY1* mRNA is barely detectable in non-Hodgkin cell lines Reh, BL-60 and SU-DHL-4.
(b) L428 and L591 cells were transfected with GFP and shControl or shMAML2. GFP^+ cells were FACS-enriched after 48 hours. Subsequent qPCR analyses showed, that *HES7* as well as *HEY1* mRNA levels are significantly reduced after MAML2 knockdown. *GAPDH* was used as internal control or for relative quantification in qPCR, respectively. Error bars denote 95% confidence intervals. *:$p<0.05$; **:$p<0.001$

3.1.15 MAML2-mediated NOTCH activity is essential for HRS cell line proliferation

As further functional test of MAML2 mediated NOTCH signaling and in order to assess its biological significance, the proliferation potential of HRS cell lines L428 and L591 and the non-Hodgkin cell line BJAB (which does show high levels of activated NOTCH1, see figure 3.18) in dependency of MAML mediated NOTCH signaling was investigated using two different approaches described below.

Inhibition of cHL specific NOTCH signaling via transient knock down of MAML2

First, MAML2 was knocked down in cell lines L428 and L591 using the shMAML2 constructs described above. Though BJAB cells do not express MAML2 (see figure 3.11), they were also transfected with shMAML and shControl as to determine whether possible effects on proliferation are due to off-target effects or general toxicity of the shRNA constructs used. Proliferation was measured via ^{3}H-thymidine incorporation. As shown in figure 3.23(a), proliferation of L428 is reduced significantly down to 76% of the respective control and in case of L591 down to 51% of the respective control. BJAB cells were not affected significantly, implying, that in the B cell background of the cell lines used, treatment with the shMAML constructs used does not generally result in reduced proliferation. In turn, MAML2 expression thus essentially contributes to the proliferation potential of HRS cell lines.

Inhibition of NOTCH signaling via usage of a competitive peptide inhibitor

To test whether competitive inhibition of MAML protein binding to the NIC/CSL/DNA (pre-NTC) complex would also lead to reduced proliferation of HRS cell lines L428 and L591, a dominant negative version of MAML1 fused to pEGFP (DnMAML1) was used to transfect these cell lines. DnMAML1 is a truncated version of native MAML1 consisting only of amino acids 13 to 74. This version of MAML1 thus lacks the transactivation domains necessary for a transcriptionally active NTC. When ectopically expressed in a cell it will competitively inhibit native MAML binding to the NIC/CSL/DNA complex [135]. DnMAML1 binds to the pre-NTC with a seemingly higher affinity then any native MAML protein and therefore is a potent and specific inhibitor of NOTCH signaling [135, 100, 145].

Transfection of L428 with DnMAML1 resulted in proliferation reduced to 73% when compared to the respective control (pEGFP). Proliferation of L591 was also reduced

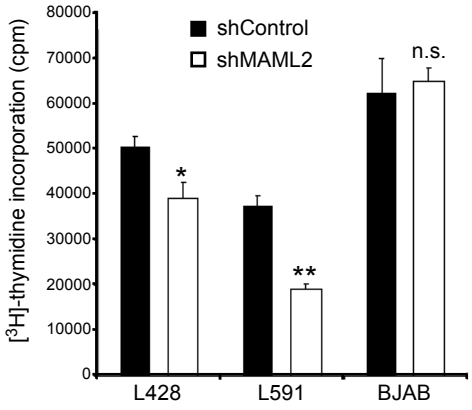

(a)

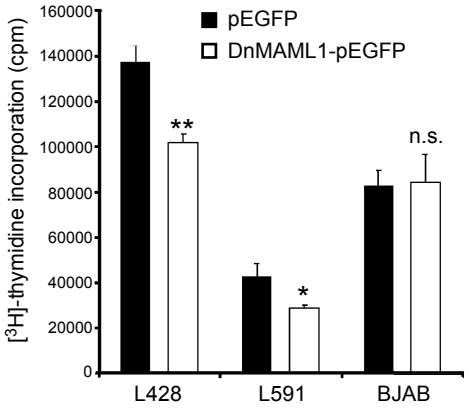

(b)

Figure 3.23: Impact of NOTCH inhibition

L428, L591 and BJAB cells were transfected with (a) GFP and shControl or shMAML2 constructs or (b), with GFP or DnMAML1-pEGFP. GFP^+ cells were FACS-enriched after 48 hours and subsequently used for ^{3}H-thymidine-incorporation based proliferation assays. Assays were harvested and measured 96 hours after initial transfection.
As seen in (a), knockdown of MAML2 protein results in significant reduction of proliferation of HRS cell lines L428 and L591, the same is the case when NOTCH signaling is inhibited using the competitive DnMAML1-pEGFP construct. Contrarily, BJAB cells are not affected by either construct, implying that treatment with these constructs does not generally affect proliferation of cells with a B cell background. Error bars denote standard deviation.
*:$p<0.01$; **:$p<0.001$; n.s., not significant.

down to 68% of the respective control (see figure 3.23(b)). In opposite, proliferation of BJAB cells tranfected with DnMAML1-pEGFP was not influenced when compared to

the control, despite the fact, that BJAB cells do show high levels of NIC1 (see figure 3.18). One may conclude, that in the specific BJAB context NOTCH1 signaling is not essential for the proliferation potential. Also, this result shows, that the treatment with DnMAML1-pEGFP is not generally toxic for cells with a B cell background.

3.1.16 Short summary and conclusions, part I

Below, the most important aspects and conclusions of part I of this work are listed:

- Statistical analyses of high-dimensional microarray data have shown, that cHL is characterized by a distinct and statistically significant NOTCH signature. It moreover revealed, that the whole gene-set defined NOTCH signaling system is differentially regulated in cHL when compared with primary samples and non-Hodgkin cell lines of other B cell associated malignancies.
- This signature is dominated by the essential NOTCH co-activator MAML2.
- A significant number of other NOTCH associated genes contributes to this signature (see appendix C).
- In contrast to normal tonsillar B cells, high MAML2 expression was detectable in malignant cells of various primary lymphomas.
- In a system, where activated NOTCH receptors are present, high-level MAML2 expression suffices to super-induce NOTCH mediated transcription.
- NOTCH signaling is aberrantly active in HRS cell lines in a cell-autonomous manner.
- NOTCH signaling is in part essential for HRS cell line proliferation and context specific NOTCH target genes.
- High-level MAML2 protein expression is partly essential for HRS cell line proliferation and context specific NOTCH target genes.

3.2 Part II: Targeting of the NOTCH transcriptional complex

As mentioned above, pathologic deregulation of NOTCH signaling is found in a wide variety of diseases. Treatment possibilities are sparse, especially when components of the NOTCH signaling system are deregulated by mutations or deletions (see section 1.2.2). Part I of this work has shown, that high-level expression of the NOTCH co-activator MAML2 provides an additional mechanism, how NOTCH signaling may be pathologically deregulated through deregulation of NTC components. As this deregulation takes place at the step of NTC assembly, it was obvious to use the NTC assembly as therapeutic target.

We thus were aiming to provide new ways of targeting NOTCH signaling at its very core, namely the NTC assembly process.

3.2.1 Inhibiting NTC assembly by small compounds

In a first approach, virtual high throughput screening (vHTS) was done in cooperation with Jens Peter von Kries' group at the Institute for Molecular Pharmacology (FMP), Berlin. Docking was done using Surflex-Dock (http://tripos.com). The keyorganics small compound database version of November 2007 was used as small compound input (www.keyorganics.co.uk). It consists of approximately 40,000 small compounds. CSL was used as target protein, the reasoning being, that a small compound binding to CSL would possibly inhibit binding of NIC and MAML proteins to CSL. As structural basis for the docking, the crystal structure of the NTC reported by Nam *et al.* [97] was used (PDB accession code: 2f8x, resolution= 3.25 Å, see figure 3.24).

To prepare the structure for virtual docking, NIC1, MAML1 and DNA structural data was omitted. Initially, we identified 10 compounds with high Surflex-Dock scorings that

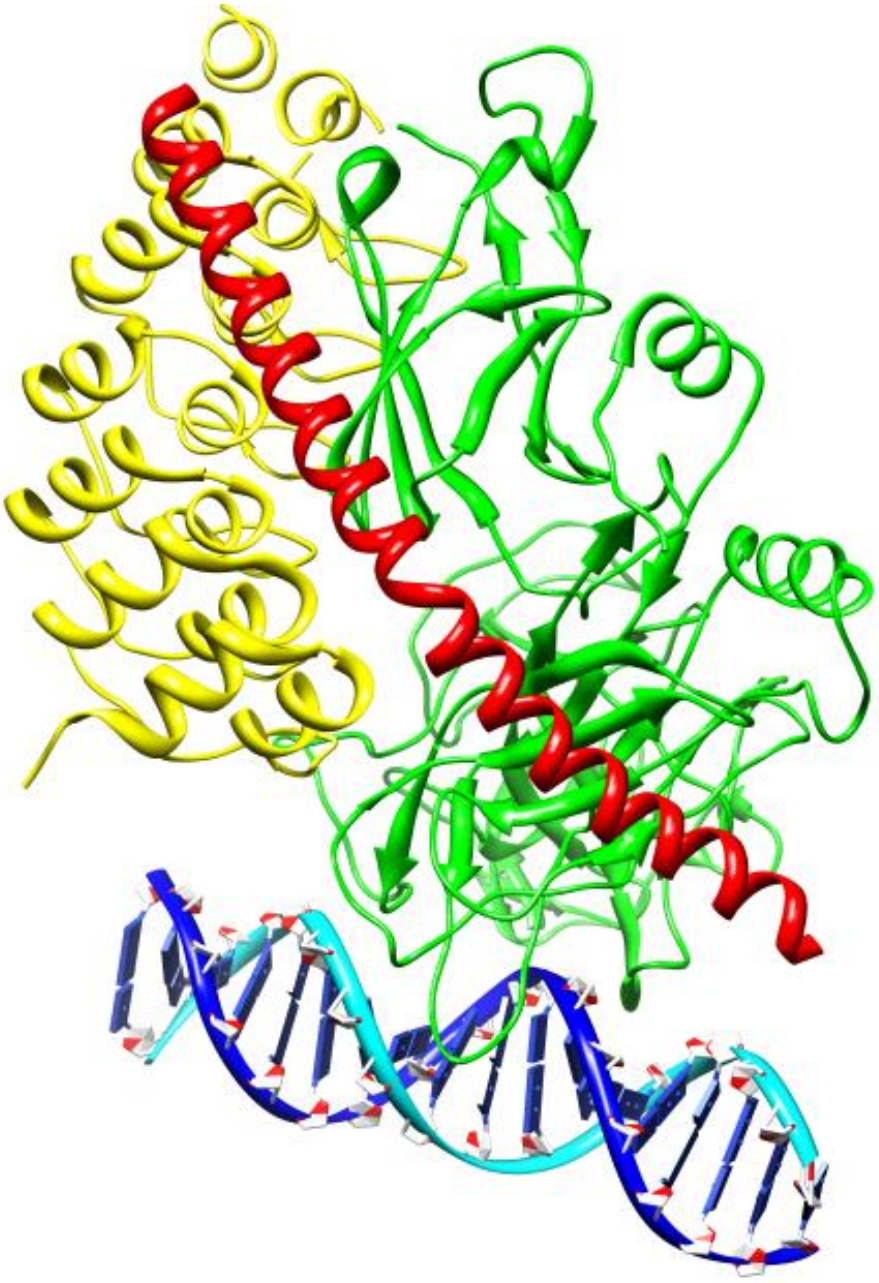

Figure 3.24: Crystal structure of the NTC, PDB code 2f8x

Crystal Structure of the NTC bound to DNA. Blue: DNA; green: CSL; yellow: Ankyrin repeat domain of NIC1; red: MAML1 amino acids 13-74. As repressive transcription factor, CSL stays bound to DNA at according CSL binding sites. Upon NOTCH1 receptor cleavage (S2 and S3 steps), NIC1 translocates to the nucleus, binds to CSL, thereby forming a dual binding interface to which co-activators of the Mastermind-like family may bind to form the transcriptionally active NTC. Crystal structure data was downloaded from www.pdb.org and rendered using the UCSF Chimera framework.

at the same time bound to CSL regions that represent the surface to which NIC or MAML proteins bind. The compounds have the following keyorganics accession numbers: 6M-003, 10B-35, 10B-049, 10E-23, 12P-818, 12R-0816, 12R-1182, 3K-521S, 3R-0688, 3R-0256. As exemplary result of the vHTS docking, the docked position of compound 6M-003 is shown in figure 3.25.

These compounds were then screened in a first functional screening in HEK293 cells transfected with the NOTCH-reporter construct described above, the control luciferase and the NIC1 construct to turn on NOTCH activity. Two compounds significantly reduced reporter activity at concentrations of 100 μM in comparison to DMSO treated control samples (for the complete table of results please see appendix D).

Further reporter assays were done with these two compounds in varying concentrations with the conclusion that at concentrations of 100 μM both compounds reduce reporter activity to 41% (6M-003) or 51% (12R-0816) of control activity (see table 3.5). At this point functionality of these compounds seemed promising, additional substantiation of this finding was done using proliferation assays of two cell lines with constitutive NOTCH1 signaling (SUP-T1 and ALL-SIL [145, 130]) and one control cell lines which does not show NOTCH1 signaling activity (Reh). Proliferation assays were performed at differing concentrations of 6M-003 and 12R0816 (1 μM, 35 μM, 65 μM, 100 μM) and DMSO as control (see figure 3.26). All cell lines tested had significantly reduced proliferation at 100 μM of either compound. This may be interpreted as the compounds having unspecific effects at such concentrations. Nevertheless, cell line ALL-SIL also showed reduced proliferation at 35 μM and 65 μM concentrations of 6M-003. It was therefore decided, to test and measure whether binding of these compounds to CSL would occur.

Figure 3.25: Result of 6M-003 docking to CSL

Result of the Surflex-Dock based 6M-003 docking to CSL. Blue: CSL; turquoise: Ankyrin repeat domain of NIC1; green: MAML1. 6M-003 is presented as centrally positioned stick-model.

3.2.2 Establishing purification of human CSL

To this end the sequence for human CSL spanning amino acids 9-435 were cloned into pSKB2LNB with a N-terminal His-tag and a PreScission-protease-site. Protein expression was induced by addition of 100 μM IPTG and was grown over night at 18°C. Protein was then purified successively using Ni-NTA His-Tag purification, cutting of the tag with PreScission-protease and subsequent final purification using size exclusion chromatogra-

compound	6M-003					12R-0816			
concentration	100 μM	65 μM	35 μM	1 μM	$1^0/_{00}$ DMSO	100 μM	65 μM	35 μM	1 μM
luciferase ratio	0.522	0.588	0.627	1.286	1.385	0.718	0.830	1.106	1.434
standard deviation	0.056	0.058	0.039	0.117	0.100	0.066	0.063	0.105	0.107

Table 3.5: NOTCH-reporter inhibition by small compounds

Dual luciferase NOTCH reporter assay was used to determine impact of compounds 6M-003 and 12R-0816 on NOTCH reporter activity in HEK293 cells. At a concentration of 100 μM, both compounds reduced reporter activity by ≈50%.

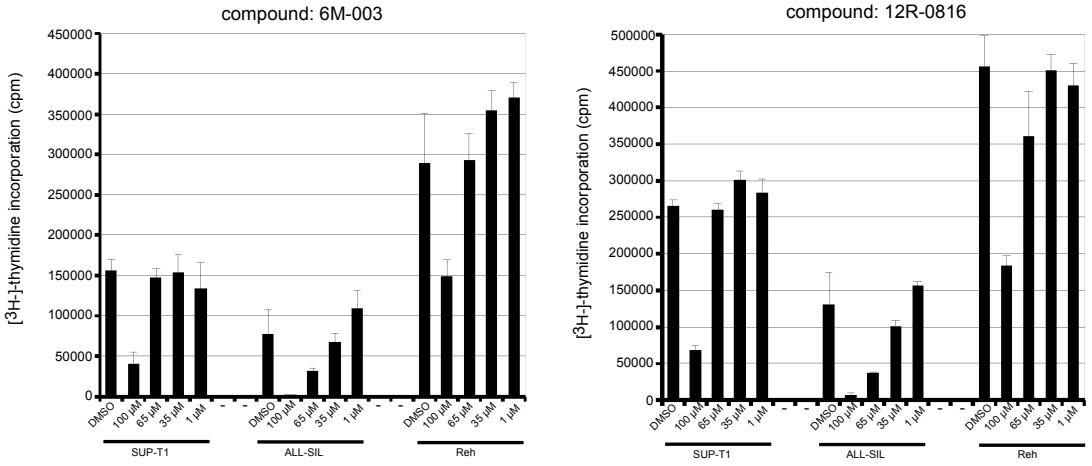

(a) (b)

Figure 3.26: Impact of 6M-003 and 12R-0816 on the proliferation of various cell lines

To assess impact of the two small compounds 6M-003 (a) and 12R-0816 (b) on proliferation, [^{3}H]-thymidine incorporation was measured in cell lines dependent on NOTCH signaling (SUPT1 and ALL-SIL [145, 130]) and the cell line Reh, which is not known to be NOTCH dependent. [^{3}H]-thymidine incorporation was measured 120 hours after adding the compounds at various concentrations or DMSO at $1^0/_{00}$ final concentration. [^{3}H]-thymidine was added 96 hours after assay start. Error bars denote standard deviation.

phy (see figure 3.27(a)). Analysis of the purified CSL on SDS-PAGE is shown in figure 3.27(b). Protein was also extracted from the gel and analyzed using mass spectrometry to verify that the band in question is CSL. Apart from various *E. coli* proteins that were detected, human CSL was identified with a MASCOT match score of 744 (please see appendix E for a MASCOT report summary). To measure binding affinity of the

compounds to CSL, Isothermal Titration Calorimetry (ITC) was used. No saturation of a presumed binding activity was measurable, it was thus assumed, that either compound does not specifically bind to CSL (see appendix F). Biological effects as seen in the NOTCH1 reporter assays therefore have to be unspecific as well, both compounds are therefore not usable for specific inhibition of NTC assembly.

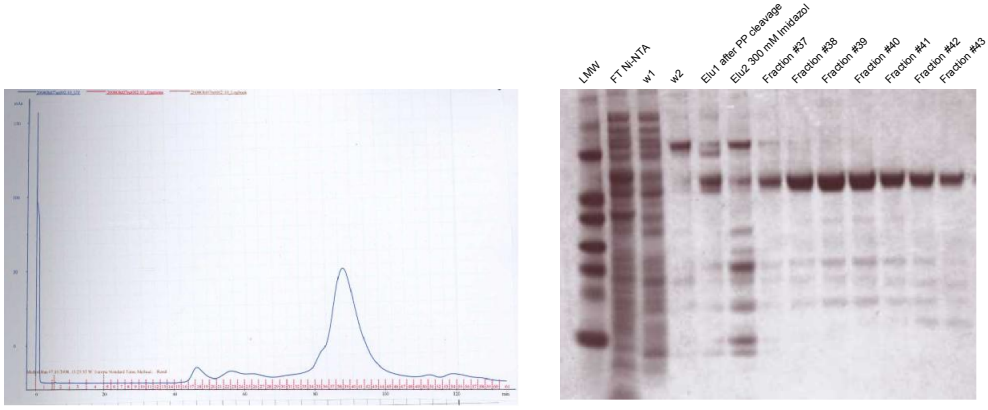

(a) (b)

Figure 3.27: Purification of human CSL

Human CSL was purified using His-tag based affinity chromatography, followed by a polishing step using size exclusion chromatography on a Sephadex G-200 column (a). (b) shows presence and purity of recombinant CSL during various steps of the purification. LMW: low molecular weight marker; FT Ni-NTA, flow through of the affinity column, note that only little CSL is seen in this fraction; w1: wash 1; w2: wash 2; Elu1: 1^{st} elution after precision protease cleavage on the affinity column; Elu2: 2^{nd} elution of affinity column using 300 mM imidazol, note, that most CSL is already eluted in Elu1; Fractions #37-#43 correspond to the big elution peak in (a). Most CSL is found in fractions #38-#40.

3.2.3 Alternative targeting of the NTC

Usage of the small compounds 6M-003 and 12R-0816 to inhibit stable complex formation of the NOTCH transcriptional complex could not be proven to work in a NOTCH specific manner. It can not be ruled out, that more sophisticated methods of measuring binding energies with for example all NTC components plus the compounds could prove to be successful in terms of specific compound-NTC binding. Yet, in regard to available

technical expertise and time-management this would have been beyond the scope of this study.

Hence, a different strategy was developed. Based on the knowledge, that the truncated version of MAML1 comprising amino acids 13 to 74 (DnMAML1), is a potent inhibitor of NOTCH signaling, it was reasoned, that this might be a lead-peptide for developing a potent NOTCH inhibitor. This peptide is still too long for scaled up chemical synthesis, which would be needed as technical prerequisite for any potential drug. Additionally, the smaller the peptide, the better its behavior in terms of bioavailability and the ratio of cytoplasmatic to nuclear localization [146, 147, 148]. It was thus reasoned, that even more truncated versions of this peptide would have to be designed and tested in order to endorse or deny the possibility of such a peptide drug. Caveats of this approach are the uncertainty of whether any synthesized peptide will subject to form the alpha-helix that is inherent to the complete MAML1 protein by self-folding as soon as it is within the cell. To circumvent this potential problem and in order to visually monitor expression, it was decided to first design peptide-GFP fusion constructs for expression directly within mammalian cells, thus producing correctly folded peptide-alpha-helix-GFP fusion proteins. For the design of the peptide sequences to be used, the binding interface as presented by the crystal structure of the NTC was screened for possible charge-based interactions and hydrogen bonds. This screen and a recent publication using mutational analysis of the MAML1 protein led to the identification of MAML1 amino acids R22, R25, R26, C30, R31 and H34 being the energetically most important residues in terms of binding enthalpy [149, 97, 150, 151]. Moreover, it has been shown, that DnMAML1 competitively inhibits binding of all three members of the mastermind-like family, as the residues important for complex formation are highly conserved among the human MAML proteins [96, 100]. Using this information lead to the design of two peptide-GFP constructs (see figure 3.28), where one comprises MAML1 amino acids 13

to 50 (hereafter referred to as DnMAML1 AA 13-50) and the other spans MAML1 amino acids 19 to 36 (hereafter referred to as DnMAML1 AA 19-36). Both were N-terminally fused to GFP for further functional analysis in appropriate *in vitro* systems.

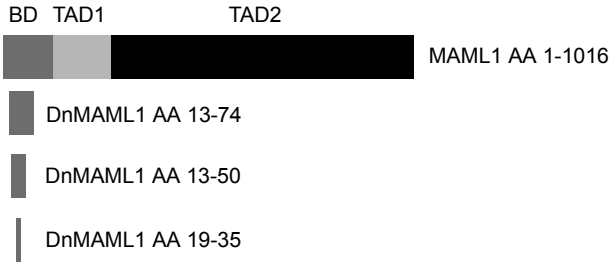

Figure 3.28: Design rationale of NTC inhibiting peptide constructs

Based on crystal structure information and mutation studies, two shortened MAML1 based peptide constructs were designed for further testing of their potential to specifically inhibit NOTCH signaling. The domains of native MAML1 (AA 1-1016) are shown, all inhibitory peptides are positioned in the binding domain (BD) that mediates binding to NIC and CSL. TAD: trans activation domain.

3.2.4 Short MAML1 based GFP-fusion constructs effectively inhibit induction of a NOTCH reporter assay

To test the various DnMAML1-GFP fusion constructs, the cell line SUP-T1 (with inherent constitutive NOTCH signaling) was transfected with the NOTCH1-reporter construct, the according control construct (both described in section 3.1.12) and either of the truncated versions of MAML1. Using the classical construct (DnMAML1 AA 13-74) the NOTCH activation dropped to 9.6% of the basal SUP-T1 level, using DnMAML1 AA 13-50 the level was reduced to 30.5% and using DnMAML1 AA 19-36 reduced basal levels of NOTCH reporter activation down to 54.0%. We concluded, that all three constructs significantly reduce reporter activation in this *in vitro* system and subsequently wanted to further substantiate this finding by additional functional studies.

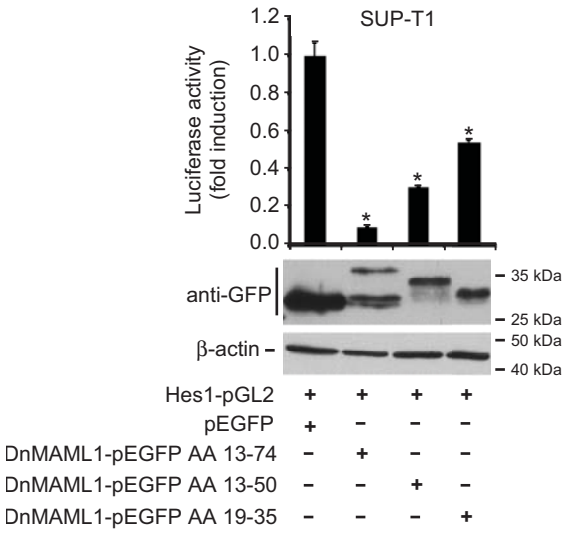

Figure 3.29: Inhibition of a NOTCH-reporter system by small peptide constructs

The T-ALL cell line SUP-T1 was used for measuring NOTCH1 reporter activity after transfection with the NOTCH1-reporter construct (Hes1-pGL2) or its respective control (pEGFP) and the various short, MAML1 based, GFP-fused peptide constructs. Cells were lysed and luciferase ratios measured 48 hours after transfection. Error bars denote standard deviation. Western blot analyses of whole cell lysates were done for controlling the expression of the various constructs. Note, that all pEGFP fusion constructs possess alternative start sites for expression of GFP only. This might explain why — e.g. in case of the DnMAML1-pEGFP AA 13-74 — apart from expression of the peptide-GFP construct, additional expression of a GFP-sized protein is detectable. *: $p<0.001$

3.2.5 Monitoring of the inhibition of NTC assembly using EMSA

To assess NTC assembly, electrophoretic mobility shift assays (EMSA) were performed with the consensus HES1 binding site as probe (described in [134]). Three core components of the NTC (NIC1, CSL, MAML1) were ectopically expressed in HEK293 cells. Each truncated version of MAML1 was then tested to see possible out-competition of native NTC formation. As seen in figure 3.30, ectopic expression of NIC1, CSL and MAML1 resulted in stable formation of the transcriptionally active high molecular weight NTC. Adding DnMAML1 AA 13-74 results in almost total out-competition (no high molecular weight NTC is detectable by EMSA) of native, full length MAML1. Subsequently a NTC with a substantially lower molecular weight is formed and visible

by EMSA analysis. Using either of the shorter constructs (DnMAML1 AA 13-50/AA 19-36) also resulted in reduced detection of the high molecular weight NTC which is vastly reduced in case of DnMAML1 AA 13-50 and well reduced when using DnMAML1 AA 19-36. Notably, no lower molecular weight complex is detectable with these two shortest constructs, presumably because formed complexes are highly unstable, thus being undetectable by EMSA analysis.

At that time, a study from Moellering *et al.* was published [145], that also focused on the development of short, MAML1 based competitive peptide inhibitor constructs. In this work they found, that indeed amino acids 21-36 of MAML1 suffice to construct a potent competitive peptide inhibitor, that can disrupt native NTC formation. As a chemical modification, Moellering *et al.* introduced an olefin bridge (a process they called peptide-stapling) that significantly enhances α-helical folding of this peptide sequence - the conformation needed for binding of MAML proteins or their derivatives to the dual binding interface of NIC and CSL. In a broad *in vitro* and *in vivo* study, these peptide constructs were shown to inhibit NOTCH signaling in a highly specific manner [145]. Therefore, our findings are in good accordance with their results.

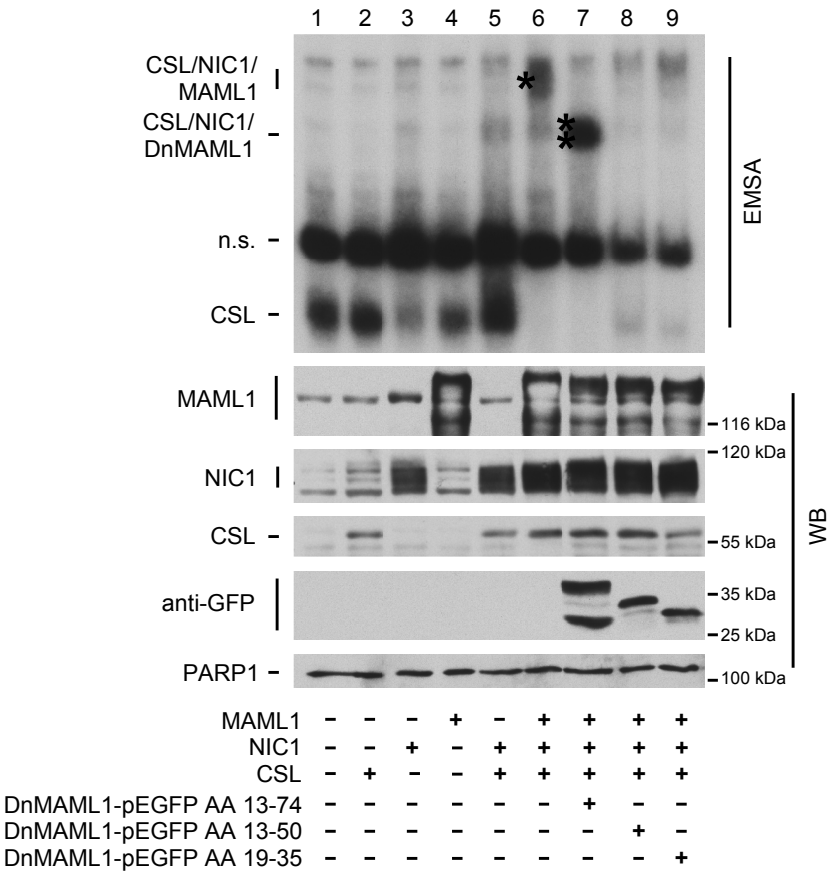

Figure 3.30: Peptide inhibition of NTC assembly

HEK293 cells were transfected with various constructs to monitor assembly of the normal NTC and the inhibition of this assembly by usage of differently sized MAML1 based peptide constructs. Cells were harvested 48 hours after transfection and used for preparation of nuclear extracts. These were then analyzed using a Hes1-probe EMSA. Expression of all constructs was monitored using western blotting, where PARP1 was used as control. Normal NTC assembly is only seen, when the four essential NTC components DNA, CSL, NIC1 and (in this case) MAML1 are present in sufficient amounts (see lane 6, marked with *). This complex assembly is inhibited by the presence of short, MAML1 based peptide constructs, in case of the classical DnMAML1 AA 13-74 this will result in the formation of a stable, transcriptionally inactive NTC (see lane 7, marked with **). Transfection with the two constructs designed in this study also significantly inhibits NTC complex assembly (see lanes 8 and 9). n.s.: unspecific band.

3.2.6 Short summary and conclusions, part II

Below, the most important aspects and conclusions of part II of this work are listed:

- vHTS of ≈40,000 small compounds from the Keyorganics small compound database led to the identification of 10 compounds that potentially may bind to human CSL in a specific manner.
- Two of these compounds (6M-003 and 12R-0816) significantly inhibited NOTCH transcriptional activation in a NOTCH1-reporter assay. They also inhibited proliferation of NOTCH1-signaling dependent cell lines (SUP-T1 and ALL-SIL). Yet, this is also the case for a cell line which presumably is not dependent on NOTCH signaling (Reh).
- Binding studies using ITC did not show specific binding of either compound to human CSL. However, it can not be ruled out that NTC assembly might be disrupted by these compounds.
- Short, MAML1 based peptide-GFP fusion constructs significantly inhibit NOTCH transcriptional activation in a NOTCH-reporter assay and NTC assembly *in vitro*.

4 Discussion

4.1 Identification of a new NOTCH-deregulating mechanism through analyses of high-dimensional data

Analyzing the cHL NOTCH signature

Using the analyses of high-dimensional microarray data, this work shows, that cHL is characterized by a distinct and global NOTCH signature which separates this malignancy clearly from other B cell associated malignancies. This NOTCH signature shows, that various genes involved in this pathway are deregulated in HRS cell lines and also in cHL primary material when extending the analyses with the dataset GSE12453. It thereby confirms earlier studies [55, 56, 74, 75] and extends the cHL-context view on NOTCH signaling from relatively view NOTCH core components and target genes to a NOTCH-global perspective. Considering the significant number of deregulated, overlapping genes comparing primary cHL samples and HRS cell lines (globally and for NOTCH associated genes), these results also imply that HRS cell lines are still very similar to cHL primary cases and thus are a well suited experimental system for cHL research.

The NOTCH gene set for this study was compiled with the aim to provide a systemic understanding and specification of the NOTCH signaling pathway. Research on the

NOTCH signaling pathway is in the focus of many scientists and in turn, much data on this pathway is being published constantly. Hence, the NOTCH gene set designed in this study will have to be recompiled from time to time, as more evidence about NOTCH associated genes becomes available and existing information is refined or rejected due to new studies.

Though making systemic understanding of NOTCH signaling more readily conceivable, our NOTCH gene set is not by itself giving any information about the relations and inter-dynamics of its components. Therefore — as future prospect — the members of this set should be used as basis for inferring directed NOTCH regulatory networks. This would be a major step in terms of gaining insights into the directionality and connectivity of NOTCH associated genes with each other. Of course this may be extended to networks that are in close proximity to NOTCH signaling. Also this set should be used when trying to confirm or reject the hypothesis of deregulated NOTCH signaling in other malignancies and may prove to be a helpful tool in this regard.

From analyzing the cHL NOTCH signature, we detected the high-level expression of the essential NOTCH co–activator MAML2, which is inappropriate when comparing HRS cell lines to non-Hodgkin cell lines. This finding was extended and confirmed for the comparison of normal, tonsillar B cells with primary material from cHL samples, and was extended to other B cell associated malignancies such as B-ALL and MCL. This should result in focused research elucidating the role and possibility of MAML2 mediated and deregulated NOTCH signaling in these malignancies, at the same time using gained information for finding of therapeutical approaches.

Our data moreover imply, that in terms of NOTCH target gene regulation (*HES7* and *HEY1*) and NOTCH dependent proliferation, high-level MAML2 expression may be rate limiting for cHL context-specific NOTCH signaling.

To confirm this hypothesis in future studies, the presence and the quantity ratio (to

the other MAML members) of MAML2 as part of an endogenous, native cHL NTC needs to be demonstrated. Yet, so far, no published study could provide data on an endogenous NTC, all studies of the NTC use recombinant or ectopically expressed NTC component proteins (see for example [96, 134, 150]). The difficulty in detection and the analysis of an endogenous NTC is most probably due to the fact, that it is present as a 1.5 MDa complex (the NTC recruits various other proteins of the basic transcriptional machinery, see above) [152]. This complex size results in various technical difficulties. Jeffries *et al.* [152] used a sophisticated set up of sub-cellular fractionation followed by SEC for detection of NTC components and were able to co-elute ectopically expressed NIC1 with native CSL and MAML proteins. This technical approach could be adapted and enhanced for future studies aiming to dissect the characteristics of native NTC complexes in cHL.

Pointing out a discrepancy

In 2005, Zweidler-McKay *et al.* [76] showed that transduction of the HRS cell line L428 with a NIC1 and GFP expressing viral construct resulted in decrease of the percentage of GFP^+ cells over time. This was interpreted as growth arrest, and — using the same experimental approach — was extended to other B cell associated malignancies. Contrarily, our findings indicate that NOTCH signaling is essential for HRS cell line proliferation. It may be speculated, that the experimental approach chosen by Zweidler-McKay *et al.* is too artificial and hard to control in terms of viral integration sites and subsequent, anti-proliferative effects. Additionally, the measurement of the percentage of GFP^+ cells as indicator for proliferation is a far more indirect parameter in comparison to e.g. ^{3}H-thymidine incorporation, which could hamper the interpretability of results.

What to consider, when analyzing the NOTCH signaling system

Adding to the known mechanisms which lead to deregulation of the NOTCH signaling pathway, namely mutations within NOTCH receptors and mutations of ubiquitin ligases that mediate the turnover of the NTC, we showed that high-level expression of NOTCH co-activators will also deregulate NOTCH signaling in a pathological manner (figure 4.1). This is also the case in cells where the obvious levels of NIC within the nucleus are relatively low (e.g. L428 and L1236) but in conjunction with high concentrations of MAML2 protein still suffice to deregulate NOTCH signaling. In opposite, high levels of NIC still do not have to result in aberrant and NOTCH-dependent proliferation of cells (e.g. in the case of BJAB cells). This points out that, when looking for deregulated NOTCH signaling in different disease entities, it is not sufficient to just assess levels of NOTCH receptor expression (as for example done in [56]), but it is rather essential to look at all activating core components — cleaved NOTCH and the Mastermind-like co-activators. Whenever possible, even all components associated with NOTCH signaling should be looked at quantitatively in order to get a global picture of the state of NOTCH signaling in a cellular system.

Not only MAML2, but regulation of various other genes may be the result of or influence cHL specific NOTCH signaling

Recent studies have shown a limited number of NOTCH associated genes to be deregulated in cHL [55, 56, 74, 75]. The deregulation of many of these genes (see above and appendix C) could be confirmed and was extended to a NOTCH-systemic analysis which has shown a significant deregulation of the NOTCH signaling system. As a most interesting gene found to be NOTCH1 regulated in HRS cell lines [75], the T-cell transcription factor GATA3 was also one of the most significant hits when analyzing the different datasets described above (see table 3.3 and also appendix C). Another

gene found in our statistical analyses in accordance with previously published data (see [55, 56]) was NOTCH2. Due to the unavailability of a specific antibody detecting the cleavage product of NOTCH2 (NIC2) we could unfortunately not analyze, whether this receptor may also contribute to a super-induction of NOTCH signaling in HRS cell lines. Future studies will have to elucidate this possibility.

Interestingly the cHL specific deregulation of the basic helix-loop-helix transcription (bHLH) factor HES7 which this study shows to be due to MAML2 deregulation may also result in another mechanism deregulating E2A activity. The deregulation of E2A in cHL is a commonly known defect and various mechanisms have been described that contribute to this deregulation. Mathas *et al.* [48] for example have shown, that high levels of ABF1 and ID2 inhibit E2A dependent transcription which ultimately contributes to the cHL-typic loss of the B cell phenotype. In a recent study HES7 — being a repressive transcription factor — was shown to inhibit E2A dependent transcription [153]. Future research will have to focus on this being another potential mechanism of inhibited E2A dependent transcription in the specific context of classical Hodgkin lymphoma.

One has to mention, that the deregulation of JAG2 was not detected by gene expression profiling, presumably because biological group-variance is too large. As result, the applied statistical tests did not deem this gene to be significantly deregulated. One has to conclude, that the analyses of high-dimensional data from disease entities is always to some degree dependent on genetic homogeneity. If possible, gene expression profiling should therefore always be completed with complementary array-qPCR for the gene sets of interest.

Many other genes with a putatively very important role in cHL-specific NOTCH signaling (see table 3.3) will have to be functionally analyzed in regard to their contribution to NOTCH deregulation in future studies.

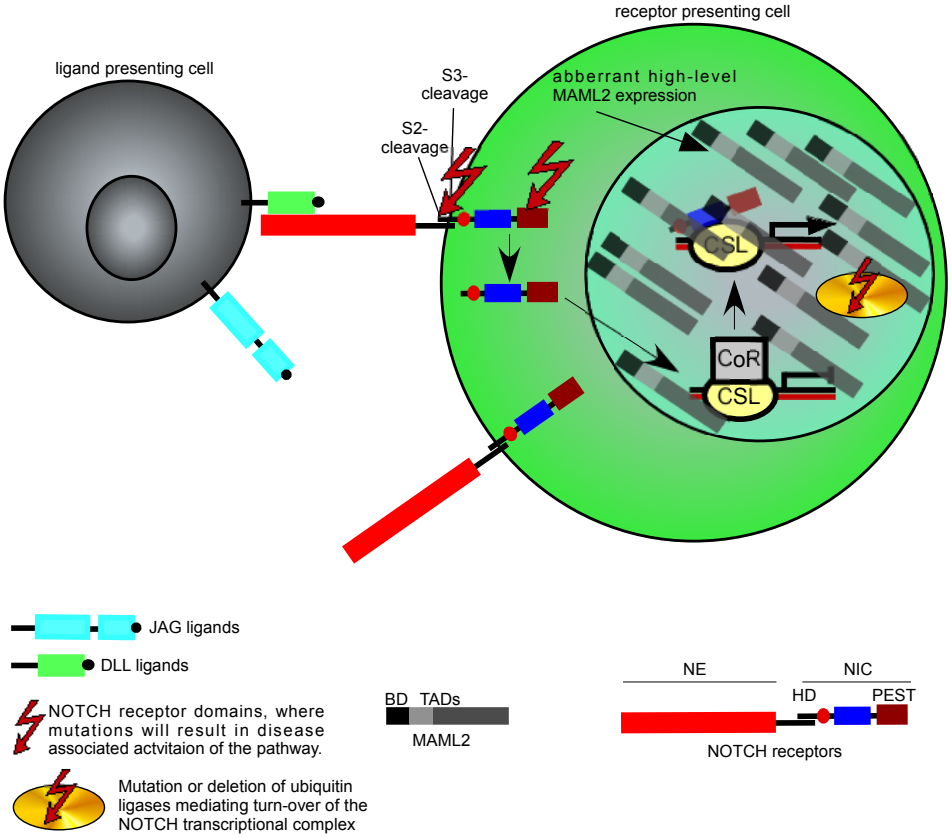

Figure 4.1: A new NOTCH-deregulation mechanism

In diseases associated with deregulated NOTCH signaling (e.g. T-ALL), two major mechanisms have been elucidated, that will result in pathological deregulation of the pathway. First, mutations of the NOTCH receptors, especially of the HD and PEST domains will lead to facilitated cleavage or reduced turn-over, respectively. Second, mutation or deletion of ubiquitin ligases involved in turn-over of the NOTCH transcriptional complex will result in increased half-life and hence, sustained transcriptional activity of the complex.
This study shows, that — in case of cHL — high-level expression of MAML2 also provides a mechanism for deregulating the NOTCH pathway significantly. This points out the importance to therapeutically target this complex at its assembly stage rather than upstream of the signaling cascade.

Cell-autonomous NOTCH activation in cHL

In this study we show evidence, that NOTCH1 signaling is not only super-induced by high-level MAML2 expression but also activated in a cell-autonomous fashion. In HRS cell lines, additionally to the activation through the cHL microenvironment as suggested by Jundt *et al.* [56] it confirms and extends studies that already suggested this cell-autonomous activation (by showing target gene regulation in HRS cell lines after NOTCH1 knockdown, see [74, 75]). As most important proof for this hypothesis, we have shown the constitutive presence of NIC1 in the nucleus of HRS cell lines.

The cleavage of the NOTCH1 receptor to NIC1 seen in all HRS cell lines at low to high levels may be due to the high-level expression of JAG2 in various HRS cell lines and the high-level expression of JAG1 in L591. The contribution of these two ligands to activated NOTCH signaling will have to be demonstrated in future studies, especially taking into account a recently published mathematical model trying to integrate *cis* and *trans* NOTCH/ligand interactions to a specific intracellular read-out [112]. This study focused on NOTCH1/DLL1 interactions, and indicates that *cis*-NOTCH/ligand interactions rather inhibit NTC activation, whereas *trans*-activations will activate NTC dependent transcription, a finding that was partly extended to JAG1 by Cordle *et al.* [154].

Mastermind-like proteins emerging as master regulators

What still remains to be elucidated, is the role of cross-effects of different MAML proteins and their individual specific effects on NOTCH signaling and the fine-tuning of NOTCH signaling. It is interesting, that MAML1 is expressed at similar levels in all cell lines tested and MAML3 is only present at robust levels in some of the cell lines tested. Yet, inhibiting the high-level expression of MAML2 is already sufficient to block NOTCH mediated proliferation and expression of certain target genes in cHL. These

results, though indicating that MAML1 and MAML3 mediated NOTCH signaling is pathologically less important in cHL, will have to be further substantiated by functional experiments, especially when one wants to elucidate their potential role in other B cell associated malignancies.

More generally, a study by Kitagawa *et al.* reported on the potentially important role of MAML1 analyzing MAML1$^{-/-}$ mice [101]. These mice show severe growth retardation and early death at day 14 of the postnatal period. Seemingly, MAML1 deficiency also results in impaired development of early thymocytes and also shows clear inhibition of the development of marginal zone B cells [92]. This emphasizes the importance of MAML1 in the development the hematopoetic compartment, whether this is purely the result of MAML1 mediated NOTCH signaling is unknown and will have to be shown in future studies. The result, that HES1 levels in MAML1$^{-/-}$ mice were not significantly reduced in comparison to MAML1$^{+/+}$ mice points into the direction, that there may be other mechanisms affected by MAML1. Also, inhibition of NOTCH signaling using dominant negative mutants of either MAML1, MAML2 or MAML3 in murine hematopoetic stem cells resulted in early inhibition of T-cell development and the appearance of intrathymic B cells [100]. This implies that either MAML member may be of vital importance for Notch-mediated cell fate decisions.

Adding to the complexity, more and more studies extend the picture of the MAML1 co-activator to other pathways then NOTCH signaling. Regulation of NF-κB signaling through Maml1 regulation of p65 and IκBα has recently been shown *in vitro*, furthermore MEF2C regulation and even p53 activity seem to be in part to be mediated through the MAML1 protein [103, 155, 156]. In addition, the activity of the MAML1 protein seems also to be regulated through certain mechanisms. Lately one study revealed, that SUMOilation may prove to be an important factor determining in how far MAML proteins are capable of activating e.g. NOTCH signaling [99].

Unfortunately, little to nothing is known about the specific role of MAML2 and MAML3 in the differentiation process of hematopoiesis and about their role in differentiated tissues as most studies focus on MAML1. However, studies with ectopic expression of the MAML2 and MAML3 proteins show that they do have a great potential in activating the NOTCH signaling pathway significantly [95, 96]. Other studies show that translocation of the MAML2 gene and its fusion to genes such as MECTC1 and TORC1 will lead to oncogenic events [104, 105] and thus imply that MAML2 has the potential to activate various intracellular signaling pathways. Our study additionally provides data that clearly speaks in favor for an important role of MAML2 in — at least — the lymphocytic context. Nevertheless, much work will have to be done in order to unravel the functions of these proteins by using for example adequate mouse models.

Putting NOTCH signaling in a wider context

A recent study has shown, that the up-regulation of the T-cell transcription factor GATA3 in HRS cell lines is caused by two major signaling pathways — NOTCH and NF-κB [75]. More generally, the fact that p65 and CSL DNA consensus-binding sites show strong similarity [157, 158] also point out, that both pathways may compete for regulation of the same target genes and will make it necessary to develop a systemic view on both pathways and their possible interplay in different cellular decision-making processes. This systemic view on NOTCH and NF-κB signaling ultimately will have to be extended to a holistic description of cHL as disease system, putting each pathway-subnetwork in its place and in relation to other pathway-subnetworks.

Overall, this newly unraveled, MAML2 dependent deregulation mechanism of NOTCH signaling adds to the complexity of this pathway. As this deregulation takes place at the DNA-protein level and in this respect the core-site of regulation of NOTCH mediated transcriptional activation it is of utmost importance to target NOTCH signaling at this level.

4.1.1 Systemic disease models for cHL — a perspective

Various major pathways of the hematopoetic system have been shown to be severely deregulated in classical Hodgkin lymphoma and there is now evidence that additionally epigenetic dysregulation plays an important role in the pathogenesis of this disease [46, 57]. The gene expression analysis we performed showed ≈4700 features to be significantly deregulated in HRS cell lines when compared to non-Hodgkin cell lines. One may easily conclude, that it will still take decades to put all these results into perspective, especially when each and every possible hypothesis will have to be validated experimentally. Rather than looking at every factor one at a time it will be of great importance to use available datasets to describe cHL in a systemic fashion. In order to do so, it will not be sufficient to use standard statistical procedures such as cluster analysis, PCA or GSEA that are being used currently to systematically describe disease entities [24, 57, 159]. While these kinds of analyses set a good basis for hypothesis generation, they lack the capability of connecting different pieces of information. This caveat can be accounted for by generation of — in case of cHL — complete B cell network models. Recent publications have shown promising results in this respect [160, 161, 162] yet in case of Bayesian and mutual-information based network models, there is still much potential of improvement in terms of for example run-time complexity, the possibilities to integrate different data types and to account for technical variance in between different datasets. Nevertheless, inference of near-complete genetic interaction and regulatory networks enables researchers to identify and select functional clusters that are most promising in disrupting the cellular interaction network of a specified disease. This will be essential as to find new therapeutic approaches possibly circumventing late toxicities due to deployment of traditional chemotherapy and radio therapy that are a common feature of traditional cHL treatment. According to network theory of biological networks one would assume, that there are only relatively few major hub-proteins within

the network and that these important proteins have a shallow interaction architecture [163]. Identifying them will provide molecules, that should be targeted therapeutically. In regard to this work, we have shown how computer-aided analyses of data from high-throughput-experiments helps to understand disease-specific pathway regulation at systemic/holistic level. Extension of these analyses to even larger datasets will at some point enable researchers to completely infer a systemic cHL disease model.

4.2 Strategies to target NTC assembly as therapeutic approach

Using vHTS for small compound identification

Virtual High Throughput Screens and computer aided compound design are basically free of charge tools to predict compound binding to proteins. This technique has successfully been applied in a growing number of studies [164, 165]. Different docking algorithms have been developed and many of them have proven useful in some studies [166]. Success though is so far mostly limited to enzymes and receptor-proteins. Both classes of molecules normally contain binding grooves for native ligands. These grooves usually have special biophysical and structural characteristics predisposing them for stable binding of compounds with complimentary characteristics. In opposite, successful small compound binding to proteins that do not display such binding grooves seems particularly hard to accomplish. The NOTCH transcriptional complex consists of proteins, that mainly present flat surfaces rather then cavities. Moreover the available crystal structure of the NTC has only a low resolution (3.25 Å, see [97]). Taking into account the cost-effectiveness and rapidity of vHTS, we decided to use this technique for a screen which identified a limited number of high-score hits. Functional screens for the NTC transcriptional activation were already established, however are seemingly prone to measuring effects that are not singularly due to targeting of NOTCH signaling. Though we identified two compounds that had shown activity in our two functional assays, a subsequent measurement of binding energy had shown that there presumably is no specific binding of either compound to CSL. This shows the caveats of the vHTS approach and the usage of small compounds in general — the docking technique relies on structural information, which in case of X-ray crystallography may not represent what is found in solution within a living cell, does not account for structural dynamics of the protein and

moreover there will be quality issues in terms of structure resolution. As NMR-based in-solution structures become more and more available even for large proteins [167], these structural informations may prove to be of higher quality and will presumably get closer to the structure one expects under the physiological conditions of a cell and thus be more suitable for vHTS screens. If there are functional and specific screens available that can measure effects on a certain protein, vHTS nevertheless is a good option in order to identify potential small molecule inhibitors. Of course the potential toxicity of these compounds may then present a further problem when going from bioanalytical assays to cellular or mouse models.

Developing peptide inhibitors

Targeting a certain protein or protein complex always should be preceded by a thorough investigation of all available information with special emphasis on resolved structures, binding studies and mutational studies. Doing this for the NOTCH transcriptional complex we established the hypothesis, that a short alpha-helical MAML1 derivative could be the basis for the design of a potent competitive inhibitor of NOTCH transcriptional complex formation. MAML1 being completely alpha helical predestines this simple structured protein for being the basis of producing chemically synthesized peptides, that depending on their size and amino acid composition would then freely diffuse across the cell and nuclear membranes [145, 146, 147, 148]. Other elegant ways such as fusing a small effector peptide to HIV-TAT [168, 169] have been described and make promising steps into the direction of the application of small peptide drugs in mouse models or even humans. Polo *et al.* for example were successful in using a TAT-fused BCL6-binding peptide which effectively induced apoptosis in BCL6-positive lymphoma cells [169]. This stresses the feasibility of this kind of therapeutic approach.

In this study we have shown, that indeed a very short MAML1 derived peptide sequence contains the core motif necessary for construction of a potent competitive in-

hibitor of NOTCH transcriptional complex formation.

At the same time this was found by Moellering *et al.* who described — in accordance with our results — that MAML1 amino acids 21-36 are sufficient for construction of an inhibitory peptide disrupting NTC assembly [145]. They moreover have shown, that the unmodified, chemically synthesized peptide MAML1 amino acids 21-36 exhibits only 23% alpha-helicity. These findings point out that, when designing a peptide drug, consideration of the desired secondary or tertiary structure is of utmost importance. Moellering *et al.* circumvented this problem by stabalizing alpha-helical folding through so-called 'peptide-stapeling' where an olefin-bridge is introduced between I27 and H31 (i.e. between position i and i+4 as to mimic alpha-helix-like hydrogen-bond formation). This resulted in 94% alpha-helicity. In subsequent experiments, Moellering *et al.* thoroughly characterised their peptides and different derivatives and have shown that indeed NOTCH transcriptional activation is inhibited *in vitro* and *in vivo*. Usage of these peptides in different NOTCH dependent human T-ALL cell lines resulted in induction of apoptosis. Additionally, lethally irradiated mice were reconstituted with haematopoetic stem cells, which were modified to have NOTCH signaling constitutively activated and then treated with the peptide inhibitor or the respective control. The subsequent tumor burden was significantly lower in mice treated with the peptide. The next step in advancing this promising drug template will be the thorough characterization of possible toxicity and the stability of the peptide *in vivo*. Also, ways how to administer the peptide to potential patients in an effective manner will have to be explored. If all this proves to be at acceptable levels, clinical trials will have to show usability of this NOTCH inhibitory peptide in the therapy of NOTCH associated diseases.

4.2.1 On a promising way — specific inhibition of transcription factor complexes

The results of part II of this work show that generally protein-complex assembly may be inhibited if some binding event may be outcompeted by usage of truncated, binding-capable but otherwise non-functional derivatives of one of the complex-composing proteins. However, applicability is always reduced to cases, where derivatives are very small in terms of molecular weight and thus are readily synthesized by chemical synthesis. At the same time it has to be guaranteed, that structural and stability requirements for the peptide are met. Size also matters in terms of transfer of the peptide from its location of application to the target. As additional caveat, inhibition of any process in healthy tissue will lead to undesirable counter effects, making it necessary to develop application and targeting strategies for most specific deployment of the peptide drug. Before deciding whether to target a disease-associated complex or single molecule with a small compound or a peptide inhibitor, a thorough biological and biophysical characterization should precede the decision. Especially in cases where the molecule of interest contains hydrophobic pockets or other surface characteristics suitable for small compound binding, this kind of approach should be preferred (e.g. this is often the case for kinases). In summary we have shown that the development of NOTCH signaling pathway specific peptide inhibitors is a promising way and tool to create and design drugs that most specifically inhibit this pathway at a crucial step, namely the NTC assembly. Various NOTCH associated malignancies (even those showing GSI resistance, see [145]) may be treatable using this peptide inhibitor. In case of cHL this might become a new way circumventing the devastating effects of traditional chemo- and radio-therapy and thus improve quality of life of patients substantially.

Appendix A

Below, all genes found in either database to be associated with the NOTCH signaling pathway are listed.

Affymetrix ID	Gene Name	BioGRID[1]	KEGG[2]	NetAffx[3]	PUBMED ID[4]
209743_s_at; 217094_s_at; 217094_s_at	ATROPHIN-1 INTERACTING PROTEIN 4	x			
201502_s_at	NUCLEAR FACTOR OF KAPPA LIGHT POLYPEPTIDE GENE ENHANCER IN B-CELLS INHIBITOR, ALPHA	x			
202360_at	MASTERMIND-LIKE 1 (DROSOPHILA)	x			
213494_s_at; 224711_at; 200047_s_at; 201901_s_at; 201902_s_at	YY1 TRANSCRIPTION FACTOR	x			
32137_at; 209784_s_at	JAGGED 2	x			
241378_at; 228261_at; 241541_at; 226644_at; 241377_s_at	MINDBOMB HOMOLOG 2 (DROSOPHILA)				15824097
221036_s_at	ANTERIOR PHARYNX DEFECTIVE 1 HOMOLOG B (C. ELEGANS)			x	
213091_at; 207159_x_at	CREB REGULATED TRANSCRIPTION COACTIVATOR 1			x	
204863_s_at; 234967_at; 234474_x_at; 212196_at; 211000_s_at; 204864_s_at; 212195_at	INTERLEUKIN 6 SIGNAL TRANSDUCER (GP130, ONCOSTATIN M RECEPTOR)			x	
229540_at; 207785_s_at; 211974_x_at	RECOMBINING BINDING PROTEIN SUPPRESSOR OF HAIRLESS (DROSOPHILA)	x			

204153_s_at; 204152_s_at	213783_at;	MANIC FRINGE HOMOLOG (DROSOPHILA)		12486116; 10935626
218512_at		WD REPEAT DOMAIN 12	x	
202064_s_at; 202061_s_at; 202063_s_at	202062_s_at; 230265_at;	SEL-1 SUPPRESSOR OF LIN-12-LIKE (C. ELEGANS)		12553058
204849_at; 235694_at		TRANSCRIPTION FACTOR-LIKE 5 (BASIC HELIX-LOOP-HELIX)		16990763
206480_at		LEUKOTRIENE C4 SYNTHASE	x	
221315_s_at; 1566816_at	1566814_at;	FIBROBLAST GROWTH FACTOR 22		16990763
209200_at; 209199_s_at	207968_s_at;	MADS BOX TRANSCRIPTION ENHANCER FACTOR 2, POLYPEPTIDE C (MYOCYTE ENHANCER FACTOR 2C)		10082551 ;16510869
207835_at; 207834_at; 202995_s_at	201787_at; 202994_s_at;	FIBULIN 1		16990763
218902_at; 223508_at		NOTCH HOMOLOG 1, TRANSLOCATION-ASSOCIATED (DROSOPHILA)	x	
206759_at; 206760_s_at		FC FRAGMENT OF IGE, LOW AFFINITY II, RECEPTOR FOR (CD23A)		11986231
209151_x_at; 215260_s_at; 228052_x_at; 213730_x_at; 213731_s_at; 209153_s_at	213732_at; 209152_s_at; 213811_x_at; 210776_x_at;	TRANSCRIPTION FACTOR 3 (E2A IMMUNOGLOBULIN ENHANCER BINDING FACTORS E12/E47)		18449208 ; 18815281

203867_s_at; 203866_at	NOTCHLESS HOMOLOG 1 (DROSOPHILA)			x	
208893_s_at; 208891_at; 208892_s_at;	DUAL SPECIFICITY PHOSPHATASE 6				16990763
206847_s_at	HOMEOBOX A7				16990763
211269_s_at; 206341_at	INTERLEUKIN 2 RECEPTOR, ALPHA				16612405
211148_s_at; 236034_at; 205572_at	ANGIOPOIETIN 2				16990763
212611_at	DELTEX 4 HOMOLOG (DROSOPHILA)			x	
225415_at	DELTEX 3-LIKE (DROSOPHILA)		x		
235106_at; 235457_at	MASTERMIND-LIKE 2 (DROSOPHILA)	x			
209239_at	NUCLEAR FACTOR OF KAPPA LIGHT POLYPEPTIDE GENE ENHANCER IN B-CELLS 1 (P105)	x			
215270_at; 228762_at	LUNATIC FRINGE HOMOLOG (DROSOPHILA)				16612405
202604_x_at; 214895_s_at	ADAM METALLOPEPTIDASE DOMAIN 10				16612405
204501_at; 214321_at	NEPHROBLASTOMA OVEREXPRESSED GENE				12050162
213260_at; 1553613_s_at	FORKHEAD BOX C1			x	
214722_at; 227067_x_at	NOTCH HOMOLOG 2 (DROSOPHILA) N-TERMINAL LIKE				14673143
209945_s_at; 1554417_s_at; 218389_s_at; 237327_at	GLYCOGEN SYNTHASE KINASE 3 BETA	x			

202284_s_at; 1555186_at	CYCLIN-DEPENDENT KINASE INHIBITOR 1A (P21, CIP1)			19091404
229195_at; 243387_at; 224476_s_at	MESODERM POSTERIOR 1 HOMOLOG (MOUSE)		x	
201465_s_at	V-JUN SARCOMA VIRUS 17 ONCOGENE HOMOLOG (AVIAN)			14645224
215732_s_at	DELTEX2 HOMOLOG (DROSOPHILA)		x	
226281_at	DELTA-NOTCH-LIKE EGF REPEAT-CONTAINING TRANSMEMBRANE		x	
227678_at; 1554349_at	XRCC6 BINDING PROTEIN 1	x		
201996_s_at; 201997_s_at; 1556059_s_at;1556058_s_at	SPEN HOMOLOG, TRANSCRIPTIONAL REGULATOR (DROSOPHILA)		x	
211252_x_at; 211837_s_at; 215492_x_at	PRE T-CELL ANTIGEN RECEPTOR ALPHA			16612405
218284_at; 205396_at; 205398_s_at	SMAD, MOTHERS AGAINST DPP HOMOLOG 3 (DROSOPHILA)	x		
207538_at; 207539_s_at	INTERLEUKIN 4			15137944
204262_s_at; 204261_s_at; 211373_s_at;	PRESENILIN 2 (ALZHEIMER DISEASE 4)			16612405
209097_s_at; 209099_x_at; 216268_s_at; 209098_s_at; 231183_s_at	JAGGED 1 (ALAGILLE SYNDROME)	x		
213147_at; 213150_at	HOMEOBOX A10			16990763
224726_at; 224722_at; 236573_at; 224720_at; 224725_at; 1558645_at	MINDBOMB HOMOLOG 1 (DROSOPHILA)		x	

203237_s_at; 203238_s_at	NOTCH HOMOLOG 3 (DROSOPHILA)	x				
215205_x_at; 208888_s_at; 207760_s_at; 208889_s_at	NUCLEAR RECEPTOR CO-REPRESSOR 2		x			
215424_s_at; 201575_at	SNW DOMAIN CONTAINING 1	x				
207195_at	CONTACTIN 6			x		
230568_x_at; 219537_x_at; 229755_x_at; 222898_s_at;	DELTA-LIKE 3 (DROSOPHILA)			x		
212349_at; 210433_at;	PROTEIN O-FUCOSYLTRANSFERASE 1			x		
203460_s_at; 207782_s_at; 238816_at; 1567440_at; 1567443_x_at; 226577_at; 1559206_at	PRESENILIN 1 (ALZHEIMER DISEASE 3)					16612405
203845_at; 239585_at	P300/CBP-ASSOCIATED FACTOR		x			
1559295_at; 235858_at; 202160_at; 211808_s_at; 237239_at	CREB BINDING PROTEIN (RUBINSTEIN-TAYBI SYNDROME)		x			
212377_s_at; 210756_s_at; 202445_s_at; 202443_x_at	NOTCH HOMOLOG 2 (DROSOPHILA)	x				
224548_at	HAIRY AND ENHANCER OF SPLIT 7 (DROSOPHILA)			x		
208292_at	BONE MORPHOGENETIC PROTEIN 10			x		
227347_x_at	HAIRY AND ENHANCER OF SPLIT 4 (DROSOPHILA)			x		
223525_at	DELTA-LIKE 4 (DROSOPHILA)					16612405
227336_at	DELTEX HOMOLOG 1 (DROSOPHILA)					16612405

220662_s_at; 226828_s_at	HAIRY/ENHANCER-OF-SPLIT RELATED WITH YRPW MOTIF-LIKE			x	
203394_s_at; 203395_s_at; 203393_at	HAIRY AND ENHANCER OF SPLIT 1, (DROSOPHILA)			x	
209073_s_at; 236930_at; 207545_s_at; 230462_at	NUMB HOMOLOG (DROSOPHILA)		x		
221333_at; 221334_s_at; 224211_at	FORKHEAD BOX P3				19267400
205247_at; 240786_at	NOTCH HOMOLOG 4 (DROSOPHILA)				16612405
210948_s_at; 221558_s_at; 221557_s_at	LYMPHOID ENHANCER-BINDING FACTOR 1				17585052
211370_s_at; 211371_at	MITOGEN-ACTIVATED PROTEIN KINASE KINASE 5				16990763
218751_s_at; 229419_at; 222729_at	F-BOX AND WD-40 DOMAIN PROTEIN 7 (ARCHIPELAGO HOMOLOG, DROSOPHILA)	x			
205745_x_at; 205746_s_at; 213532_at; 237897_at	ADAM METALLOPEPTIDASE DOMAIN 17 (TUMOR NECROSIS FACTOR, ALPHA, CONVERTING ENZYME)			x	
209905_at; 214651_s_at	HOMEOBOX A9				16990763
211277_x_at; 200602_at; 214953_s_at	AMYLOID BETA (A4) PRECURSOR PROTEIN (PEPTIDASE NEXIN-II, ALZHEIMER DISEASE)			x	
239230_at	HAIRY AND ENHANCER OF SPLIT 5 (DROSOPHILA)				16990763
221318_at	NEUROGENIC DIFFERENTIATION 4			x	

208230_s_at; 208241_at; 206343_s_at; 208232_x_at; 206237_s_at; 208231_at	NEUREGULIN 1				x	
213844_at	HOMEOBOX A5					16990763
228508_at; 242794_at; 207946_at; 207946_at	MASTERMIND-LIKE 3 (DROSOPHILA)	x				
227209_at; 1554784_at; 227202_at; 211203_s_at	CONTACTIN 1				x	
212968_at	RADICAL FRINGE HOMOLOG (DROSOPHILA)					17170755
232204_at; 233261_at; 229487_at; 227646_at	EARLY B-CELL FACTOR					1881528
237076_at; 208759_at	NICASTRIN					16612405
222022_at; 235721_at; 221835_at; 49051_g_at; 49049_at	DELTEX 3 HOMOLOG (DROSOPHILA)				x	
202182_at	GCN5 GENERAL CONTROL OF AMINO-ACID SYNTHESIS 5-LIKE 2 (YEAST)			x		
200792_at; 215308_at	X-RAY REPAIR COMPLEMENTING DEFECTIVE REPAIR IN CHINESE HAMSTER CELLS 6 (KU AUTOANTIGEN, 70KDA)	x				
204369_at; 235980_at; 231854_at	PHOSPHOINOSITIDE-3-KINASE, CATALYTIC, ALPHA POLYPEPTIDE	x				
227938_s_at; 224215_s_at	DELTA-LIKE 1 (DROSOPHILA)				x	
218839_at; 44783_s_at	HAIRY/ENHANCER-OF-SPLIT RELATED WITH YRPW MOTIF 1				x	

211193_at; 211195_s_at; 1555581_a_at; 211194_s_at	211834_s_at; 207382_at; 209863_s_at;	TUMOR PROTEIN P73-LIKE			x	
209878_s_at; 201783_s_at		V-REL RETICULOENDOTHELIOSIS VIRAL ONCOGENE HOMOLOG A, NUCLEAR FACTOR OF KAPPA LIGHT POLYPEPTIDE GENE ENHANCER IN B-CELLS 3, P65 (AVIAN)	x			
1556015_a_at; 1556014_at		MESODERM POSTERIOR 2 HOMOLOG (MOUSE)			x	
204890_s_at; 204891_s_at		LYMPHOCYTE-SPECIFIC PROTEIN TYROSINE KINASE	x			
209571_at		CBF1 INTERACTING COREPRESSOR		x		
226499_at		SIMILAR TO ANKYRIN-REPEAT PROTEIN NRARP				16612405
222921_s_at; 219743_at		HAIRY/ENHANCER-OF-SPLIT RELATED WITH YRPW MOTIF 2			x	
218302_at		PRESENILIN ENHANCER 2 HOMOLOG (C. ELEGANS)			x	
209987_s_at; 209988_s_at; 209986_at	209985_s_at; 213768_s_at;	ACHAETE-SCUTE COMPLEX-LIKE 1 (DROSOPHILA)			x	
244097_at; 205544_s_at		COMPLEMENT COMPONENT (3D EPSTEIN BARR VIRUS) RECEPTOR 2				11390591

209602_s_at; 209604_s_at	209603_at;	GATA BINDING PROTEIN 3	16317090

[1], General Repository for interaction datasets; [2], Kyoto Encyclopedia of Genes and Genomes; [3], NetAffx (http://www.affymetrix.com) was screened for array features listed under the term 'NOTCH signaling pathway';

[5], the pubmed database (http://www.ncbi.nlm.nih.gov/pubmed) was screened for articles linking genes to NOTCH signaling, unique PUBMED IDs are listed.

Appendix B

Summary of the Quality Control for Gene Expression Omnibus entry GSE12453. The results of various quality measurements are summarized below. Especially array #26 shows several quality problems, yet these are accounted for by the applied pre-processing procedures.

Array Name	MA plots	Spatial distribution	Boxplots	Heatmap	RLE	NUSE
GSM312811_pHL	ok	ok	ok	ok	ok	ok
GSM312812_pHL	ok	ok	ok	ok	ok	ok
GSM312813_pHL	ok	ok	ok	ok	ok	ok
GSM312814_pHL	ok	ok	ok	ok	ok	ok
GSM312815_pHL	ok	ok	ok	ok	ok	ok
GSM312816_pHL	ok	ok	ok	ok	ok	ok
GSM312817_pHL	ok	ok	ok	ok	ok	ok
GSM312818_pHL	ok	*	ok	ok	ok	ok
GSM312819_pHL	ok	ok	ok	ok	ok	ok
GSM312820_pHL	ok	ok	ok	ok	ok	ok
GSM312821_pHL	ok	ok	ok	ok	ok	ok
GSM312822_pHL	ok	*	ok	ok	ok	ok
GSM312851_pBL	ok	ok	ok	ok	ok	ok
GSM312853_pBL	ok	ok	ok	ok	ok	ok
GSM312854_pBL	ok	ok	ok	ok	ok	ok
GSM312856_pBL	ok	ok	ok	ok	ok	ok
GSM312857_pBL	ok	ok	ok	ok	ok	ok
GSM312858_pDLBCL	ok	ok	ok	ok	ok	ok
GSM312859_pDLBCL	ok	ok	ok	ok	ok	ok
GSM312860_pDLBCL	ok	ok	ok	ok	ok	ok
GSM312861_pDLBCL	ok	ok	ok	ok	ok	ok
GSM312862_pDLBCL	ok	ok	ok	ok	ok	ok
GSM312863_pDLBCL	ok	ok	ok	ok	ok	ok
GSM312864_pDLBCL	ok	ok	ok	ok	ok	ok
GSM312865_pDLBCL	ok	ok	ok	ok	ok	ok
GSM312867_pDLBCL	*	ok	ok	*	*	ok
GSM312868_pDLBCL	ok	ok	ok	ok	ok	ok
GSM312869_pDLBCL	ok	ok	ok	ok	ok	ok

*, in the marked characteristic, the array differs from all other ones. pHL, primary Hodgkin Lymphoma sample; pDLBCL, primary Diffuse Large B Cell Lymphoma sample; pBL, primary Burkitt Lymphoma sample.

Appendix C

Deregulated NOTCH associated genes in comparisons of different data sets are listed below (primary sample data, cell line data and merged data). Number codings are as follows: -1 = significantly up–regulated in cHL; 0 = not significantly regulated in between the groups; 1 = significantly down–regulated in cHL.

Affymetrix Probe ID	Gene Symbol	primary data: non-Hodgkin vs. cHL	cell line data: non-Hodgkin vs. HRS	merged data: non-Hodgkin vs. HRS
217094_s_at	ITCH	0	0	0
236235_at	ITCH	0	0	0
201502_s_at	NFKBIA	-1	-1	-1
202360_at	MAML1	0	0	0
213494_s_at	YY1	1	0	0
224711_at	YY1	1	0	1
200047_s_at	YY1	1	0	1
201901_s_at	YY1	1	0	1
201902_s_at	YY1	0	0	0
32137_at	JAG2	0	0	0
209784_s_at	JAG2	0	0	0
241378_at	MIB2	0	0	0
228261_at	MIB2	1	0	1
241541_at	MIB2	1	0	1
226644_at	MIB2	0	0	0
241377_s_at	MIB2	0	0	0
221036_s_at	APH1B	0	0	0
213091_at	CRTC1	0	0	0
207159_x_at	CRTC1	0	0	0
204863_s_at	IL6ST	0	0	0
234967_at	IL6ST	0	0	0
234474_x_at	IL6ST	0	0	0
212196_at	IL6ST	0	-1	-1
211000_s_at	IL6ST	0	-1	0
204864_s_at	IL6ST	0	0	0
212195_at	IL6ST	0	-1	-1
229540_at	RBPJ	0	0	0
207785_s_at	RBPJ	0	0	0
211974_x_at	RBPJ	0	0	-1
204153_s_at	MFNG	0	1	1
213783_at	MFNG	0	0	0
204152_s_at	MFNG	0	1	0
218512_at	WDR12	0	0	1
202064_s_at	SEL1L	0	-1	-1
202062_s_at	SEL1L	0	-1	0
202061_s_at	SEL1L	0	-1	-1
230265_at	SEL1L	0	-1	0
202063_s_at	SEL1L	0	0	0
204849_at	TCFL5	0	0	1
235694_at	TCFL5	1	0	1
206480_at	LTC4S	0	0	0
221315_s_at	FGF22	0	0	0
1566814_at	FGF22	0	0	0
1566816_at	FGF22	0	0	0
209200_at	MEF2C	1	1	1
207968_s_at	MEF2C	0	1	0
209199_s_at	MEF2C	1	1	1
207835_at	FBLN1	0	0	0
201787_at	FBLN1	0	0	0
202994_s_at	FBLN1	0	0	0
207834_at	FBLN1	0	0	0
202995_s_at	FBLN1	0	0	0
218902_at	NOTCH1	0	0	0
223508_at	NOTCH1	0	0	0
206759_at	FCER2	0	-1	0
206760_s_at	FCER2	0	-1	0

209151_x_at	TCF3	0	1	0
213732_at	TCF3	0	0	0
215260_s_at	TCF3	0	1	1
209152_s_at	TCF3	1	1	1
228052_x_at	TCF3	0	0	0
213811_x_at	TCF3	1	1	1
213730_x_at	TCF3	1	1	1
210776_x_at	TCF3	1	1	1
213731_s_at	TCF3	0	0	0
209153_s_at	TCF3	1	1	1
203867_s_at	NLE1	0	0	0
203866_at	NLE1	0	0	0
208893_s_at	DUSP6	0	0	0
208891_at	DUSP6	0	0	0
208892_s_at	DUSP6	0	0	0
206847_s_at	HOXA7	0	0	0
211269_s_at	IL2RA	-1	-1	-1
206341_at	IL2RA	0	-1	0
211148_s_at	ANGPT2	0	0	0
236034_at	ANGPT2	0	0	0
205572_at	ANGPT2	0	0	0
212611_at	DTX4	1	1	1
225415_at	DTX3L	0	0	0
235106_at	MAML2	0	-1	-1
235457_at	MAML2	-1	-1	-1
209239_at	NFKB1	0	0	0
215270_at	LFNG	0	0	0
228762_at	LFNG	0	0	0
202604_x_at	ADAM10	0	0	-1
214895_s_at	ADAM10	0	0	0
204501_at	NOV	0	0	0
214321_at	NOV	0	0	0
213260_at	FOXC1	0	-1	0
1553613_s_at	FOXC1	0	0	-1
214722_at	NOTCH2NL	0	-1	-1
227067_x_at	NOTCH2NL	0	-1	0
209945_s_at	GSK3B	0	0	0
1554417_s_at	APH1A	0	0	0
218389_s_at	APH1A	0	0	0
237327_at	APH1A	0	0	0
202284_s_at	CDKN1A	-1	0	-1
1555186_at	CDKN1A	0	0	0
229195_at	MESP1	0	0	0
243387_at	MESP1	0	0	0
224476_s_at	MESP1	0	-1	0
201465_s_at	JUN	-1	-1	-1
215732_s_at	DTX2	0	0	0
226281_at	DNER	0	0	0
227678_at	XRCC6BP1	0	0	0
1554349_at	XRCC6BP1	0	0	0
201996_s_at	SPEN	0	0	0
201997_s_at	SPEN	0	0	0
1556059_s_at	SPEN	0	0	0
1556058_s_at	SPEN	0	0	0
211252_x_at	PTCRA	0	0	0
211837_s_at	PTCRA	0	0	0
215492_x_at	PTCRA	0	0	0
218284_at	SMAD3	0	1	0
205396_at	SMAD3	0	0	0
205398_s_at	SMAD3	0	0	0
207538_at	IL4	0	0	0
207539_s_at	IL4	0	0	0
204262_s_at	PSEN2	0	-1	-1
204261_s_at	PSEN2	0	-1	0
211373_s_at	PSEN2	-1	-1	-1
209097_s_at	JAG1	0	0	0
209099_x_at	JAG1	0	0	0
216268_s_at	JAG1	0	0	0
209098_s_at	JAG1	0	0	0
231183_s_at	JAG1	0	0	0
213147_at	HOXA10	0	0	0
213150_at	HOXA10	0	-1	0
224726_at	MIB1	0	0	0
224722_at	MIB1	0	1	0
236573_at	MIB1	0	0	0
224720_at	MIB1	0	0	0
224725_at	MIB1	0	0	0
1558645_at	MIB1	0	0	0
203237_s_at	NOTCH3	0	0	0
203238_s_at	NOTCH3	0	0	0
215205_x_at	NCOR2	0	0	0
208888_s_at	NCOR2	0	0	0
207760_s_at	NCOR2	0	0	0
208889_s_at	NCOR2	0	0	0
215424_s_at	SNW1	0	0	0
201575_at	SNW1	0	0	0
207195_at	CNTN6	0	0	0
230568_x_at	DLL3	0	0	0
219537_x_at	DLL3	0	0	0
229755_x_at	DLL3	0	0	0

222898_s_at	DLL3	0	1	0
212349_at	POFUT1	0	0	0
210433_at	POFUT1	0	0	0
203460_s_at	PSEN1	0	0	0
207782_s_at	PSEN1	0	-1	0
238816_at	PSEN1	0	0	0
226577_at	PSEN1	0	-1	0
1559206_at	PSEN1	0	0	0
203845_at	KAT2B	0	0	0
239585_at	KAT2B	0	0	0
235858_at	CREBBP	0	0	0
202160_at	CREBBP	0	0	0
211808_s_at	CREBBP	0	0	0
212377_s_at	NOTCH2	0	-1	-1
210756_s_at	NOTCH2	0	-1	0
202445_s_at	NOTCH2	0	-1	-1
202443_x_at	NOTCH2	0	-1	-1
224548_at	HES7	0	-1	0
208292_at	BMP10	0	0	0
227347_x_at	HES4	0	0	0
223525_at	DLL4	0	0	0
227336_at	DTX1	1	1	1
207946_at	MAML3	0	0	0
220662_s_at	HEYL	0	0	0
226828_s_at	HEYL	0	0	0
203394_s_at	HES1	0	0	0
203395_s_at	HES1	0	0	0
203393_at	HES1	0	0	0
209073_s_at	NUMB	0	0	0
236930_at	NUMB	0	0	-1
207545_s_at	NUMB	0	-1	0
230462_at	NUMB	0	0	0
221333_at	FOXP3	0	0	0
221334_s_at	FOXP3	0	0	0
224211_at	FOXP3	0	0	0
205247_at	NOTCH4	0	0	0
240786_at	NOTCH4	0	0	0
210948_s_at	LEF1	0	1	0
221558_s_at	LEF1	0	1	0
221557_s_at	LEF1	0	1	0
211370_s_at	MAP2K5	0	0	0
211371_at	MAP2K5	0	0	0
218751_s_at	FBXW7	0	0	0
229419_at	FBXW7	0	0	0
222729_at	FBXW7	0	0	0
205745_x_at	ADAM17	0	0	0
205746_s_at	ADAM17	0	0	0
213532_at	ADAM17	0	0	0
237897_at	ADAM17	0	0	0
209905_at	HOXA9	0	0	0
214651_s_at	HOXA9	0	0	0
211277_x_at	APP	0	0	0
200602_at	APP	0	1	0
214953_s_at	APP	0	1	0
239230_at	HES5	0	0	0
221318_at	NEUROD4	0	0	0
208230_s_at	NRG1	0	0	0
208241_at	NRG1	0	0	0
206343_s_at	NRG1	0	0	0
208232_x_at	NRG1	0	0	0
206237_s_at	NRG1	0	0	0
208231_at	NRG1	0	0	0
213844_at	HOXA5	0	0	0
228508_at	MAML3	0	0	0
242794_at	MAML3	0	0	0
207946_at	MAML3	0	0	0
227209_at	CNTN1	0	0	0
1554784_at	CNTN1	0	0	0
227202_at	CNTN1	0	0	0
211203_s_at	CNTN1	0	0	0
212968_at	RFNG	1	0	0
232204_at	EBF1	0	1	1
233261_at	EBF1	0	1	1
229487_at	EBF1	0	1	1
227646_at	EBF1	0	1	0
237076_at	NCSTN	0	0	0
208759_at	NCSTN	0	0	0
222022_at	DTX3	0	0	0
235721_at	DTX3	0	0	0
221835_at	DTX3	0	0	0
49051_g_at	DTX3	0	0	0
49049_at	DTX3	0	0	0
202182_at	KAT2A	1	0	0
200792_at	XRCC6	0	0	0
215308_at	XRCC6	0	0	0
204369_at	PIK3CA	0	0	0
235980_at	PIK3CA	0	0	0
231854_at	PIK3CA	0	0	0
227938_s_at	DLL1	0	0	0
224215_s_at	DLL1	0	0	0

218839_at	HEY1	0	0	0
44783_s_at	HEY1	0	0	-1
211834_s_at	TP63	0	0	0
211195_s_at	TP63	0	0	0
207382_at	TP63	0	0	0
1555581_a_at	TP63	0	0	0
209863_s_at	TP63	0	0	0
211194_s_at	TP63	0	-1	0
209878_s_at	RELA	0	0	0
201783_s_at	RELA	0	0	0
1556015_a_at	MESP2	0	0	0
1556014_at	MESP2	0	0	0
204890_s_at	LCK	0	1	1
204891_s_at	LCK	0	1	1
209571_at	CIR1	0	0	0
226499_at	NRARP	0	0	0
222921_s_at	HEY2	0	0	0
219743_at	HEY2	0	0	0
218302_at	PSENEN	0	0	0
209987_s_at	ASCL1	0	0	0
209985_s_at	ASCL1	0	0	0
209988_s_at	ASCL1	0	0	0
213768_s_at	ASCL1	0	0	0
209986_at	ASCL1	0	0	0
244097_at	CR2	0	0	0
205544_s_at	CR2	0	0	0
209602_s_at	GATA3	0	-1	-1
209603_at	GATA3	0	-1	-1
209604_s_at	GATA3	-1	-1	-1

Appendix D

The 10 Keyorganics compounds identified by vHTS to bind to CSL, were initially tested using the NOTCH-reporter assay described above, using HEK293 cells as test systems. Compounds dissolved in DMSO or DMSO only were administered 2 hours after transfection of the reporter constructs. Results are shown below.

Keyorganics accession number	concentration	luciferase ratio	standard deviation
12R-0816	100 μM	2.12	0.01
12R-0816	10 μM	3.66	0.06
12R-0816	1 μM	3.70	0.12
12R-0816	0.1 μM	3.11	0.09
12R-1182	100 μM	8.19	0.25
12R-1182	10 μM	3.85	0.02
12R-1182	1 μM	3.42	0.81
12R-1182	0.1 μM	3.55	0.05
3R-0256	100 μM	4.01	0.08
3R-0256	10 μM	3.82	0.10
3R-0256	1 μM	3.92	0.06
3R-0256	0.1 μM	3.57	0.09
3R-0688	100 μM	3.87	0.20
3R-0688	10 μM	3.78	0.45
3R-0688	1 μM	2.77	1.64
3R-0688	0.1 μM	3.58	0.41
3K-521S	100 μM	2.96	0.42
3K-521S	10 μM	4.11	0.03
3K-521S	1 μM	4.38	0.25
3K-521S	0.1 μM	3.08	1.83
6M-003	100 μM	1.44	0.47
6M-003	10 μM	2.79	1.63
6M-003	1 μM	3.20	1.96
6M-003	0.1 μM	2.47	1.31
10B-035	100 μM	3.22	0.04
10B-035	10 μM	3.39	0.13
10B-035	1 μM	3.31	0.12
10B-035	0.1 μM	2.99	0.09
10B-049	100 μM	4.36	0.04
10B-049	10 μM	3.72	0.06
10B-049	1 μM	3.20	0.07
10B-049	0.1 μM	3.41	0.08
10E-23	100 μM	3.12	0.08
10E-23	10 μM	3.82	0.08
10E-23	1 μM	3.38	0.11
10E-23	0.1 μM	3.20	0.08
12P-818	100 μM	2.94	0.09
12P-818	10 μM	3.83	0.08
12P-818	1 μM	3.21	0.12
12P-818	0.1 μM	3.35	0.03
DMSO	$1^0/_{00}$	3.34	0.08
DMSO	$1^0/_{00}$	3.29	0.06

Appendix E

Below, a Mascot Search Result report identifying our purified protein to be human CSL is attached. Note: SUH_human is synonymous with human CSL.

Mascot Search Results

Protein View

Match to: **SUH_HUMAN** Score: **744**
Recombining binding protein suppressor of hairless - Homo sapiens (Human)
Found in search of MSC388.pkl

Nominal mass (M_r): **55628**; Calculated pI value: **6.80**
NCBI BLAST search of SUH_HUMAN against nr
Unformatted sequence string for pasting into other applications

Taxonomy: Homo sapiens

Variable modifications: Carbamidomethyl (C),Oxidation (M),Propionamide (C)
Cleavage by Trypsin: cuts C-term side of KR unless next residue is P
Sequence Coverage: **23%**

Matched peptides shown in **Bold Red**

```
     1 MDHTEGLPAE EPPAHAPSPG KFGERPPPKR LTREAMRNYL KERGDQTVLI
    51 LHAKVAQKSY GNEKRFFCPP PCVYLMGSGW KKKKEQMERD GCSEQESQPC
   101 AFIGIGNSDQ EMQQLNLEGK NYCTAKTLYI SDSDKRKHFM LSVKMFYGNS
   151 DDIGVFLSKR IKVISKPSKK KQSLKNADLC IASGTKVALF NRLRSQTVST
   201 RYLHVEGGNF HASSQQWGAF FIHLLDDDES EGEEFTVRDG YIHYGQTVKL
   251 VCSVTGMALP RLIIRKVDKQ TALLDADDPV SQLHKCAFYL KDTERMYLCL
   301 SQERIIQFQA TPCPKEPNKE MINDGASWTI ISTDKAEYTF YEGMGPVLAP
   351 VTPVPVVESL QLNGGGDVAM LELTGQNFTP NLRVWFGDVE AETMYRCGES
   401 MLCVVPDISA FREGWRWVRQ PVQVPVTLVR NDGIIYSTSL TFTYTPEPGP
   451 RPHCSAAGAI LRANSSQVPP NESNTNSEGS YTNASTNSTS VTSSTATVVS
   501
```

Residue Number Increasing Mass Decreasing Mass

Start - End	Observed	Mr(expt)	Mr(calc)	Delta	Miss	Sequence
42 - 54	493.94	1478.79	1478.82	-0.03	1	K.ERGDQTVLILHAK.V (Ions score 37)
44 - 54	398.87	1193.60	1193.68	-0.08	0	R.GDQTVLILHAK.V (Ions score 41)
44 - 54	597.83	1193.65	1193.68	-0.03	0	R.GDQTVLILHAK.V (Ions score 41)
127 - 136	399.83	1196.47	1196.60	-0.13	1	K.TLYISDSDKR.K (Ions score 56)
127 - 136	599.26	1196.51	1196.60	-0.09	1	K.TLYISDSDKR.K (Ions score 65)
138 - 144	431.21	860.42	860.46	-0.04	0	K.HFMLSVK.M (Ions score 43)
145 - 159	846.81	1691.61	1691.79	-0.18	0	K.MFYGNSDDIGVFLSK.R (Ions score 100)
145 - 159	846.90	1691.79	1691.79	0.00	0	K.MFYGNSDDIGVFLSK.R (Ions score 29)
145 - 159	846.90	1691.79	1691.79	0.00	0	K.MFYGNSDDIGVFLSK.R (Ions score 64)
145 - 159	846.90	1691.79	1691.79	0.00	0	K.MFYGNSDDIGVFLSK.R (Ions score 67)

145 - 159	846.90	1691.79	1691.79	0.01	0	K.MFYGNSDDIGVFLSK.R
(Ions score 49)						
145 - 159	846.91	1691.80	1691.79	0.02	0	K.MFYGNSDDIGVFLSK.R
(Ions score 16)						
239 - 249	640.78	1279.54	1279.62	-0.08	0	R.DGYIHYGQTVK.L
(Ions score 51)						
250 - 261	631.86	1261.70	1261.65	0.05	0	K.LVCSVTGMALPR.L
Oxidation (M) (Ions score 5)						
270 - 285	584.28	1749.81	1749.89	-0.08	0	K.QTALLDADDPVSQLHK.C
(Ions score 88)						
316 - 335	750.36	2248.05	2248.07	-0.02	1	
K.EPNKEMINDGASWTIISTDK.A (Ions score 68)						
320 - 335	890.92	1779.82	1779.83	-0.01	0	K.EMINDGASWTIISTDK.A
(Ions score 113)						
320 - 335	890.93	1779.84	1779.83	0.00	0	K.EMINDGASWTIISTDK.A
(Ions score 17)						
320 - 335	890.93	1779.84	1779.83	0.01	0	K.EMINDGASWTIISTDK.A
(Ions score 18)						
320 - 335	890.93	1779.84	1779.83	0.01	0	K.EMINDGASWTIISTDK.A
(Ions score 36)						
384 - 396	801.84	1601.66	1601.72	-0.06	0	R.VWFGDVEAETMYR.C
(Ions score 71)						
384 - 396	534.91	1601.69	1601.72	-0.02	0	R.VWFGDVEAETMYR.C
(Ions score 16)						
384 - 396	801.86	1601.70	1601.72	-0.02	0	R.VWFGDVEAETMYR.C
(Ions score 88)						
384 - 396	801.87	1601.72	1601.72	-0.00	0	R.VWFGDVEAETMYR.C
(Ions score 67)						
384 - 396	801.87	1601.72	1601.72	0.00	0	R.VWFGDVEAETMYR.C
(Ions score 75)						
384 - 396	801.87	1601.72	1601.72	0.00	0	R.VWFGDVEAETMYR.C
(Ions score 69)						
384 - 396	801.87	1601.72	1601.72	0.00	0	R.VWFGDVEAETMYR.C
(Ions score 68)						
384 - 396	801.87	1601.72	1601.72	0.00	0	R.VWFGDVEAETMYR.C
(Ions score 62)						
384 - 396	809.86	1617.71	1617.71	-0.01	0	R.VWFGDVEAETMYR.C
Oxidation (M) (Ions score 59)						

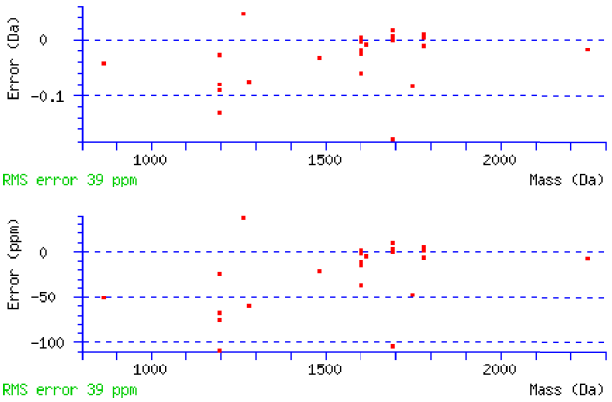

Appendix F

Exemplary ITC measurement for compound 6M-003 and purified, recombinant, human CSL. Note, that no binding saturation takes place, indicating, that compound 6M-003 does not specifically bind to CSL.

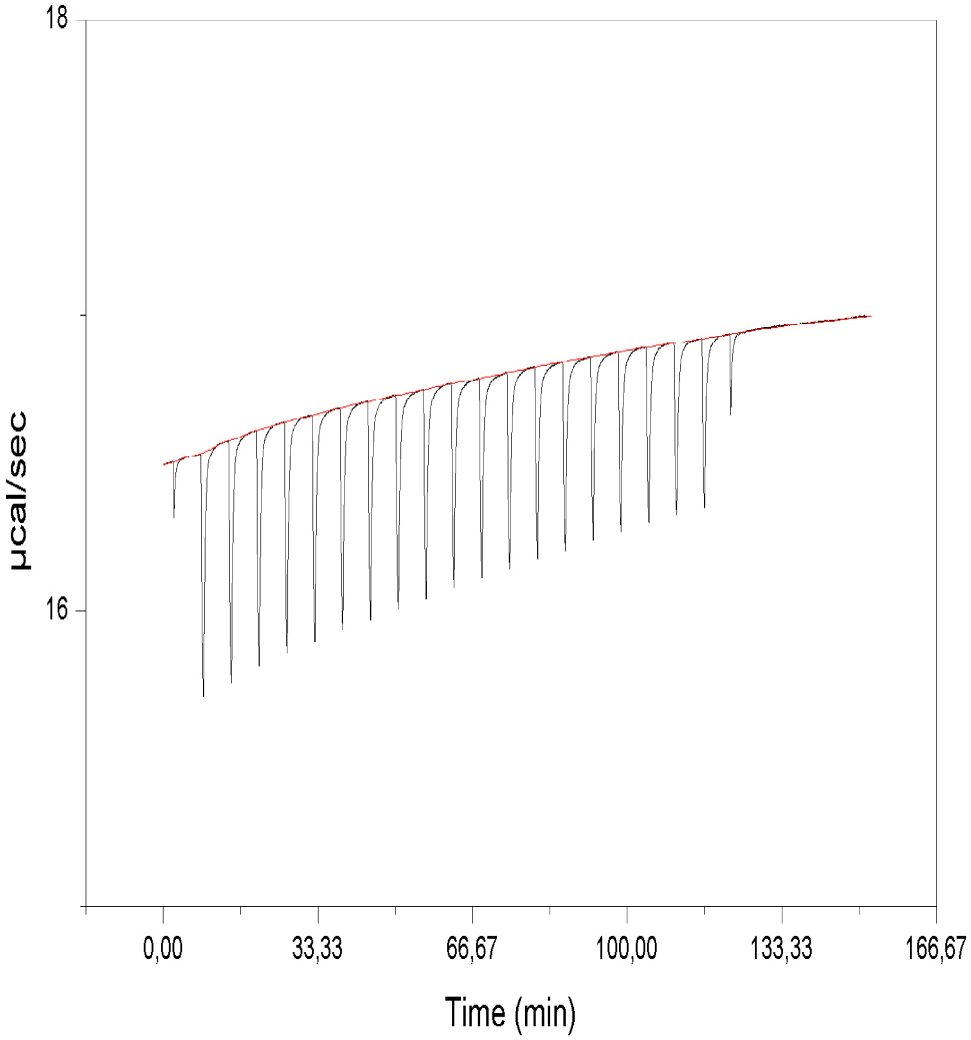

Abbreviations

SI units are not stated.

Abbreviation	*Explanation*
AA	amino acid
bp	base pairs
B-ALL	B cell acute lymphoblastic leukemia
BCA	bicinchoninic acid
BD	binding domain
BL	Burkitt's lymphoma
BME	β-mercaptoethanol
cHL	classical Hodgkin lymphoma
cpm	counts per minute
CT	cycle threshold
Da	Dalton
DAPT	N-[N-(3,5-Difluoro-phenacetyl)-L-alanyl]-S-phenylglycine t-butyl ester
DLBCL	diffuse large B cell lymphoma
DNA	Deoxyribonucleic acid
dNTP	deoxynucleotide triphosphate
DTT	dithiotreitol
e.g.	exempli gratia
EBV	Epstein Barr virus
EDTA	ethylenediaminetetraacetate
EMSA	electrophoretic mobility shift assay
FACS	fluorescence activated cell sorting
FPLC	fast protein liquid chromatography
g	gravity
GFP	green fluorescent protein
GO	gene ontology
GSEA	Gene Set Enrichment Analysis
GSI	γ-secretase inhibitor
HD	heterodimerization domain
HRS	Hodgkin Reed Sternberg
HPLC	high-performance liquid chromatography
ITC	isothermal titration calorimetry
IPTG	Isopropyl-β-D-thiogalactopyranoside
MAML	Mastermind-like
MCL	Mantle cell lymphoma

min	minutes
mRNA	messenger ribonucleic acid
NIC	NOTCH intracellular domain
n.s.	not significant
NTC	NOTCH transcriptional complex
NUSE	normalized unscaled standard error
p	probability
PBS	phosphate buffered saline
PCA	principal components analysis
PCR	polymerase-chain-reaction
PDB	protein data bank
qPCR	quantitative PCR
RLE	relative log expression
RNA	ribonucleic acid
RT	room temperature
RT-PCR	reverse transcriptase PCR
sd	standard deviation
SDS-PAGE	Sodiumdodecylsulfate-polyacrylamide gel electrophoresis
sec	seconds
SEC	size exclusion chromatography
sqPCR	semi-quantitative PCR
T-ALL	T cell acute lymphoblastic leukemia
TAD	transactivation domain
TBE	Tris Borate EDTA
TBS	Tris buffered saline
Tris	tris(hydroxymethyl)aminomethane
U	Units
vHTS	virtual high throughput screen
WB	western blotting
WHO	World Health Organization

Bibliography

[1] T Hodgkin. On some morbid appearances of the absorbent glands and spleen. *Med. Chir. Trans.*, 17:68–114, 1832.

[2] D. M. Parkin and C. S. Muir. Cancer incidence in five continents. comparability and quality of data. *IARC Sci Publ*, 120:45–173, 1992.

[3] R. K. Thomas, D. Re, T. Zander, J. Wolf, and V. Diehl. Epidemiology and etiology of hodgkin's lymphoma. *Ann Oncol*, 13 Suppl 4:147–52, 2002.

[4] Andreasd Engert and Sandra Horning. *Hodgkin Lymphoma - A comprehensive update on Diagnostics and Clinics*. Springerl, Heidelberg, Germany, 2010.

[5] B. Lindelof and G. Eklund. Analysis of hereditary component of cancer by use of a familial index by site. *Lancet*, 358(9294):1696–8, 2001.

[6] A. Engert, A. Plutschow, H. T. Eich, A. Lohri, B. Dorken, P. Borchmann, B. Berger, R. Greil, K. C. Willborn, M. Wilhelm, J. Debus, M. J. Eble, M. Sokler, A. Ho, A. Rank, A. Ganser, L. Trumper, C. Bokemeyer, H. Kirchner, J. Schubert, Z. Kral, M. Fuchs, H. K. Muller-Hermelink, R. P. Muller, and V. Diehl. Reduced treatment intensity in patients with early-stage hodgkin's lymphoma. *N Engl J Med*, 363(7):640–52, 2010.

[7] C Ferme. Four abvd and involved-field radiotherapy in unfavourable supradiaphragmatic clinical stages (cs) i-ii hodgkin's lymphoma: preliminary results of the eortc-gela h9-u trial. *Blood*, 106, 2005.

[8] A Engert. Hd12 randomised trial comparing 8 dose-escalated cycles of beacopp with 4 escalated and 4 baseline cycles in patients with advanced stage hodgkin lymphoma (hl). *Blood*, 108, 2006.

[9] S. Sleijfer. Bleomycin-induced pneumonitis. *Chest*, 120(2):617–24, 2001.

[10] E. Azoulay, S. Herigault, M. Levame, L. Brochard, B. Schlemmer, A. Harf, and C. Delclaux. Effect of granulocyte colony-stimulating factor on bleomycin-induced acute lung injury and pulmonary fibrosis. *Crit Care Med*, 31(5):1442–8, 2003.

[11] G. M. Dores, C. Metayer, R. E. Curtis, C. F. Lynch, E. A. Clarke, B. Glimelius, H. Storm, E. Pukkala, F. E. van Leeuwen, E. J. Holowaty, M. Andersson, T. Wiklund, T. Joensuu, M. B. van't Veer, M. Stovall, M. Gospodarowicz, and L. B.

Travis. Second malignant neoplasms among long-term survivors of hodgkin's disease: a population-based evaluation over 25 years. *J Clin Oncol*, 20(16):3484–94, 2002.

[12] F. E. van Leeuwen, W. J. Klokman, M. B. Veer, A. Hagenbeek, A. D. Krol, U. A. Vetter, M. Schaapveld, P. van Heerde, J. M. Burgers, R. Somers, and B. M. Aleman. Long-term risk of second malignancy in survivors of hodgkin's disease treated during adolescence or young adulthood. *J Clin Oncol*, 18(3):487–97, 2000.

[13] L. B. Travis, D. Hill, G. M. Dores, M. Gospodarowicz, F. E. van Leeuwen, E. Holowaty, B. Glimelius, M. Andersson, E. Pukkala, C. F. Lynch, D. Pee, S. A. Smith, M. B. Van't Veer, T. Joensuu, H. Storm, M. Stovall, Jr. Boice, J. D., E. Gilbert, and M. H. Gail. Cumulative absolute breast cancer risk for young women treated for hodgkin lymphoma. *J Natl Cancer Inst*, 97(19):1428–37, 2005.

[14] D. C. Hodgson, E. S. Gilbert, G. M. Dores, S. J. Schonfeld, C. F. Lynch, H. Storm, P. Hall, F. Langmark, E. Pukkala, M. Andersson, M. Kaijser, H. Joensuu, S. D. Fossa, and L. B. Travis. Long-term solid cancer risk among 5-year survivors of hodgkin's lymphoma. *J Clin Oncol*, 25(12):1489–97, 2007.

[15] D. C. Weber, S. Johanson, N. Peguret, L. Cozzi, and D. R. Olsen. Predicted risk of radiation-induced cancers after involved field and involved node radiotherapy with or without intensity modulation for early-stage hodgkin lymphoma in female patients. *Int J Radiat Oncol Biol Phys*, 2010.

[16] I. Meattini, L. Livi, C. Saieva, L. Marrazzo, A. Rampini, C. Iermano, M. G. Papi, B. Detti, S. Scoccianti, and G. Biti. Breast cancer following hodgkin's disease: the experience of the university of florence. *Breast J*, 16(3):290–6, 2010.

[17] A. M. Evens, M. Hutchings, and V. Diehl. Treatment of hodgkin lymphoma: the past, present, and future. *Nat Clin Pract Oncol*, 5(9):543–56, 2008.

[18] M Sieber and et al. Treatment of advanced stage hodgkin's disease with copp/abv/imep versus copp/abvd and consolidating radiotherapy: final results of the ghsg lymphoma study group hd6 trial. *Ann Oncol.*, 15:276–82, 2004.

[19] Carl Sternberg. Über eine eigenartige unter dem bilde der pseudoleukämie verlaufende tuberkolose des lymphatischen apparates. *Z. Heilkunde*, 19:21–90, 1898.

[20] Dorothy Reed. On the pathological changes in hodgkin's disease with special referencfe to its relation to tubercolosis. *John Hopkins Hosp. Rep.*, 10:133–193, 1902.

[21] H. Stein and M. Hummel. Cellular origin and clonality of classic hodgkin's lymphoma: immunophenotypic and molecular studies. *Semin Hematol*, 36(3):233–41, 1999.

[22] T. S. Barry, E. S. Jaffe, L. Sorbara, M. Raffeld, and S. Pittaluga. Peripheral t-cell lymphomas expressing cd30 and cd15. *Am J Surg Pathol*, 27(12):1513–22, 2003.

[23] D. Re, R. Kuppers, and V. Diehl. Molecular pathogenesis of hodgkin's lymphoma. *J Clin Oncol*, 23(26):6379–86, 2005.

[24] V. Brune, E. Tiacci, I. Pfeil, C. Doring, S. Eckerle, C. J. van Noesel, W. Klapper, B. Falini, A. von Heydebreck, D. Metzler, A. Brauninger, M. L. Hansmann, and R. Kuppers. Origin and pathogenesis of nodular lymphocyte-predominant hodgkin lymphoma as revealed by global gene expression analysis. *J Exp Med*, 205(10): 2251–68, 2008.

[25] R. Kuppers, K. Rajewsky, M. Zhao, G. Simons, R. Laumann, R. Fischer, and M. L. Hansmann. Hodgkin disease: Hodgkin and reed-sternberg cells picked from histological sections show clonal immunoglobulin gene rearrangements and appear to be derived from b cells at various stages of development. *Proc Natl Acad Sci U S A*, 91(23):10962–6, 1994.

[26] R. Kuppers, U. Klein, I. Schwering, V. Distler, A. Brauninger, G. Cattoretti, Y. Tu, G. A. Stolovitzky, A. Califano, M. L. Hansmann, and R. Dalla-Favera. Identification of hodgkin and reed-sternberg cell-specific genes by gene expression profiling. *J Clin Invest*, 111(4):529–37, 2003.

[27] M. Janz, B. Dorken, and S. Mathas. Reprogramming of b lymphoid cells in human lymphoma pathogenesis. *Cell Cycle*, 5(10):1057–61, 2006.

[28] H. Kanzler, R. Kuppers, M. L. Hansmann, and K. Rajewsky. Hodgkin and reed-sternberg cells in hodgkin's disease represent the outgrowth of a dominant tumor clone derived from (crippled) germinal center b cells. *J Exp Med*, 184(4):1495–505, 1996.

[29] T. Marafioti, M. Hummel, H. D. Foss, H. Laumen, P. Korbjuhn, I. Anagnostopoulos, H. Lammert, G. Demel, J. Theil, T. Wirth, and H. Stein. Hodgkin and reed-sternberg cells represent an expansion of a single clone originating from a germinal center b-cell with functional immunoglobulin gene rearrangements but defective immunoglobulin transcription. *Blood*, 95(4):1443–50, 2000.

[30] S. Mathas, A. Lietz, I. Anagnostopoulos, F. Hummel, B. Wiesner, M. Janz, F. Jundt, B. Hirsch, K. Johrens-Leder, H. P. Vornlocher, K. Bommert, H. Stein, and B. Dorken. c-flip mediates resistance of hodgkin/reed-sternberg cells to death receptor-induced apoptosis. *J Exp Med*, 199(8):1041–52, 2004.

[31] R. Kuppers. The biology of hodgkin's lymphoma. *Nat Rev Cancer*, 9(1):15–27, 2009.

[32] K. Willenbrock, R. Kuppers, C. Renne, V. Brune, S. Eckerle, E. Weidmann, A. Brauninger, and M. L. Hansmann. Common features and differences in the

transcriptome of large cell anaplastic lymphoma and classical hodgkin's lymphoma. *Haematologica*, 91(5):596–604, 2006.

[33] B. F. Skinnider, A. J. Elia, R. D. Gascoyne, L. H. Trumper, F. von Bonin, U. Kapp, B. Patterson, B. E. Snow, and T. W. Mak. Interleukin 13 and interleukin 13 receptor are frequently expressed by hodgkin and reed-sternberg cells of hodgkin lymphoma. *Blood*, 97(1):250–5, 2001.

[34] B. F. Skinnider and T. W. Mak. The role of cytokines in classical hodgkin lymphoma. *Blood*, 99(12):4283–97, 2002.

[35] B. Lamprecht, S. Kreher, I. Anagnostopoulos, K. Johrens, G. Monteleone, F. Jundt, H. Stein, M. Janz, B. Dorken, and S. Mathas. Aberrant expression of the th2 cytokine il-21 in hodgkin lymphoma cells regulates stat3 signaling and attracts treg cells via regulation of mip-3alpha. *Blood*, 112(8):3339–47, 2008.

[36] D. Aldinucci, D. Lorenzon, L. Cattaruzza, A. Pinto, A. Gloghini, A. Carbone, and A. Colombatti. Expression of ccr5 receptors on reed-sternberg cells and hodgkin lymphoma cell lines: involvement of ccl5/rantes in tumor cell growth and microenvironmental interactions. *Int J Cancer*, 122(4):769–76, 2008.

[37] M. Fischer, M. Juremalm, N. Olsson, C. Backlin, C. Sundstrom, K. Nilsson, G. Enblad, and G. Nilsson. Expression of ccl5/rantes by hodgkin and reed-sternberg cells and its possible role in the recruitment of mast cells into lymphomatous tissue. *Int J Cancer*, 107(2):197–201, 2003.

[38] U. Kapp, A. Dux, E. Schell-Frederick, N. Banik, M. Hummel, S. Mucke, C. Fonatsch, J. Bullerdiek, C. Gottstein, A. Engert, and et al. Disseminated growth of hodgkin's-derived cell lines l540 and l540cy in immune-deficient scid mice. *Ann Oncol*, 5 Suppl 1:121–6, 1994.

[39] D. Aldinucci, A. Gloghini, A. Pinto, R. De Filippi, and A. Carbone. The classical hodgkin's lymphoma microenvironment and its role in promoting tumour growth and immune escape. *J Pathol*, 221(3):248–63, 2010.

[40] C. Steidl, T. Lee, S. P. Shah, P. Farinha, G. Han, T. Nayar, A. Delaney, S. J. Jones, J. Iqbal, D. D. Weisenburger, M. A. Bast, A. Rosenwald, H. K. Muller-Hermelink, L. M. Rimsza, E. Campo, J. Delabie, R. M. Braziel, J. R. Cook, R. R. Tubbs, E. S. Jaffe, G. Lenz, J. M. Connors, L. M. Staudt, W. C. Chan, and R. D. Gascoyne. Tumor-associated macrophages and survival in classic hodgkin's lymphoma. *N Engl J Med*, 362(10):875–85, 2010.

[41] T. Tanijiri, T. Shimizu, K. Uehira, T. Yokoi, H. Amuro, H. Sugimoto, Y. Torii, K. Tajima, T. Ito, R. Amakawa, and S. Fukuhara. Hodgkin's reed-sternberg cell line (km-h2) promotes a bidirectional differentiation of cd4+cd25+foxp3+ t cells and cd4+ cytotoxic t lymphocytes from cd4+ naive t cells. *J Leukoc Biol*, 82(3): 576–84, 2007.

[42] R. Kuppers. Mechanisms of b-cell lymphoma pathogenesis. *Nat Rev Cancer*, 5(4): 251–62, 2005.

[43] H. J. Gruss, F. Herrmann, V. Gattei, A. Gloghini, A. Pinto, and A. Carbone. Cd40/cd40 ligand interactions in normal, reactive and malignant lymphohematopoietic tissues. *Leuk Lymphoma*, 24(5-6):393–422, 1997.

[44] S. W. Van Gool, J. Delabie, P. Vandenberghe, L. Coorevits, C. De Wolf-Peeters, and J. L. Ceuppens. Expression of b7-2 (cd86) molecules by reed-sternberg cells of hodgkin's disease. *Leukemia*, 11(6):846–51, 1997.

[45] A. Carbone, A. Gloghini, V. Gattei, D. Aldinucci, M. Degan, P. De Paoli, V. Zagonel, and A. Pinto. Expression of functional cd40 antigen on reed-sternberg cells and hodgkin's disease cell lines. *Blood*, 85(3):780–9, 1995.

[46] B. Lamprecht, K. Walter, S. Kreher, R. Kumar, M. Hummel, D. Lenze, K. Kochert, M. A. Bouhlel, J. Richter, E. Soler, R. Stadhouders, K. Johrens, K. D. Wurster, D. F. Callen, M. F. Harte, M. Giefing, R. Barlow, H. Stein, I. Anagnostopoulos, M. Janz, P. N. Cockerill, R. Siebert, B. Dorken, C. Bonifer, and S. Mathas. Derepression of an endogenous long terminal repeat activates the csf1r proto-oncogene in human lymphoma. *Nat Med*, 16(5):571–9, 1p following 579, 2010.

[47] J. M. Pongubala, D. L. Northrup, D. W. Lancki, K. L. Medina, T. Treiber, E. Bertolino, M. Thomas, R. Grosschedl, D. Allman, and H. Singh. Transcription factor ebf restricts alternative lineage options and promotes b cell fate commitment independently of pax5. *Nat Immunol*, 9(2):203–15, 2008.

[48] S. Mathas, M. Janz, F. Hummel, M. Hummel, B. Wollert-Wulf, S. Lusatis, I. Anagnostopoulos, A. Lietz, M. Sigvardsson, F. Jundt, K. Johrens, K. Bommert, H. Stein, and B. Dorken. Intrinsic inhibition of transcription factor e2a by hlh proteins abf-1 and id2 mediates reprogramming of neoplastic b cells in hodgkin lymphoma. *Nat Immunol*, 7(2):207–15, 2006.

[49] C. B. Hertel, X. G. Zhou, S. J. Hamilton-Dutoit, and S. Junker. Loss of b cell identity correlates with loss of b cell-specific transcription factors in hodgkin/reed-sternberg cells of classical hodgkin lymphoma. *Oncogene*, 21(32):4908–20, 2002.

[50] C. Renne, J. I. Martin-Subero, M. Eickernjager, M. L. Hansmann, R. Kuppers, R. Siebert, and A. Brauninger. Aberrant expression of id2, a suppressor of b-cell-specific gene expression, in hodgkin's lymphoma. *Am J Pathol*, 169(2):655–64, 2006.

[51] Y. Yokota, A. Mansouri, S. Mori, S. Sugawara, S. Adachi, S. Nishikawa, and P. Gruss. Development of peripheral lymphoid organs and natural killer cells depends on the helix-loop-helix inhibitor id2. *Nature*, 397(6721):702–6, 1999.

[52] C. Hacker, R. D. Kirsch, X. S. Ju, T. Hieronymus, T. C. Gust, C. Kuhl, T. Jorgas, S. M. Kurz, S. Rose-John, Y. Yokota, and M. Zenke. Transcriptional profiling identifies id2 function in dendritic cell development. *Nat Immunol*, 4(4):380–6, 2003.

[53] E. Torlakovic, A. Tierens, H. D. Dang, and J. Delabie. The transcription factor pu.1, necessary for b-cell development is expressed in lymphocyte predominance, but not classical hodgkin's disease. *Am J Pathol*, 159(5):1807–14, 2001.

[54] D. Re, M. Muschen, T. Ahmadi, C. Wickenhauser, A. Staratschek-Jox, U. Holtick, V. Diehl, and J. Wolf. Oct-2 and bob-1 deficiency in hodgkin and reed sternberg cells. *Cancer Res*, 61(5):2080–4, 2001.

[55] U. Kapp, W. C. Yeh, B. Patterson, A. J. Elia, D. Kagi, A. Ho, A. Hessel, M. Tipsword, A. Williams, C. Mirtsos, A. Itie, M. Moyle, and T. W. Mak. Interleukin 13 is secreted by and stimulates the growth of hodgkin and reed-sternberg cells. *J Exp Med*, 189(12):1939–46, 1999.

[56] F. Jundt, I. Anagnostopoulos, R. Forster, S. Mathas, H. Stein, and B. Dorken. Activated notch1 signaling promotes tumor cell proliferation and survival in hodgkin and anaplastic large cell lymphoma. *Blood*, 99(9):3398–403, 2002.

[57] A. Ehlers, E. Oker, S. Bentink, D. Lenze, H. Stein, and M. Hummel. Histone acetylation and dna demethylation of b cells result in a hodgkin-like phenotype. *Leukemia*, 22(4):835–41, 2008.

[58] A. Feuerborn, C. Moritz, F. Von Bonin, M. Dobbelstein, L. Trumper, B. Sturzenhofecker, and D. Kube. Dysfunctional p53 deletion mutants in cell lines derived from hodgkin's lymphoma. *Leuk Lymphoma*, 47(9):1932–40, 2006.

[59] E. M. Maggio, E. Stekelenburg, A. Van den Berg, and S. Poppema. Tp53 gene mutations in hodgkin lymphoma are infrequent and not associated with absence of epstein-barr virus. *Int J Cancer*, 94(1):60–6, 2001.

[60] M. Montesinos-Rongen, A. Roers, R. Kuppers, K. Rajewsky, and M. L. Hansmann. Mutation of the p53 gene is not a typical feature of hodgkin and reed-sternberg cells in hodgkin's disease. *Blood*, 94(5):1755–60, 1999.

[61] K. C. Chang, N. T. Khen, D. Jones, and I. J. Su. Epstein-barr virus is associated with all histological subtypes of hodgkin lymphoma in vietnamese children with special emphasis on the entity of lymphocyte predominance subtype. *Hum Pathol*, 36(7):747–55, 2005.

[62] I. Anagnostopoulos, M. L. Hansmann, K. Franssila, M. Harris, N. L. Harris, E. S. Jaffe, J. Han, J. M. van Krieken, S. Poppema, T. Marafioti, J. Franklin, M. Sextro, V. Diehl, and H. Stein. European task force on lymphoma project on lymphocyte

predominance hodgkin disease: histologic and immunohistologic analysis of submitted cases reveals 2 types of hodgkin disease with a nodular growth pattern and abundant lymphocytes. *Blood*, 96(5):1889–99, 2000.

[63] J. L. Kutok and F. Wang. Spectrum of epstein-barr virus-associated diseases. *Annu Rev Pathol*, 1:375–404, 2006.

[64] B. E. Henderson, R. Dworsky, M. C. Pike, J. Baptista, H. Menck, S. Preston-Martin, and T. Mack. Risk factors for nodular sclerosis and other types of hodgkin's disease. *Cancer Res*, 39(11):4507–11, 1979.

[65] H. Hjalgrim, J. Askling, K. Rostgaard, S. Hamilton-Dutoit, M. Frisch, J. S. Zhang, M. Madsen, N. Rosdahl, H. B. Konradsen, H. H. Storm, and M. Melbye. Characteristics of hodgkin's lymphoma after infectious mononucleosis. *N Engl J Med*, 349(14):1324–32, 2003.

[66] H. Hjalgrim, K. E. Smedby, K. Rostgaard, D. Molin, S. Hamilton-Dutoit, E. T. Chang, E. Ralfkiaer, C. Sundstrom, H. O. Adami, B. Glimelius, and M. Melbye. Infectious mononucleosis, childhood social environment, and risk of hodgkin lymphoma. *Cancer Res*, 67(5):2382–8, 2007.

[67] B. Jungnickel, A. Staratschek-Jox, A. Brauninger, T. Spieker, J. Wolf, V. Diehl, M. L. Hansmann, K. Rajewsky, and R. Kuppers. Clonal deleterious mutations in the ikappabalpha gene in the malignant cells in hodgkin's lymphoma. *J Exp Med*, 191(2):395–402, 2000.

[68] C. Renne, N. Hinsch, K. Willenbrock, M. Fuchs, W. Klapper, A. Engert, R. Kuppers, M. L. Hansmann, and A. Brauninger. The aberrant coexpression of several receptor tyrosine kinases is largely restricted to ebv-negative cases of classical hodgkin's lymphoma. *Int J Cancer*, 120(11):2504–9, 2007.

[69] D. Bechtel, J. Kurth, C. Unkel, and R. Kuppers. Transformation of bcr-deficient germinal-center b cells by ebv supports a major role of the virus in the pathogenesis of hodgkin and posttransplantation lymphomas. *Blood*, 106(13):4345–50, 2005.

[70] C. Mancao, M. Altmann, B. Jungnickel, and W. Hammerschmidt. Rescue of "crippled" germinal center b cells from apoptosis by epstein-barr virus. *Blood*, 106 (13):4339–44, 2005.

[71] C. Mancao and W. Hammerschmidt. Epstein-barr virus latent membrane protein 2a is a b-cell receptor mimic and essential for b-cell survival. *Blood*, 110(10): 3715–21, 2007.

[72] T. Portis, P. Dyck, and R. Longnecker. Epstein-barr virus (ebv) lmp2a induces alterations in gene transcription similar to those observed in reed-sternberg cells of hodgkin lymphoma. *Blood*, 102(12):4166–78, 2003.

[73] L. J. Anderson and R. Longnecker. Epstein-barr virus latent membrane protein 2a exploits notch1 to alter b-cell identity in vivo. *Blood*, 113(1):108–16, 2009.

[74] F. Jundt, O. Acikgoz, S. H. Kwon, R. Schwarzer, I. Anagnostopoulos, B. Wiesner, S. Mathas, M. Hummel, H. Stein, H. M. Reichardt, and B. Dorken. Aberrant expression of notch1 interferes with the b-lymphoid phenotype of neoplastic b cells in classical hodgkin lymphoma. *Leukemia*, 22(8):1587–94, 2008.

[75] J. Stanelle, C. Doring, M. L. Hansmann, and R. Kuppers. Mechanisms of aberrant gata-3 expression in classical hodgkin lymphoma and its consequences for the cytokine profile of hodgkin and reed/sternberg cells. *Blood*, 2010.

[76] P. A. Zweidler-McKay, Y. He, L. Xu, C. G. Rodriguez, F. G. Karnell, A. C. Carpenter, J. C. Aster, D. Allman, and W. S. Pear. Notch signaling is a potent inducer of growth arrest and apoptosis in a wide range of b-cell malignancies. *Blood*, 106(12):3898–906, 2005.

[77] F. Radtke, N. Fasnacht, and H. R. Macdonald. Notch signaling in the immune system. *Immunity*, 32(1):14–27, 2010.

[78] T.H. Morgan. The theory of the gene. *Am. Nat.*, 51:513–544, 1917.

[79] D.F. Poulson. The effects of certain x-chromosome deficiencies on the embryonic deleopment of *Drosophila melaonagaster*. *J. Exp. Zool.*, 83:271–325, 1940.

[80] A. Robert-Moreno, L. Espinosa, J. L. de la Pompa, and A. Bigas. Rbpjkappa-dependent notch function regulates gata2 and is essential for the formation of intra-embryonic hematopoietic cells. *Development*, 132(5):1117–26, 2005.

[81] K. Kumano, S. Chiba, A. Kunisato, M. Sata, T. Saito, E. Nakagami-Yamaguchi, T. Yamaguchi, S. Masuda, K. Shimizu, T. Takahashi, S. Ogawa, Y. Hamada, and H. Hirai. Notch1 but not notch2 is essential for generating hematopoietic stem cells from endothelial cells. *Immunity*, 18(5):699–711, 2003.

[82] L. M. Calvi, G. B. Adams, K. W. Weibrecht, J. M. Weber, D. P. Olson, M. C. Knight, R. P. Martin, E. Schipani, P. Divieti, F. R. Bringhurst, L. A. Milner, H. M. Kronenberg, and D. T. Scadden. Osteoblastic cells regulate the haematopoietic stem cell niche. *Nature*, 425(6960):841–6, 2003.

[83] A. Kunisato, S. Chiba, E. Nakagami-Yamaguchi, K. Kumano, T. Saito, S. Masuda, T. Yamaguchi, M. Osawa, R. Kageyama, H. Nakauchi, M. Nishikawa, and H. Hirai. Hes-1 preserves purified hematopoietic stem cells ex vivo and accumulates side population cells in vivo. *Blood*, 101(5):1777–83, 2003.

[84] B. Varnum-Finney, C. Brashem-Stein, and I. D. Bernstein. Combined effects of notch signaling and cytokines induce a multiple log increase in precursors with lymphoid and myeloid reconstituting ability. *Blood*, 101(5):1784–9, 2003.

[85] J. J. Bell and A. Bhandoola. The earliest thymic progenitors for t cells possess myeloid lineage potential. *Nature*, 452(7188):764–7, 2008.

[86] T. B. Feyerabend, G. Terszowski, A. Tietz, C. Blum, H. Luche, A. Gossler, N. W. Gale, F. Radtke, H. J. Fehling, and H. R. Rodewald. Deletion of notch1 converts pro-t cells to dendritic cells and promotes thymic b cells by cell-extrinsic and cell-intrinsic mechanisms. *Immunity*, 30(1):67–79, 2009.

[87] H. Wada, K. Masuda, R. Satoh, K. Kakugawa, T. Ikawa, Y. Katsura, and H. Kawamoto. Adult t-cell progenitors retain myeloid potential. *Nature*, 452 (7188):768–72, 2008.

[88] E. Fiorini, E. Merck, A. Wilson, I. Ferrero, W. Jiang, U. Koch, F. Auderset, E. Laurenti, F. Tacchini-Cottier, M. Pierres, F. Radtke, S. A. Luther, and H. R. Macdonald. Dynamic regulation of notch 1 and notch 2 surface expression during t cell development and activation revealed by novel monoclonal antibodies. *J Immunol*, 183(11):7212–22, 2009.

[89] K. Hozumi, N. Negishi, D. Suzuki, N. Abe, Y. Sotomaru, N. Tamaoki, C. Mailhos, D. Ish-Horowicz, S. Habu, and M. J. Owen. Delta-like 1 is necessary for the generation of marginal zone b cells but not t cells in vivo. *Nat Immunol*, 5(6): 638–44, 2004.

[90] T. Saito, S. Chiba, M. Ichikawa, A. Kunisato, T. Asai, K. Shimizu, T. Yamaguchi, G. Yamamoto, S. Seo, K. Kumano, E. Nakagami-Yamaguchi, Y. Hamada, S. Aizawa, and H. Hirai. Notch2 is preferentially expressed in mature b cells and indispensable for marginal zone b lineage development. *Immunity*, 18(5):675–85, 2003.

[91] K. Tanigaki, H. Han, N. Yamamoto, K. Tashiro, M. Ikegawa, K. Kuroda, A. Suzuki, T. Nakano, and T. Honjo. Notch-rbp-j signaling is involved in cell fate determination of marginal zone b cells. *Nat Immunol*, 3(5):443–50, 2002.

[92] L. Wu, I. Maillard, M. Nakamura, W. S. Pear, and J. D. Griffin. The transcriptional coactivator maml1 is required for notch2-mediated marginal zone b-cell development. *Blood*, 110(10):3618–23, 2007.

[93] S. J. Bray. Notch signalling: a simple pathway becomes complex. *Nat Rev Mol Cell Biol*, 7(9):678–89, 2006.

[94] L. Wu, J. C. Aster, S. C. Blacklow, R. Lake, S. Artavanis-Tsakonas, and J. D. Griffin. Maml1, a human homologue of drosophila mastermind, is a transcriptional co-activator for notch receptors. *Nat Genet*, 26(4):484–9, 2000.

[95] L. Wu, T. Sun, K. Kobayashi, P. Gao, and J. D. Griffin. Identification of a family of mastermind-like transcriptional coactivators for mammalian notch receptors. *Mol Cell Biol*, 22(21):7688–700, 2002.

[96] S. E. Lin, T. Oyama, T. Nagase, K. Harigaya, and M. Kitagawa. Identification of new human mastermind proteins defines a family that consists of positive regulators for notch signaling. *J Biol Chem*, 277(52):50612–20, 2002.

[97] Y. Nam, P. Sliz, L. Song, J. C. Aster, and S. C. Blacklow. Structural basis for cooperativity in recruitment of maml coactivators to notch transcription complexes. *Cell*, 124(5):973–83, 2006.

[98] C. J. Fryer, J. B. White, and K. A. Jones. Mastermind recruits cycc:cdk8 to phosphorylate the notch icd and coordinate activation with turnover. *Mol Cell*, 16(4):509–20, 2004.

[99] M. J. Lindberg, A. E. Popko-Scibor, M. L. Hansson, and A. E. Wallberg. Sumo modification regulates the transcriptional activity of maml1. *FASEB J*, 24(7): 2396–404, 2010.

[100] I. Maillard, A. P. Weng, A. C. Carpenter, C. G. Rodriguez, H. Sai, L. Xu, D. Allman, J. C. Aster, and W. S. Pear. Mastermind critically regulates notch-mediated lymphoid cell fate decisions. *Blood*, 104(6):1696–702, 2004.

[101] T. Oyama, K. Harigaya, A. Muradil, K. Hozumi, S. Habu, H. Oguro, A. Iwama, K. Matsuno, R. Sakamoto, M. Sato, N. Yoshida, and M. Kitagawa. Mastermind-1 is required for notch signal-dependent steps in lymphocyte development in vivo. *Proc Natl Acad Sci U S A*, 104(23):9764–9, 2007.

[102] A. S. McElhinny, J. L. Li, and L. Wu. Mastermind-like transcriptional coactivators: emerging roles in regulating cross talk among multiple signaling pathways. *Oncogene*, 27(38):5138–47, 2008.

[103] B. Jin, H. Shen, S. Lin, J. L. Li, Z. Chen, J. D. Griffin, and L. Wu. The mastermind-like 1 (maml1) co-activator regulates constitutive nf-kappab signaling and cell survival. *J Biol Chem*, 285(19):14356–65, 2010.

[104] H. A. Khan, A. Loya, R. Azhar, N. U. Din, and D. Bell. Central mucoepidermoid carcinoma, a case report with molecular analysis of the torc1/maml2 gene fusion. *Head Neck Pathol*, 4(3):261–4, 2010.

[105] R. R. Seethala, S. Dacic, K. Cieply, L. M. Kelly, and M. N. Nikiforova. A reappraisal of the mect1/maml2 translocation in salivary mucoepidermoid carcinomas. *Am J Surg Pathol*, 34(8):1106–21, 2010.

[106] A. Robert-Moreno, J. Guiu, C. Ruiz-Herguido, M. E. Lopez, J. Ingles-Esteve, L. Riera, A. Tipping, T. Enver, E. Dzierzak, T. Gridley, L. Espinosa, and A. Bigas. Impaired embryonic haematopoiesis yet normal arterial development in the absence of the notch ligand jagged1. *EMBO J*, 27(13):1886–95, 2008.

[107] R. C. Beck, M. Padival, D. Yeh, J. Ralston, K. R. Cooke, and J. B. Lowe. The notch ligands jagged2, delta1, and delta4 induce differentiation and expansion of functional human nk cells from cd34(+) cord blood hematopoietic progenitor cells. *Biol Blood Marrow Transplant*, 15(9):1026–37, 2009.

[108] M. E. Fortini. Notch signaling: the core pathway and its posttranslational regulation. *Dev Cell*, 16(5):633–47, 2009.

[109] T. Lieber, S. Kidd, E. Alcamo, V. Corbin, and M. W. Young. Antineurogenic phenotypes induced by truncated notch proteins indicate a role in signal transduction and may point to a novel function for notch in nuclei. *Genes Dev*, 7(10):1949–65, 1993.

[110] S. Stifani, C. M. Blaumueller, N. J. Redhead, R. E. Hill, and S. Artavanis-Tsakonas. Human homologs of a drosophila enhancer of split gene product define a novel family of nuclear proteins. *Nat Genet*, 2(4):343, 1992.

[111] Y. Nam, P. Sliz, W. S. Pear, J. C. Aster, and S. C. Blacklow. Cooperative assembly of higher-order notch complexes functions as a switch to induce transcription. *Proc Natl Acad Sci U S A*, 104(7):2103–8, 2007.

[112] D. Sprinzak, A. Lakhanpal, L. Lebon, L. A. Santat, M. E. Fontes, G. A. Anderson, J. Garcia-Ojalvo, and M. B. Elowitz. Cis-interactions between notch and delta generate mutually exclusive signalling states. *Nature*, 465(7294):86–90, 2010.

[113] M. Itoh, C. H. Kim, G. Palardy, T. Oda, Y. J. Jiang, D. Maust, S. Y. Yeo, K. Lorick, G. J. Wright, L. Ariza-McNaughton, A. M. Weissman, J. Lewis, S. C. Chandrasekharappa, and A. B. Chitnis. Mind bomb is a ubiquitin ligase that is essential for efficient activation of notch signaling by delta. *Dev Cell*, 4(1):67–82, 2003.

[114] E. C. Lai and G. M. Rubin. Neuralized is essential for a subset of notch pathway-dependent cell fate decisions during drosophila eye development. *Proc Natl Acad Sci U S A*, 98(10):5637–42, 2001.

[115] E. Pavlopoulos, C. Pitsouli, K. M. Klueg, M. A. Muskavitch, N. K. Moschonas, and C. Delidakis. neuralized encodes a peripheral membrane protein involved in delta signaling and endocytosis. *Dev Cell*, 1(6):807–16, 2001.

[116] C. Pitsouli and C. Delidakis. The interplay between dsl proteins and ubiquitin ligases in notch signaling. *Development*, 132(18):4041–50, 2005.

[117] E. C. Lai, F. Roegiers, X. Qin, Y. N. Jan, and G. M. Rubin. The ubiquitin ligase drosophila mind bomb promotes notch signaling by regulating the localization and activity of serrate and delta. *Development*, 132(10):2319–32, 2005.

[118] K. Bruckner, L. Perez, H. Clausen, and S. Cohen. Glycosyltransferase activity of fringe modulates notch-delta interactions. *Nature*, 406(6794):411–5, 2000.

[119] R. J. Fleming, Y. Gu, and N. A. Hukriede. Serrate-mediated activation of notch is specifically blocked by the product of the gene fringe in the dorsal compartment of the drosophila wing imaginal disc. *Development*, 124(15):2973–81, 1997.

[120] B. G. Ju, S. Jeong, E. Bae, S. Hyun, S. B. Carroll, J. Yim, and J. Kim. Fringe forms a complex with notch. *Nature*, 405(6783):191–5, 2000.

[121] D. J. Moloney, V. M. Panin, S. H. Johnston, J. Chen, L. Shao, R. Wilson, Y. Wang, P. Stanley, K. D. Irvine, R. S. Haltiwanger, and T. F. Vogt. Fringe is a glycosyltransferase that modifies notch. *Nature*, 406(6794):369–75, 2000.

[122] V. M. Panin, V. Papayannopoulos, R. Wilson, and K. D. Irvine. Fringe modulates notch-ligand interactions. *Nature*, 387(6636):908–12, 1997.

[123] M. A. McGill and C. J. McGlade. Mammalian numb proteins promote notch1 receptor ubiquitination and degradation of the notch1 intracellular domain. *J Biol Chem*, 278(25):23196–203, 2003.

[124] T. Ishitani, T. Hirao, M. Suzuki, M. Isoda, S. Ishitani, K. Harigaya, M. Kitagawa, K. Matsumoto, and M. Itoh. Nemo-like kinase suppresses notch signalling by interfering with formation of the notch active transcriptional complex. *Nat Cell Biol*, 12(3):278–85, 2010.

[125] R. McDaniell, D. M. Warthen, P. A. Sanchez-Lara, A. Pai, I. D. Krantz, D. A. Piccoli, and N. B. Spinner. Notch2 mutations cause alagille syndrome, a heterogeneous disorder of the notch signaling pathway. *Am J Hum Genet*, 79(1):169–73, 2006.

[126] J. T. Park, M. Li, K. Nakayama, T. L. Mao, B. Davidson, Z. Zhang, R. J. Kurman, C. G. Eberhart, M. Shih Ie, and T. L. Wang. Notch3 gene amplification in ovarian cancer. *Cancer Res*, 66(12):6312–8, 2006.

[127] S. Pece, M. Serresi, E. Santolini, M. Capra, E. Hulleman, V. Galimberti, S. Zurrida, P. Maisonneuve, G. Viale, and P. P. Di Fiore. Loss of negative regulation by numb over notch is relevant to human breast carcinogenesis. *J Cell Biol*, 167(2):215–21, 2004.

[128] W. S. Pear and J. C. Aster. T cell acute lymphoblastic leukemia/lymphoma: a human cancer commonly associated with aberrant notch1 signaling. *Curr Opin Hematol*, 11(6):426–33, 2004.

[129] A. P. Weng, A. A. Ferrando, W. Lee, J. P. th Morris, L. B. Silverman, C. Sanchez-Irizarry, S. C. Blacklow, A. T. Look, and J. C. Aster. Activating mutations of notch1 in human t cell acute lymphoblastic leukemia. *Science*, 306(5694):269–71, 2004.

[130] J. O'Neil, J. Grim, P. Strack, S. Rao, D. Tibbitts, C. Winter, J. Hardwick, M. Welcker, J. P. Meijerink, R. Pieters, G. Draetta, R. Sears, B. E. Clurman, and A. T. Look. Fbw7 mutations in leukemic cells mediate notch pathway activation and resistance to gamma-secretase inhibitors. *J Exp Med*, 204(8):1813–24, 2007.

[131] M. S. Wolfe. Inhibition and modulation of gamma-secretase for alzheimer's disease. *Neurotherapeutics*, 5(3):391–8, 2008.

[132] E. Siemers, M. Skinner, R. A. Dean, C. Gonzales, J. Satterwhite, M. Farlow, D. Ness, and P. C. May. Safety, tolerability, and changes in amyloid beta concentrations after administration of a gamma-secretase inhibitor in volunteers. *Clin Neuropharmacol*, 28(3):126–32, 2005.

[133] E. R. Siemers, J. F. Quinn, J. Kaye, M. R. Farlow, A. Porsteinsson, P. Tariot, P. Zoulnouni, J. E. Galvin, D. M. Holtzman, D. S. Knopman, J. Satterwhite, C. Gonzales, R. A. Dean, and P. C. May. Effects of a gamma-secretase inhibitor in a randomized study of patients with alzheimer disease. *Neurology*, 66(4):602–4, 2006.

[134] C. J. Fryer, E. Lamar, I. Turbachova, C. Kintner, and K. A. Jones. Mastermind mediates chromatin-specific transcription and turnover of the notch enhancer complex. *Genes Dev*, 16(11):1397–411, 2002.

[135] A. P. Weng, Y. Nam, M. S. Wolfe, W. S. Pear, J. D. Griffin, S. C. Blacklow, and J. C. Aster. Growth suppression of pre-t acute lymphoblastic leukemia cells by inhibition of notch signaling. *Mol Cell Biol*, 23(2):655–64, 2003.

[136] M. Janz, M. Hummel, M. Truss, B. Wollert-Wulf, S. Mathas, K. Johrens, C. Hagemeier, K. Bommert, H. Stein, B. Dorken, and R. C. Bargou. Classical hodgkin lymphoma is characterized by high constitutive expression of activating transcription factor 3 (atf3), which promotes viability of hodgkin/reed-sternberg cells. *Blood*, 107(6):2536–9, 2006.

[137] R Development Core Team. R: A language and environment for statistical computing, 2009.

[138] R. C. Gentleman, V. J. Carey, D. M. Bates, B. Bolstad, M. Dettling, S. Dudoit, B. Ellis, L. Gautier, Y. Ge, J. Gentry, K. Hornik, T. Hothorn, W. Huber, S. Iacus, R. Irizarry, F. Leisch, C. Li, M. Maechler, A. J. Rossini, G. Sawitzki, C. Smith, G. Smyth, L. Tierney, J. Y. Yang, and J. Zhang. Bioconductor: open software development for computational biology and bioinformatics. *Genome Biol*, 5(10): R80, 2004.

[139] G. K. Smyth. Linear models and empirical bayes methods for assessing differential expression in microarray experiments. *Stat Appl Genet Mol Biol*, 3:Article3, 2004.

[140] A. Subramanian, P. Tamayo, V. K. Mootha, S. Mukherjee, B. L. Ebert, M. A. Gillette, A. Paulovich, S. L. Pomeroy, T. R. Golub, E. S. Lander, and J. P. Mesirov. Gene set enrichment analysis: a knowledge-based approach for interpreting genome-wide expression profiles. *Proc Natl Acad Sci U S A*, 102(43): 15545–50, 2005.

[141] F. Weerkamp, T. C. Luis, B. A. Naber, E. E. Koster, L. Jeannotte, J. J. van Dongen, and F. J. Staal. Identification of notch target genes in uncommitted t-cell progenitors: No direct induction of a t-cell specific gene program. *Leukemia*, 20 (11):1967–77, 2006.

[142] Yosef Benjamini, Yoav; Hochberg. Controlling the false discovery rate: a practical and powerful approach to multiple testing. *Journal of the Royal Statistical Society*, 57(1):289–300, 1995.

[143] L. W. Ellisen, J. Bird, D. C. West, A. L. Soreng, T. C. Reynolds, S. D. Smith, and J. Sklar. Tan-1, the human homolog of the drosophila notch gene, is broken by chromosomal translocations in t lymphoblastic neoplasms. *Cell*, 66(4):649–61, 1991.

[144] S. Jarriault, C. Brou, F. Logeat, E. H. Schroeter, R. Kopan, and A. Israel. Signalling downstream of activated mammalian notch. *Nature*, 377(6547):355–8, 1995.

[145] R. E. Moellering, M. Cornejo, T. N. Davis, C. Del Bianco, J. C. Aster, S. C. Blacklow, A. L. Kung, D. G. Gilliland, G. L. Verdine, and J. E. Bradner. Direct inhibition of the notch transcription factor complex. *Nature*, 462(7270):182–8, 2009.

[146] S. R. Schwarze, K. A. Hruska, and S. F. Dowdy. Protein transduction: unrestricted delivery into all cells? *Trends Cell Biol*, 10(7):290–5, 2000.

[147] P. Lundberg and U. Langel. A brief introduction to cell-penetrating peptides. *J Mol Recognit*, 16(5):227–33, 2003.

[148] T. Holm, H. Johansson, P. Lundberg, M. Pooga, M. Lindgren, and U. Langel. Studying the uptake of cell-penetrating peptides. *Nat Protoc*, 1(2):1001–5, 2006.

[149] Y. Nam, A. P. Weng, J. C. Aster, and S. C. Blacklow. Structural requirements for assembly of the csl.intracellular notch1.mastermind-like 1 transcriptional activation complex. *J Biol Chem*, 278(23):21232–9, 2003.

[150] O. Y. Lubman, M. X. Ilagan, R. Kopan, and D. Barrick. Quantitative dissection of the notch:csl interaction: insights into the notch-mediated transcriptional switch. *J Mol Biol*, 365(3):577–89, 2007.

[151] C. Del Bianco, J. C. Aster, and S. C. Blacklow. Mutational and energetic studies of notch 1 transcription complexes. *J Mol Biol*, 376(1):131–40, 2008.

[152] S. Jeffries, D. J. Robbins, and A. J. Capobianco. Characterization of a high-molecular-weight notch complex in the nucleus of notch(ic)-transformed rke cells and in a human t-cell leukemia cell line. *Mol Cell Biol*, 22(11):3927–41, 2002.

[153] Y. Bessho, G. Miyoshi, R. Sakata, and R. Kageyama. Hes7: a bhlh-type repressor gene regulated by notch and expressed in the presomitic mesoderm. *Genes Cells*, 6(2):175–85, 2001.

[154] J. Cordle, S. Johnson, J. Z. Tay, P. Roversi, M. B. Wilkin, B. H. de Madrid, H. Shimizu, S. Jensen, P. Whiteman, B. Jin, C. Redfield, M. Baron, S. M. Lea, and P. A. Handford. A conserved face of the jagged/serrate dsl domain is involved in notch trans-activation and cis-inhibition. *Nat Struct Mol Biol*, 15(8):849–57, 2008.

[155] H. Shen, A. S. McElhinny, Y. Cao, P. Gao, J. Liu, R. Bronson, J. D. Griffin, and L. Wu. The notch coactivator, maml1, functions as a novel coactivator for mef2c-mediated transcription and is required for normal myogenesis. *Genes Dev*, 20(6): 675–88, 2006.

[156] Y. Zhao, R. B. Katzman, L. M. Delmolino, I. Bhat, Y. Zhang, C. B. Gurumurthy, A. Germaniuk-Kurowska, H. V. Reddi, A. Solomon, M. S. Zeng, A. Kung, H. Ma, Q. Gao, G. Dimri, A. Stanculescu, L. Miele, L. Wu, J. D. Griffin, D. E. Wazer, H. Band, and V. Band. The notch regulator maml1 interacts with p53 and functions as a coactivator. *J Biol Chem*, 282(16):11969–81, 2007.

[157] L. D. Vales and E. M. Friedl. Binding of c/ebp and rbp (cbf1) to overlapping sites regulates interleukin-6 gene expression. *J Biol Chem*, 277(45):42438–46, 2002.

[158] S. H. Lee, X. Wang, and J. DeJong. Functional interactions between an atypical nf-kappab site from the rat cyp2b1 promoter and the transcriptional repressor rbp-jkappa/cbf1. *Nucleic Acids Res*, 28(10):2091–8, 2000.

[159] S. Eckerle, V. Brune, C. Doring, E. Tiacci, V. Bohle, C. Sundstrom, R. Kodet, M. Paulli, B. Falini, W. Klapper, A. B. Chaubert, K. Willenbrock, D. Metzler, A. Brauninger, R. Kuppers, and M. L. Hansmann. Gene expression profiling of isolated tumour cells from anaplastic large cell lymphomas: insights into its cellular origin, pathogenesis and relation to hodgkin lymphoma. *Leukemia*, 23 (11):2129–38, 2009.

[160] K. Basso, A. A. Margolin, G. Stolovitzky, U. Klein, R. Dalla-Favera, and A. Califano. Reverse engineering of regulatory networks in human b cells. *Nat Genet*, 37 (4):382–90, 2005.

[161] A. A. Margolin, I. Nemenman, K. Basso, C. Wiggins, G. Stolovitzky, R. Dalla Favera, and A. Califano. Aracne: an algorithm for the reconstruction of gene regulatory networks in a mammalian cellular context. *BMC Bioinformatics*, 7 Suppl 1: S7, 2006.

[162] M. Wang, V. Augusto Benedito, P. Xuechun Zhao, and M. Udvardi. Inferring large-scale gene regulatory networks using a low-order constraint-based algorithm. *Mol Biosyst*, 6(6):988–98, 2010.

[163] Uri Alon. *An introduction to systems biology : design principles of biological circuits*. Chapman & Hall, Boca Raton, FL, 2007.

[164] P. D. Lyne. Structure-based virtual screening: an overview. *Drug Discov Today*, 7(20):1047–55, 2002.

[165] L. C. Cerchietti, A. F. Ghetu, X. Zhu, G. F. Da Silva, S. Zhong, M. Matthews, K. L. Bunting, J. M. Polo, C. Fares, C. H. Arrowsmith, S. N. Yang, M. Garcia, A. Coop, Jr. Mackerell, A. D., G. G. Prive, and A. Melnick. A small-molecule inhibitor of bcl6 kills dlbcl cells in vitro and in vivo. *Cancer Cell*, 17(4):400–11, 2010.

[166] J. Janin. Protein-protein docking tested in blind predictions: the capri experiment. *Mol Biosyst*, 2010.

[167] G. T. Montelione and T. Szyperski. Advances in protein nmr provided by the nigms protein structure initiative: impact on drug discovery. *Curr Opin Drug Discov Devel*, 13(3):335–49, 2010.

[168] L. C. Cerchietti, S. N. Yang, R. Shaknovich, K. Hatzi, J. M. Polo, A. Chadburn, S. F. Dowdy, and A. Melnick. A peptomimetic inhibitor of bcl6 with potent antilymphoma effects in vitro and in vivo. *Blood*, 113(15):3397–405, 2009.

[169] J. M. Polo, T. Dell'Oso, S. M. Ranuncolo, L. Cerchietti, D. Beck, G. F. Da Silva, G. G. Prive, J. D. Licht, and A. Melnick. Specific peptide interference reveals bcl6 transcriptional and oncogenic mechanisms in b-cell lymphoma cells. *Nat Med*, 10 (12):1329–35, 2004.

[170] J. M. Kilby, J. P. Lalezari, J. J. Eron, M. Carlson, C. Cohen, R. C. Arduino, J. C. Goodgame, J. E. Gallant, P. Volberding, R. L. Murphy, F. Valentine, M. S. Saag, E. L. Nelson, P. R. Sista, and A. Dusek. The safety, plasma pharmacokinetics, and antiviral activity of subcutaneous enfuvirtide (t-20), a peptide inhibitor of gp41-mediated virus fusion, in hiv-infected adults. *AIDS Res Hum Retroviruses*, 18(10):685–93, 2002.

[171] L. Nogova, T. Rudiger, and A. Engert. Biology, clinical course and management of nodular lymphocyte-predominant hodgkin lymphoma. *Hematology Am Soc Hematol Educ Program*, pages 266–72, 2006.

[172] EM Noordijk. First results of the eortc-gela h9 randomized trials: the h9-f trial and h9-u trial in patients with favourable or unfavourable early stage hodgkin's lymphoma. *J Clin Oncol*, 23:561, 2005.

List of Figures

List of Tables

Danksagung

In allererster Linie möchte ich mich bei Herrn Dr. Stephan Mathas bedanken. Allgemein dafür, die vorliegende Arbeit in seiner Arbeitsgruppe durchführen zu können und im speziellen für seine wertvollen wissenschaftlichen und projektplanerischen Ideen, seine Unterstützung und Beharrlichkeit und seine konstruktive Offenheit gegenüber meinen Ideen. All dies hat ganz wesentlich zum Erfolg dieser Arbeit beigetragen.

Besonderer Dank gilt auch Herrn Dr. Martin Janz für seine kritische Analyse von Ergebnissen und Hypothesen dieser Arbeit und fr die Bereitstellung diverser hochdimensionaler Datensätze, die den Grundstock dieser Arbeit gelegt haben. Weiterhin möchte ich Katrin Ullrich, Melanie Manzke, Caroline Gärtner und Björn Lamprecht vielmals für ihre experimentelle Unterstützung danken. Gleiches gilt für Herrn Dr. Otto Albrecht, der die Massenspektrometrie durchgeführt und auch ausgewertet hat. Frau Kathrin Wurster danke ich für das kritische Korrekturlesen dieser Arbeit. Prof. Dr. Bernd Dörken möchte ich für seine fortwährende Unterstützung danken.

Zu guter letzt möchte ich meiner Familie und vor allem Leopold und Claudia für ihren Rückhalt und ihre unersetzlichen Aufmunterungen — besonders in den arbeitsintensivsten Phasen dieses Projekts — danken.

Selbständigkeitserklärung

Ich erkläre, dass ich die vorliegende Arbeit selbständig und nur unter Verwendung der angegebenen Literatur und Hilfsmittel angefertigt habe. Ich versichere, dass alle aus anderen Quellen übernommenen Daten und Konzepte, sowie Ergebnisse aus Kooperationsprojekten unter Angabe der Referenz gekennzeichnet sind. Außerdem versichere ich, dass mir die aktuelle Promotionsordnung bekannt ist und ich mich nicht anderwärts um einen Doktorgrad bewerbe, bzw. noch keinen entsprechenden Doktorgrad besitze. Diese Arbeit wurde in gleicher oder ähnlicher Form nicht einer anderen Prüfungsbehörde vorgelegt.

Berlin, den 27.10.2010 Karl Köchert